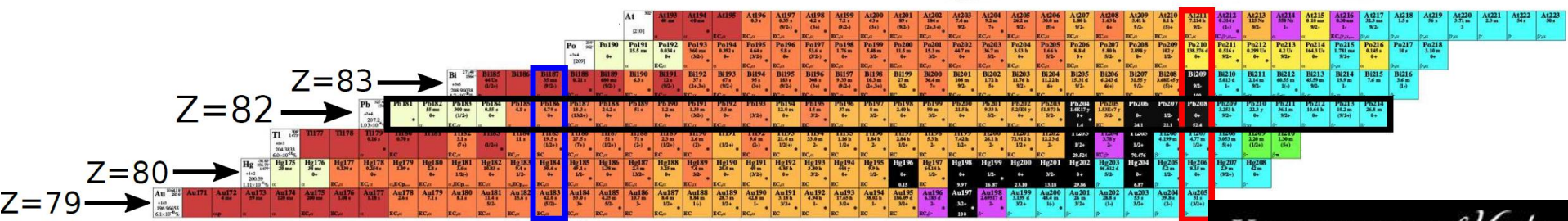


The studies of neutron-rich Tl-Po isotopes facilitated by selective laser spectroscopy at ISOLDE Decay Station (CERN) (nice physics with modern experimental nuclear and atomic techniques)

Andrei Andreyev
University of York(UK)

- Introduction on shapes and charge radii
- Method: Isotope Shift(IS) and Hyperfine Splitting (HFS) measurements
- ISOLDE and our detection tools
- Exemplary study case: neutron-deficient Hg isotopes – is there life after shape staggering?
- N=126 charge radii kink problem
- Neutron-rich Tl and Hg isotopes
- Conclusions



Collaboration

University of York, United Kingdom

A. N. Andreyev, J. G. Cubiss, R. Harding, C. Raison, C. Page, Z. Yue...

Université Paris-Saclay

S. Hilaire, S. Péru,

Université Libre de Bruxelles

S. Goriely

Gatchina, JINR-Dubna, Russia

I. N. Borzov, A. E. Barzakh, D. V. Fedorov, P. Molkanov

RILIS, CRIS and ISOLDE, Geneva, Switzerland

B. A. Marsh, K. Chrysalidis, R. Heinke, C. Bernerd, V. N. Fedosseev, M. D. Seliverstov, K. Lynch, T. Day Goodacre...

Institut für Physik, Johannes Gutenberg-Universität Mainz, Mainz, Germany

S. Raeder, K. D. A. Wendt

Instituut voor Kern- en Stralingsphysica, K.U. Leuven, Leuven, Belgium

S. Sels, L. Ghys, C. Van Beveren, E. Rapisarda, D. Pauwels, D. Radulov, H. De Witte, Yu. Kudryavtsev, M. Huyse, P. Van Duppen, K. Rezynkina, L. Gaffney, T. E. Cocolios...

Comenius University, Bratislava, Slovakia

S. Antalic, B. Andel....

MR-TOF@ISOLTRAP team:

S. Kreim, V. Manea, F. Wienholtz, M. Meugeot, M. Rosenbusch, L. Neis +...

University of Surrey, United Kingdom

Z. Podolyak, S. Pascu...

University of Manchester, UK

J. Billowes, M. Bissel...

Many PhD students, both nuclear and atomic/laser spectroscopy

York city, UK, ~150.000 population



University of York (est. 1963)

Academic staff	2,295
Students	23,420
<u>Undergraduates</u>	15,350
<u>Postgraduates</u>	8,070

York's Nuclear Physics group
10 academics
10+ postdocs
25+ PhD students

Some fun ☺

陕西地图VS英国地图

35 million



陕西

69 million



英国

面积：20.6万平方公里

北部：黄土高原

著名建筑：钟楼、大雁塔

邻居：河南

资源：煤、石油、天然气

代表食品：肉夹馍

别称：大唐不夜城

艺人：郭达



面积：20.9万平方公里

北部：苏格兰高地

著名建筑：大笨钟、伦敦塔

邻居：荷兰

资源：煤、石油、天然气

代表食品：汉堡包

别称：日不落帝国

艺人：杰森斯坦森



York-Zhuhai Collaboration: Nuclear structure in heavy exotic nuclei (C.F.Jiao et al)

PHYSICAL REVIEW C 112, 024328 (2025)

August 2025

β - and α -decay spectroscopy of ^{182}Au

J. Miščík^{1,*}, B. Andel¹, A. N. Andreyev^{2,3}, A. E. Barzakh⁴, J. G. Cubiss^{2,†}, A. Algora^{5,6}, S. Antalic¹, M. Athanasakis-Kaklamanakis⁷, M. Au⁷, S. Bara⁸, R. A. Bark⁹, M. J. G. Borge¹⁰, A. Camaiani¹⁰, K. Chrysalidis⁷, T. E. Cocilios⁸, C. Costache¹³, H. De Witte⁸, R. Y. Dong¹⁴, D. V. Fedorov⁴, V. N. Fedossev¹⁷, L. M. Fraile¹⁵, H. O. U. Fynbo¹⁶, R. Grzywacz¹⁷, R. Heinke⁷, C. F. Jiao¹⁴, J. Johnson⁸, P. M. Jones⁹, D. S. Judson¹⁸, D. T. Kattikat Melcom¹⁹, M. M. Khan^{8,20}, J. Klimo⁸, A. Korgul²¹, M. Labiche²², R. Lică¹³, Z. Liu²³, M. Madurga¹⁷, N. Marginean¹³, P. Marini^{19,‡}, B. A. Marsh^{7,§}, C. Mihai¹³, P. L. Molkanov⁴, E. Nácher⁵, C. Neacsu¹³, J. N. Orce²⁴, R. D. Page¹⁸, J. Pakarinen^{25,28}, P. Papadakis²², S. Pascu¹³, A. Pereia¹⁰, M. Piera-Sifkowska²¹, Zs. Podolyák²⁶, M. D. Seliverstov⁴, A. Sitarčík¹, E. Stamatı^{7,27}, A. Stoica¹³, A. Stott², M. Stryjczyk^{25,28,29}, O. Tengblad¹⁰, I. Tsekhanovich¹⁹, A. Turturea¹³, J. M. Urdas¹⁵, P. Van Duppen⁸, N. Warr³⁰, and A. Youssef⁸

(ISOLDE Decay Station Collaboration)

¹Department of Nuclear Physics and Biophysics, Comenius University in Bratislava, 84248 Bratislava, Slovakia

²School of Physics, Engineering and Technology, University of York, York YO10 5DD, United Kingdom

³Advanced Science Research Center, Japan Atomic Energy Agency, Tokai-mura, Ibaraki 319-1195, Japan

⁴Affiliated with an institute covered by a cooperation agreement with CERN at the time of the experiment

⁵Instituto de Física Corpuscular, CSIC-Universidad de Valencia, E-46071 Valencia, Spain

⁶Institute of Nuclear Research (ATOMKI), P.O.Box 51, H-4001 Debrecen, Hungary

⁷CERN, CH-1211 Geneve 23, Switzerland

⁸KU Leuven, Instituut voor Kern- en Stralingsfysica, 3001 Leuven, Belgium

⁹iThemba LABS, National Research Foundation, P. O. Box 722, Somerset West 7129, South Africa

¹⁰Instituto de Estructura de la Materia, CSIC, 28006 Madrid, Spain

¹¹Dipartimento di Fisica, Università di Firenze, I-50019 Sesto Fiorentino, Italy

¹²Istituto Nazionale di Fisica Nucleare, Sezione di Firenze, I-50019 Sesto Fiorentino, Italy

¹³Horia Hulubei National Institute of Physics and Nuclear Engineering (IFIN-HH), R-077125 Bucharest, Romania

¹⁴School of Physics and Astronomy, Sun Yat-sen University, Zhuhai 519082, China

¹⁵Grupo de Física Nuclear and IPARCOS, Universidad Complutense de Madrid, CEI Moncloa, E-28040 Madrid, Spain

Competition between shape-coexisting $11/2^-$ states in neutron-deficient odd-mass thallium isotopes **In preparation 2026**

R. Y. Dong^{a,b}, C. F. Jiao^{a,b,*}, A. N. Andreyev^{c,d}, A. E. Barzakh^e, Z. Liu^{f,g}, S. Y. Zhang^h

^aSchool of Physics and Astronomy, Sun Yat-sen University, Zhuhai 519082, China

^bGuangdong Provincial Key Laboratory of Quantum Metrology and Sensing, Sun Yat-sen University, Zhuhai 519082, China

^cDepartment of Physics, University of York, York, YO10 5DD, United Kingdom

^dAdvanced Science Research Center (ASRC), Japan Atomic Energy Agency, Tokai-mura, Japan

^ePetersburg Nuclear Physics Institute, NRC Kurchatov Institute, Gatchina 188300, Russia

^fInstitute of Modern Physics, Chinese Academy of Sciences, Lanzhou 730000, China

^gUniversity of Chinese Academy of Sciences, Beijing 100049, China

^hSchool of Physics and State Key Laboratory of Nuclear Physics and Technology, Peking University, Beijing 100871, China

Abstract

Unlike the near-constant excitation energies of low-lying $I\pi = 11/2^-$ states in neighboring Au isotopes, an anomalous suppression in the excitation energies of one-proton $11/2^-$ states is observed in neutron-deficient Tl isotopes. We study the evolution of low-lying one-proton states in neutron-deficient odd-mass Tl isotopes, in particular the $11/2^-$ states, by means of configuration-

York-Zhuhai Collaboration: Probing the shell evolution in heavy nuclei (C.Yuan et al.)

Phys. Lett. B 871 (2025) 140013

November 2025



Contents lists available at ScienceDirect

Physics Letters B

journal homepage: www.elsevier.com/locate/physletb



Letter

Electromagnetic moments of $^{215,217}\text{Bi}$: Probing shell evolution beyond $N = 126$



A. N. Andreyev ^{1,2}, A. Barzakh ^{1,3,*}, M. D. Seliverstov ¹, Z. Yue ¹, Menglan Liu ^{1,4},
Cenxi Yuan ^{1,4}, A. Algora ^{1,5}, B. Andel ^{1,6}, S. Antalic ^{1,6}, M. Al Monthery ^{1,7}, D. Atanasov ^{1,8},
J. Benito ¹, G. Benzoni ¹, T. Berry ¹, M. L. Bissell ¹, K. Blaum ^{1,9}, M. J.
K. Chrysalidis ^{1,10}, C. Clisu ^{1,10}, T. E. Cocolios ^{1,10}, C. Costache ^{1,10}, J. G. Cub
T. Day Goodacre ^{1,11,supplementary}, G. J. Farooq-Smith ^{1,11}, D. V. Fedorov ^{1,12}, V
L. M. Fraile ¹, H. O. U. Fynbo ¹, V. Gadelshin ¹, L. P. Gaffney ^{1,13}, R. F G
C. Granados ^{1,14}, P. T. Greenlees ¹, R. D. Harding ^{1,15}, L. J. Harkness-Bren
A. Herlert ^{1,16}, M. Huyse ¹, A. Illana ^{1,17}, J. Jolie ^{1,18}, D. S. Judson ¹, J. Kai
P. Larmonier ¹, I. Lazarus ^{1,19}, D. Leimbach ^{1,20}, R. Lică ¹, Z. Liu ^{1,21,af}, D. Li
M. Madurga ^{1,22}, V. Manea ¹, N. Marginean ¹, R. Marginean ¹, B. A. Mars
P. Molkanov ¹, P. Mosat ¹, M. Mougeot ¹, J. R. Murias ¹, E. Nacher ¹, A.
L. Nies ¹, R. D. Page ¹, S. Pascu ¹, A. Perea ¹, V. Pucknell ^{1,ad}, P. Rahkila ¹
E. Rapisarda ¹, K. Rezynkina ¹, M. Rosenbush ^{1,23,ak}, R. E. Rossel ¹, S. Rotl
V. Sánchez-Tembleque ¹, K. Schomacker ^{1,24}, L. Schweikhard ^{1,25}, C. Seiffe
L. Stan ¹, M. Stryjczyk ^{1,26,al}, D. Studer ¹, J. Sundberg ^{1,ac}, C. Sürder ^{1,am},
P. Van Duppen ^{1,10}, V. Vedia ¹, M. Verlinde ¹, S. Viñals ¹, N. Warr ^{1,ab}, A.
F. Wienholtz ^{1,aj,am}, R. N. Wolf ^{1,h,aj,ao}

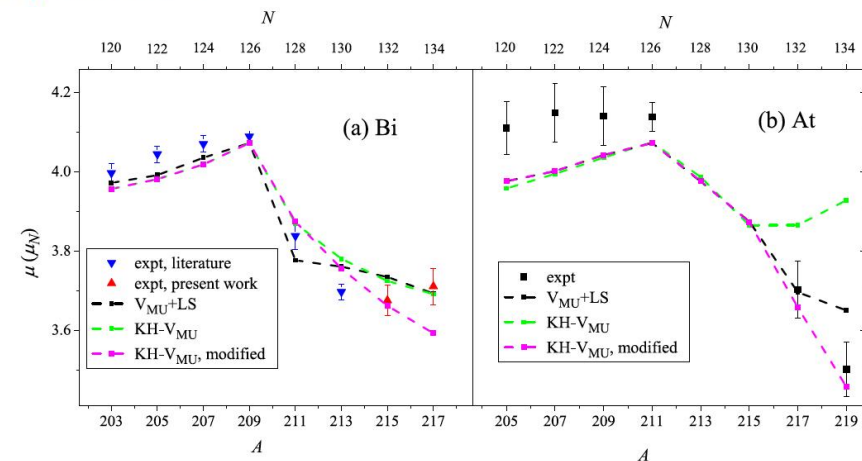


Fig. 5. Comparison of μ values from experiment and CISM calculations for $I^\pi = 9/2^-$ states of bismuth and astatine isotopes. (a) Bismuth isotopes. Upward triangles:

^a School of Physics, Engineering and Technology, University of York, YO10 5DD, York, United Kingdom

^b Affiliated with an institute covered by a cooperation agreement with CERN at the time of the experiment, Russia

^c Sino-French Institute of Nuclear Engineering and Technology, Sun Yat-Sen University, 519082, Zhuhai Guangdong, China

^d Instituto de Física Corpuscular, CSIC - Universidad de Valencia, E-46980, Valencia, Spain

^e HUN-REN Institute of Nuclear research (ATOMKI), P.O.Box 51, H-4001, Debrecen, Hungary

Mendeleev's Chart of Elements (a chemist's point of view)

IA

1 qīng H 氢 Hydrogen 1.0079
3 lǐ Li 锂 Lithium 6.941
4 pí Be 铍 Beryllium 9.0122
11 nà Na 钠 Sodium 22.988

IIA

3 lǐ Li 锂 Lithium 6.941
12 méi Mg 镁 Magnesium 24.305
11 nà Na 钠 Sodium 22.988



元素周期表

VIII
IIIB IVB VB VIB VIIB

VII

IB IIB

0

2 hái He 氦 Helium 4.002602
10 nǎi Ne 氖 Neon 20.1797
18 yá Ar 氩 Argon 39.948

IIIA IVA VA VIA VIIA

5 péng B 硼 Boron 10.811	6 tān C 碳 Carbon 12.0107	7 dàn N 氮 Nitrogen 14.0067	8 yāng O 氧 Oxygen 15.9994	9 fú F 氟 Fluorine 18.9984032	10 nǎi Ne 氖 Neon 20.1797
13 lǔ Al 铝 Aluminium 26.9815386	14 guī Si 硅 Silicon 28.0855	15 lín P 磷 Phosphorus 30.973762	16 liú S 硫 Sulfur 32.065	17 lǔ Cl 氯 Chlorine 35.453	18 yá Ar 氩 Argon 39.948
31 jiā Ga 钪 Gallium 69.723	32 zhē Ge 锗 Germanium 72.64	33 shēn As 砷 Arsenic 74.82160	34 xi Se 砹 Selenium 78.96	35 xiù Br 溴 Bromine 79.904	36 kè Kr 氪 Krypton 83.798

19 jiá K 钾 Potassium 39.098	20 gài Ca 钙 Calcium 40.08	21 kàng Sc 钆 Scandium 44.956	22 tài Ti 钛 Titanium 47.857	23 fān V 钐 Vanadium 50.9415	24 gé Cr 钸 Chromium 51.9961	25 mèng Mn 锰 Manganese 54.938045	26 tié Fe 钢 Iron 55.845	27 gǔ Co 钴 Cobalt 58.93195	28 niè Ni 镍 Nickel 58.6934	29 tóng Cu 铜 Copper 63.546	30 xīn Zn 锌 Zinc 65.38	31 jiā Ga 钪 Gallium 69.723	32 zhē Ge 锇 Germanium 72.64	33 shēn As 砷 Arsenic 74.82160	34 xi Se 砹 Selenium 78.96	35 xiù Br 溴 Bromine 79.904	36 kè Kr 氪 Krypton 83.798
37 rú Rb 铷 Rubidium 85.467	38 sī Sr 钾 Strontium 87.62	39 yǐ Y 钇 Yttrium 88.906	40 gǎo Zr 钇 Zirconium 91.22	41 ní Nb 钨 Niobium 92.90658	42 mù Mo 钼 Molybdenum 95.96	43 dé Tc 钔 Technetium 97.9072	44 liào Ru 钿 Ruthenium 101.07	45 liào Rh 钑 Rhodium 102.90550	46 bǎ Pd 钑 Palladium 106.42	47 yīn Ag 银 Silver 107.8682	48 gé Cd 钪 Cadmium 112.411	49 yīn In 钕 Indium 114.818	50 xi Sn 锡 Tin 121.710	51 tī Sb 锦 Srimony 121.760	52 dí Te 砘 Tellurium 127.60	53 diān I 砹 Iodine 126.90447	54 xiān Xe 氙 Xenon 131.293
55 sè Cs 铯 Cesium 132.905	56 bēi Ba 钡 Barium 137.33	La-Lu lan 镧系 Lanthanides	72 hā Hf 钫 Hafnium 178.49	73 tān Ta 钨 Tantalum 180.94788	74 wù W 钨 tungsten 183.84	75 lái Re 钇 Rhenium 186.207	76 é Os 钇 Osmium 190.23	77 yí Ir 钇 Rhodium 192.217	78 bō Pt 钯 Platinum 195.084	79 jīn Au 金 Gold 196.966569	80 gōng Hg 梞 Mercury 200.59	81 tā Tl 钻 Thallium 204.2833	82 qiān Pb 钋 Lead 207.2	83 bì Bi 钇 Bismuth 208.98040	84 pō Po 钍 Polonium 208.9824	85 ài At 砹 Astatine 209.9871	86 dōng Rn 氪 Radon 222.0176
87 fāng Fr 钇 Francium 223	88 lái Ra 钇 Radium 226.03	Ac-Lr 钇系 Actinides	104 lú Rf 钇 Rutherfordium (261)	105 dù Db 钇 Dubnium (262)	106 xi Sg 钇 Seaborgium (263)	107 bō Bh 钇 Bohrium (262)	108 héi Hs 钇 Hassium (265)	109 mài Mt 钇 Meltsmerium (266)	110 dā Ds 钇 darmstadtium (269)	111 lún Rg 钇 Roentgenium (272)	112 gé Cn 钇 Copernicium (285)	113 ní Nh 钇 Nihonium (284)	114 fú Fl 钇 Flerovium (289)	115 mó Mc 钇 Moscovium (288)	116 lì Lv 钇 Livermorium (292)	117 tián Ts 砈 Tennessine (294)	118 áo Og 氙 Oganesson (294)
119	120																

元素序号
元素符号
相对原子质量
元素名称

57 fān La 镧 lanthanum 138.905	58 shí Ce 钕 cerium 140.12	59 pú Pr 钕 praseodymium 140.91	60 nǚ Nd 钕 neodymium 144.2	61 pò Pm 钕 promethium 147	62 zhǎn Sm 钕 samarium 150.4	63 yóu Eu 钕 europium 151.96	64 gāo Gd 钕 gadolinium 157.25	65 tè Tb 钕 terbium 158.93	66 dí Dy 钕 dysprosium 162.5	67 huó Ho 钕 holmium 164.93	68 èr Er 钕 erbium 167.2	69 dió Tm 钇 thulium 168.943	70 yí Yb 钇 ytterbium 173	71 lǔ Lu 钇 lutetium 174.96
89 à Ac 钇 actinium 227.03	90 tú Th 钇 thorium 232.04	91 pú Pa 钇 protactinium 231.04	92 yóu U 钇 uranium 238.03	93 nǎ Np 钇 neptunium 237.05	94 bù Pu 钇 plutonium 244	95 méi Am 钇 americium 243	96 jù Cm 钇 curium 247	97 péi Bk 钇 berkelium 247	98 kǎi Cf 钇 californium 251	99 ái Es 钇 einsteinium 254	100 fēi Fm 钇 fermium 257	101 mēn Md 钇 mendelevium 258	102 nuo No 钇 nobelium 259	103 lao Lr 钇 lawrencium 260

主族金属 副族金属 非金属元素 稀有气体 人造元素

118 elements are known so far

中国科学院近代物理研究所

Chart of Isotopes (a nuclear physicist's point of view)

Nuclear Chart: decay mode of the ground state nuclide(NUBASE2020)

核素图：基态原子核的衰变类型(NUBASE2020)

■ 稳定核素 Sta 283 stable isotopes

■ β^- 衰变 β^- decay

■ β^+ 或 EC 衰变 β^+ or EC decay

■ α 衰变 α decay

■ 自发裂变 Spontaneous fission

■ 中子发射 Neutron decay

■ 质子发射 Proton decay

■ 衰变类型未知 Decay mode: ?

Proton Number
质子数

↑ Ca(20)

Ni(28)

Sn(50)

Pb(82)

82

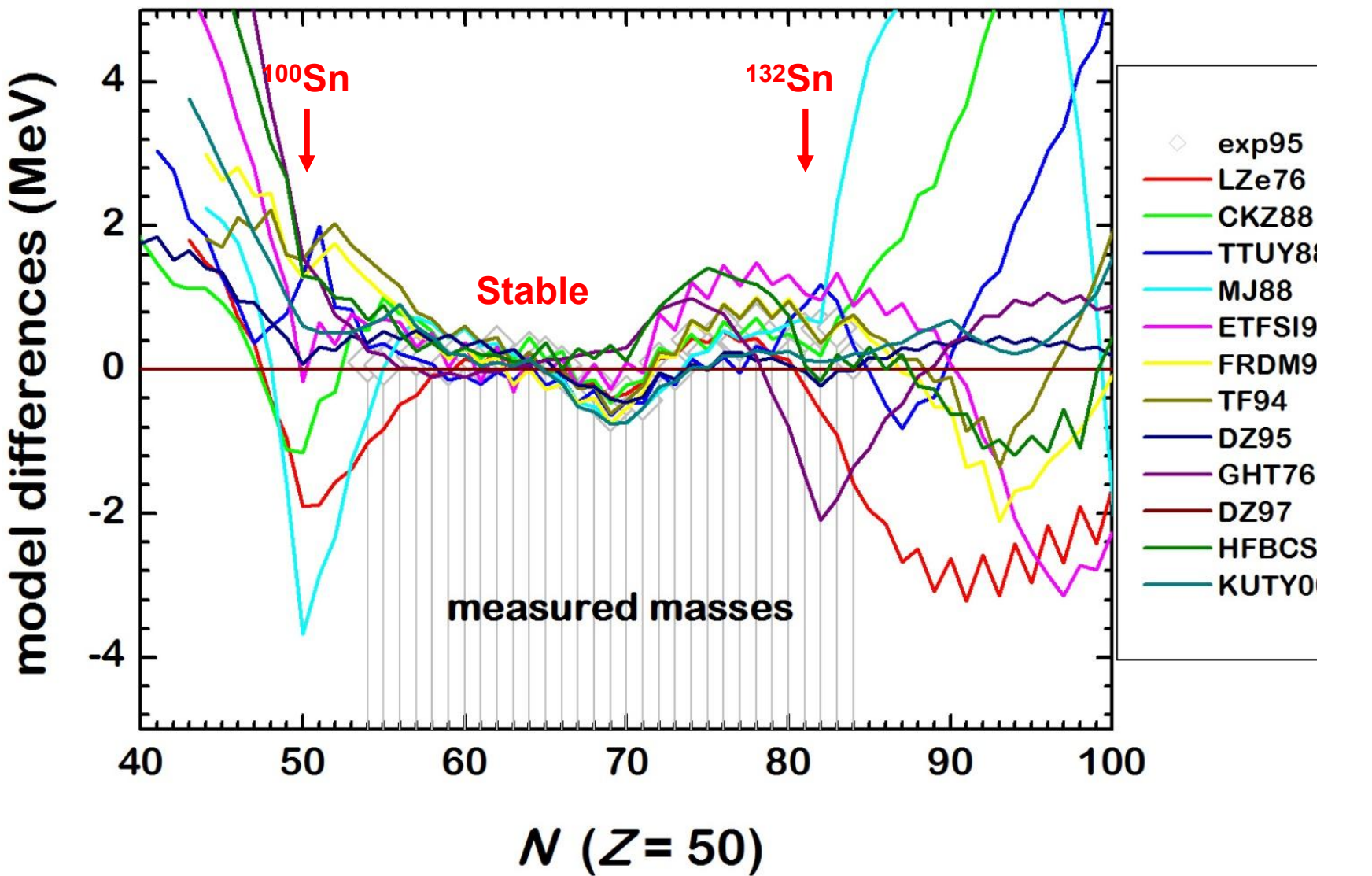
Og(Z=118)

184

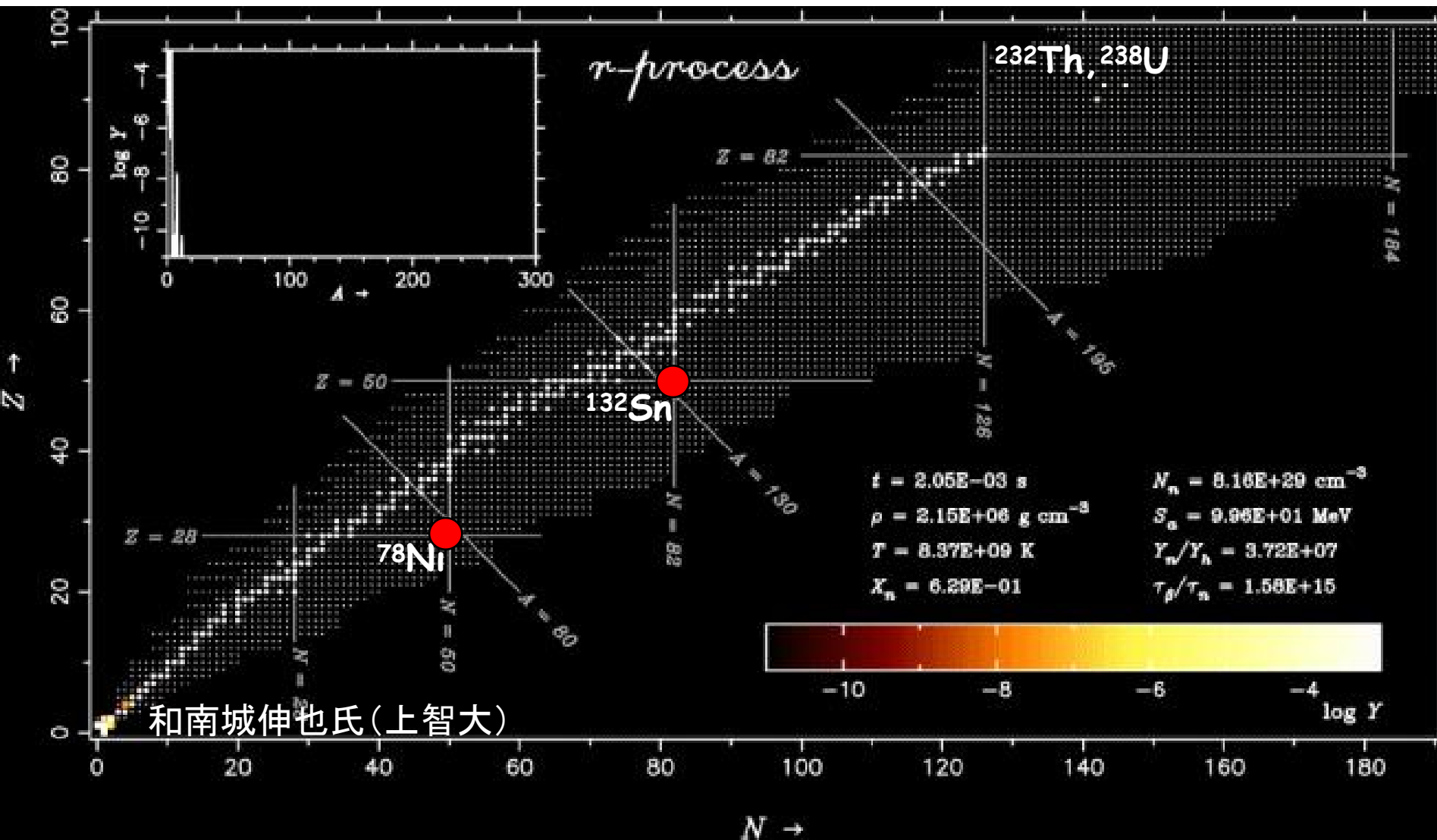
~3300 isotopes are known
~4000 can be discovered,
including new elements

A key question: are the underlying physics phenomena the same for very exotic (neutron-deficient or neutron-rich) isotopes as for stable isotopes?

Example: Calculations of mass for Sn isotopes (or why we need to go far off stability)



R-process network calculations



R-process network calculations require data for very neutron-rich nuclei: half-lives, decay modes, neutron-capture cross sections, fission barriers and mass distributions.

(Basic) Introduction on Nuclear Radii and Shapes

Or is $R=r_o A^{1/3}$?
(as it is said in all textbooks)

Traditional Techniques to Measure Charge Radii/Densities of Nuclei



ROBERT HOFSTADTER

The electron-scattering method and its application to the structure of nuclei and nucleons

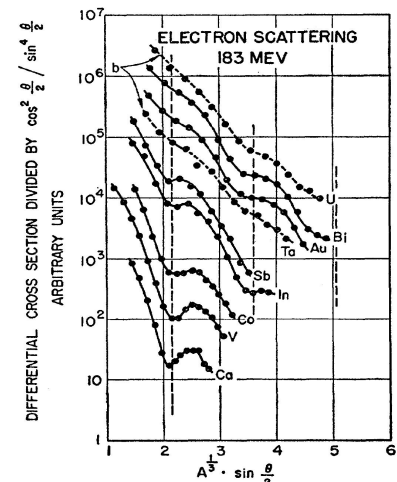
Nobel Lecture, December 11, 1961

<https://www.nobelprize.org/uploads/2018/06/hofstadter-lecture.pdf>
Review of Modern Physics, 28, 1956

1915-1990

Electron Angular Distribution

also as a function of e^- energy



Charge Distribution

$$\rho(r) = \frac{\rho_0}{1 + e^{(r-R)/a}}, \quad r = \text{distance from the center}$$

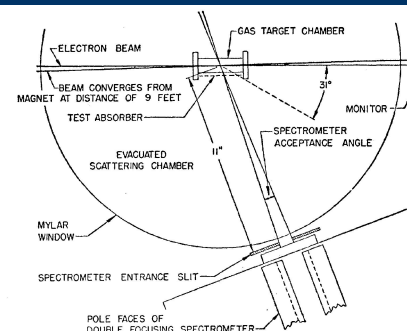
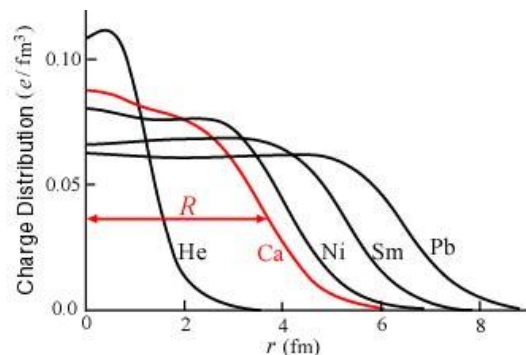


FIG. 17. Schematic diagram of scattering geometry employed with the gas target chamber.

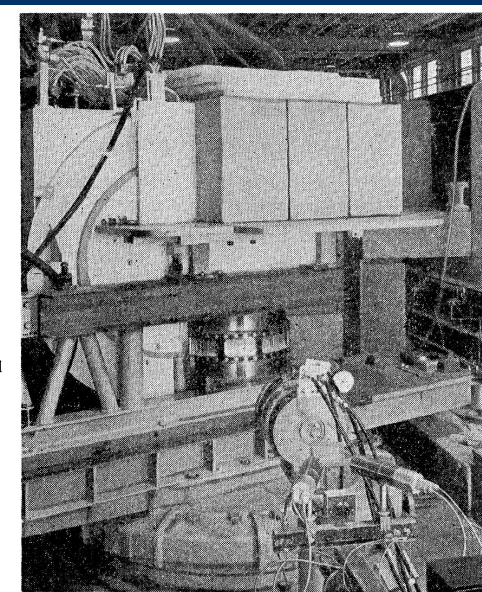
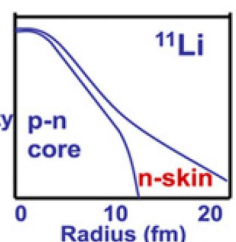


FIG. 15. The semicircular 190-Mev spectrometer, to the left, is shown on the gun mount. The upper platform carries the lead and paraffin shielding that encloses the Čerenkov counter. The gas scattering chamber is shown below with the thin window encircling it. Ion chamber monitors appear in the foreground.

Charge Radius R
 $R=r_o A^{1/3}$

- Measurements of Muonic X rays – also charge distributions
- Optical Isotope Shift (IS) measurements for stable isotopes – provide radius
- Electron scattering/Muonic X rays provide absolute charge radii/densities for STABLE/LONG-LIVED isotopes, but both methods require large amount of material (often many mg's)
- Modern experiments with UNSTABLE isotopes allow the use of IS measurements for short-lived nuclides, up to ~ a few ms (depends on intensity), up to 0.01 pps!
- Also, the electron scattering on RIBs in colliding geometry started (SCRIT@RIKEN)

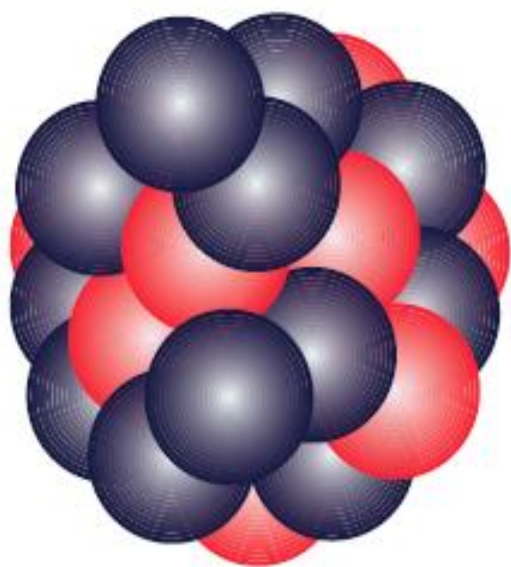
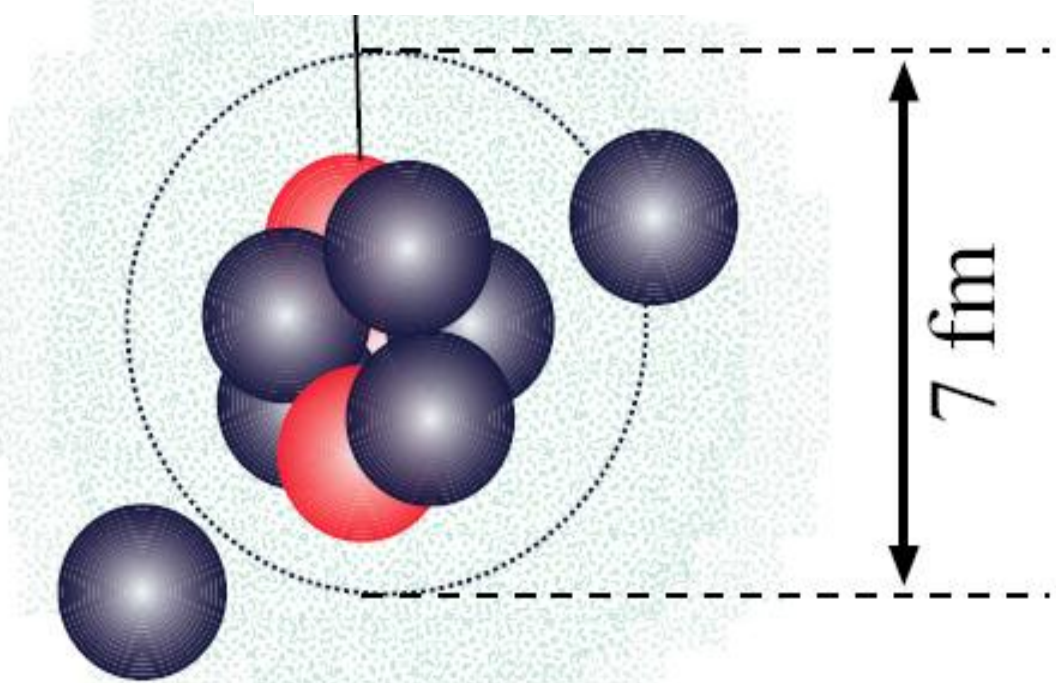
Radioactive Ion Beams (RIBs). Breaking Old Rules in Nuclear Physics: Is $R=r_0 A^{1/3}$?



^{11}Li ($Z=3, N=8$)

(halo nucleus)

^{48}Ca ($Z=N=20$)

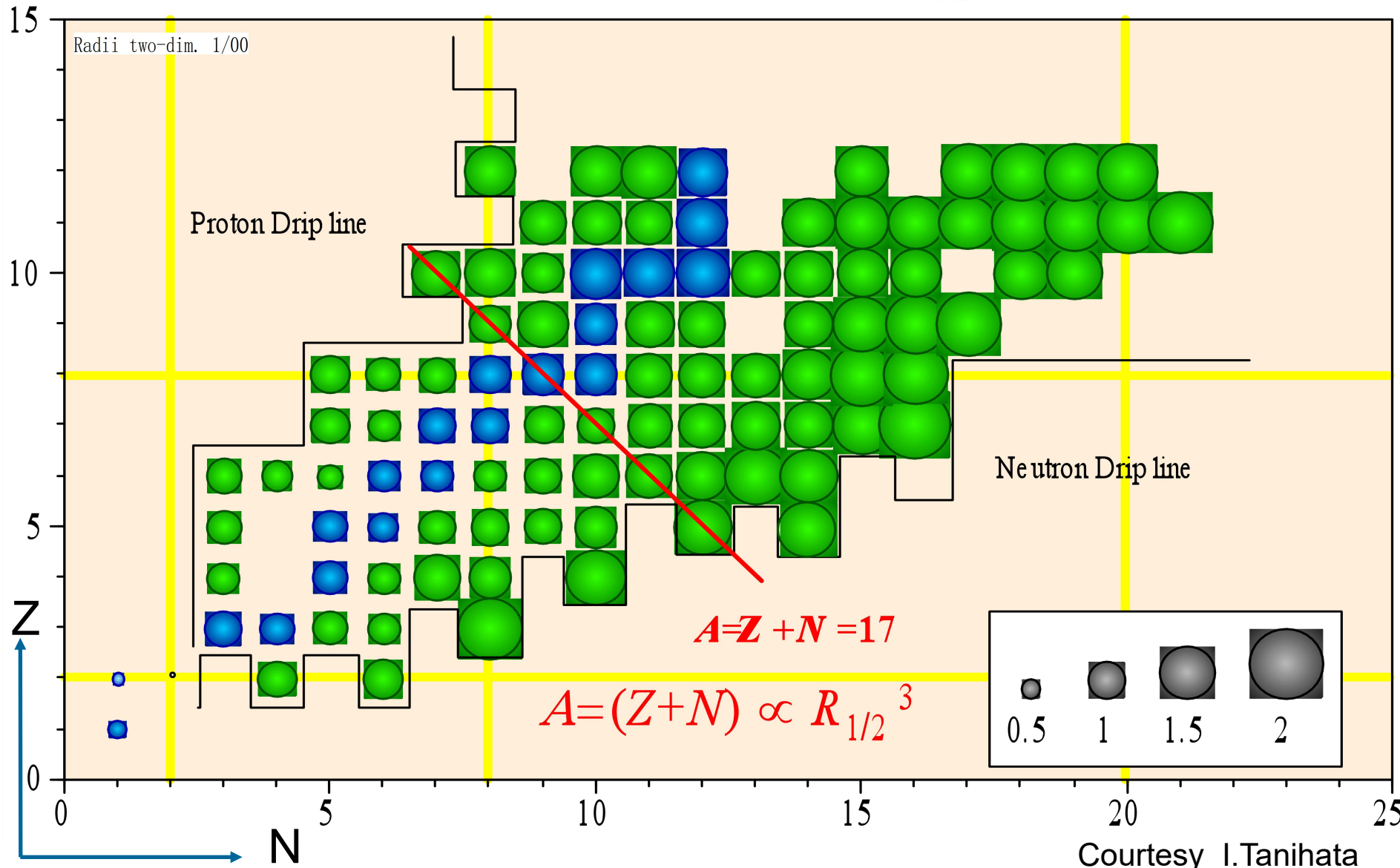


$$\text{If } R = r_0 A^{1/3} \text{ then } D(^{48}\text{Ca})/D(^{11}\text{Li}) = 2 * (48/11)^{1/3} \sim 3.2$$

RIBs: Breaking Old Rules in Nuclear Physics: is $R=r_0 A^{1/3}$?

Nuclear Radii

$(R^m_{rms} - 1.47) \text{ fm}$

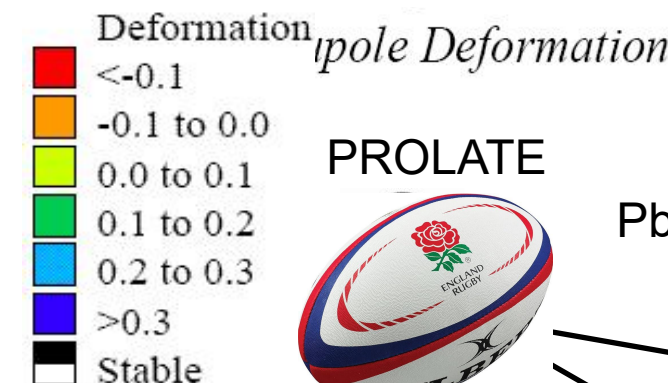


Shapes and Deformations of Atomic Nuclei

Moller Chart of Nuclides 2000

Ground state β_2 deformation

<http://ie.lbl.gov/systematics>



PROLATE



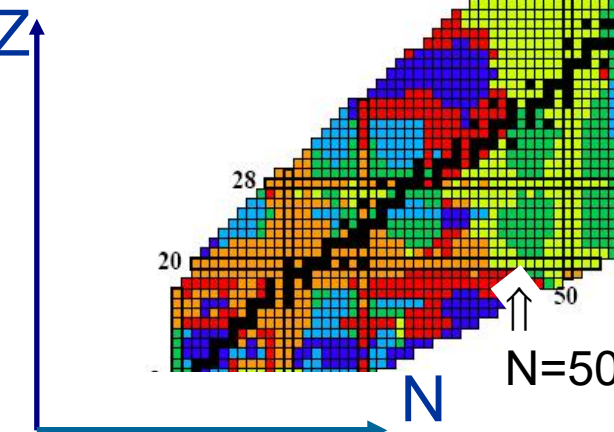
OBLATE



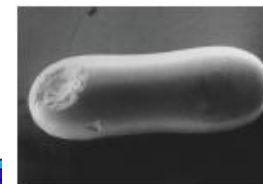
Sn (Z=50) \Rightarrow

Pb (Z=82) \Rightarrow

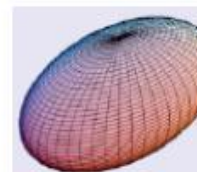
N=82



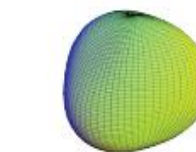
Superdeformation
Hyperdeformation



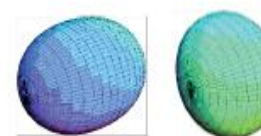
Jacobi shapes



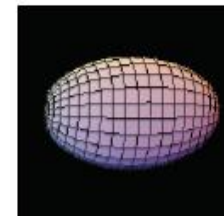
Triaxial shapes
3-dimensional rotation



Higher-order shapes
(with high-rank symmetrie)
tetrahedral, octahedral

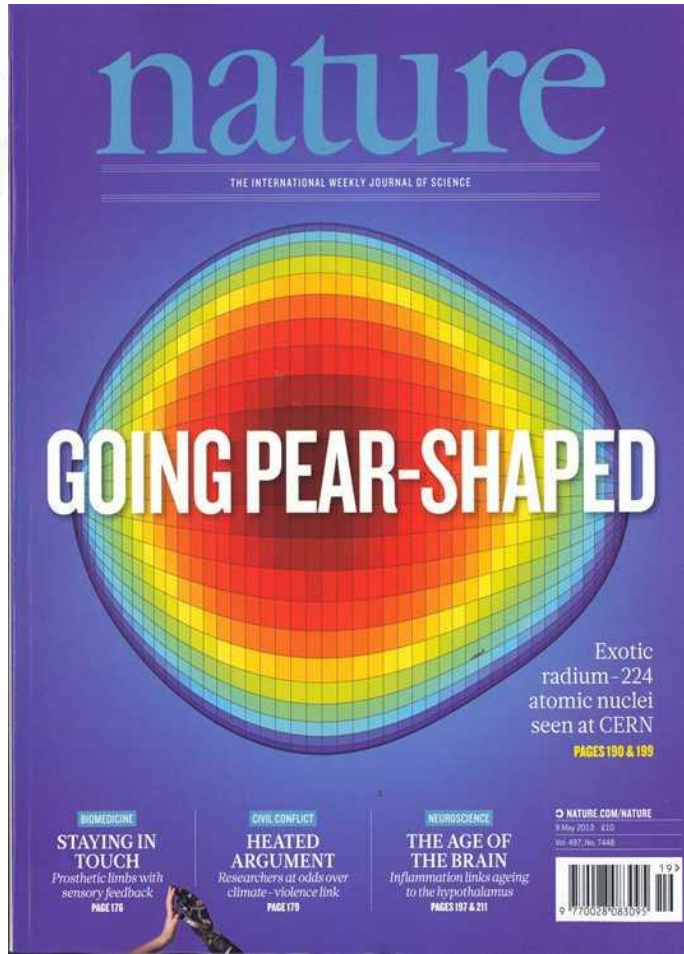


Shape coexistence



dynamic deformation
vibrations etc.

Pear-Shaped Nuclei?

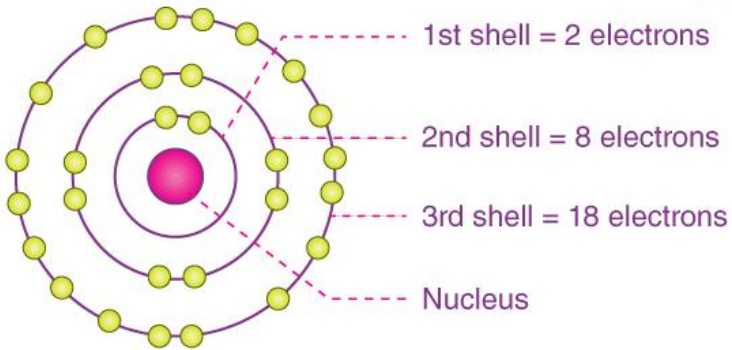


Studies of pear-shaped nuclei using accelerated radioactive beams
L. P. Gaffney et al. Nature 497, 199 (2013)

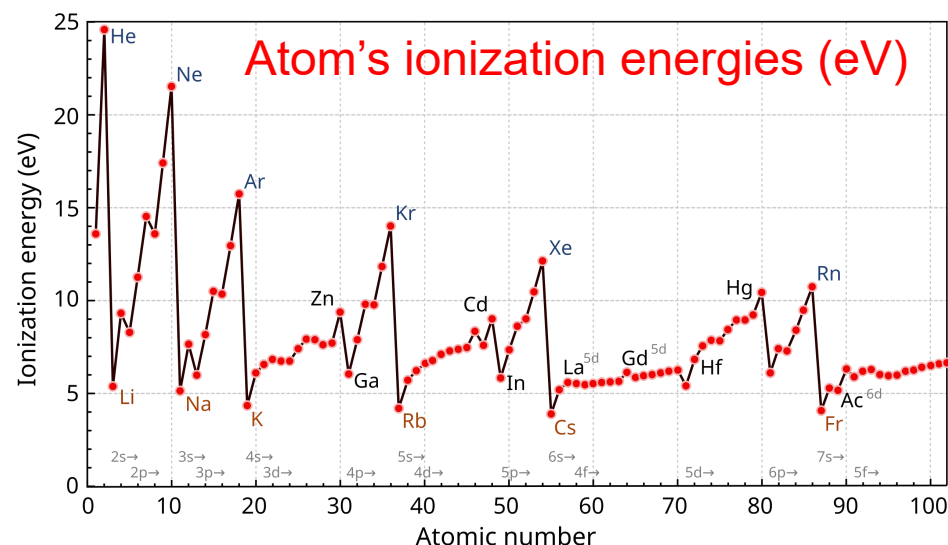
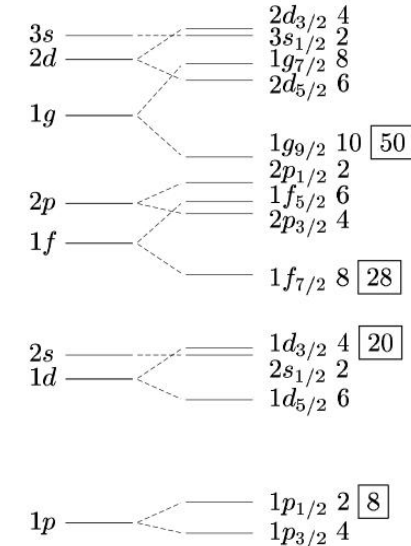
A reminder: Shell Model Structure in atoms and nuclei

Atoms: Energy scale – eV/keV's

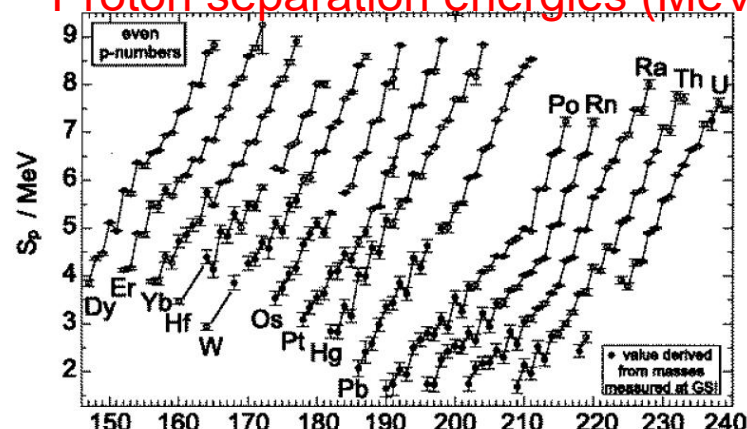
Shell structure, magic numbers 2,10,18,36...



Nuclei: Energy scale – keV's/MeV's
Magic numbers: 2,8,20,28,50,**82, 126**

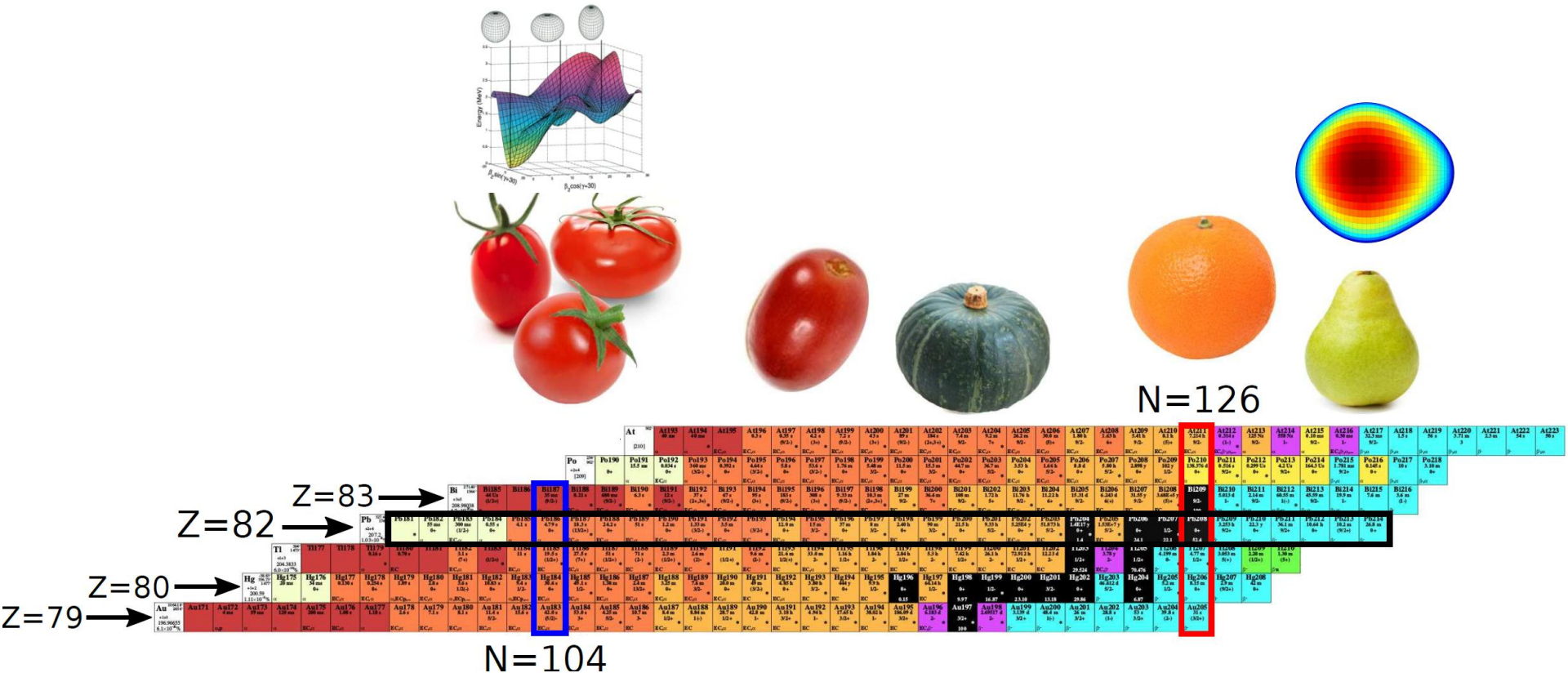


Proton separation energies (MeV)



Laser-assisted Nuclear Spectroscopy Studies in the neutron-rich Tl-Po nuclei at ISOLDE-CERN

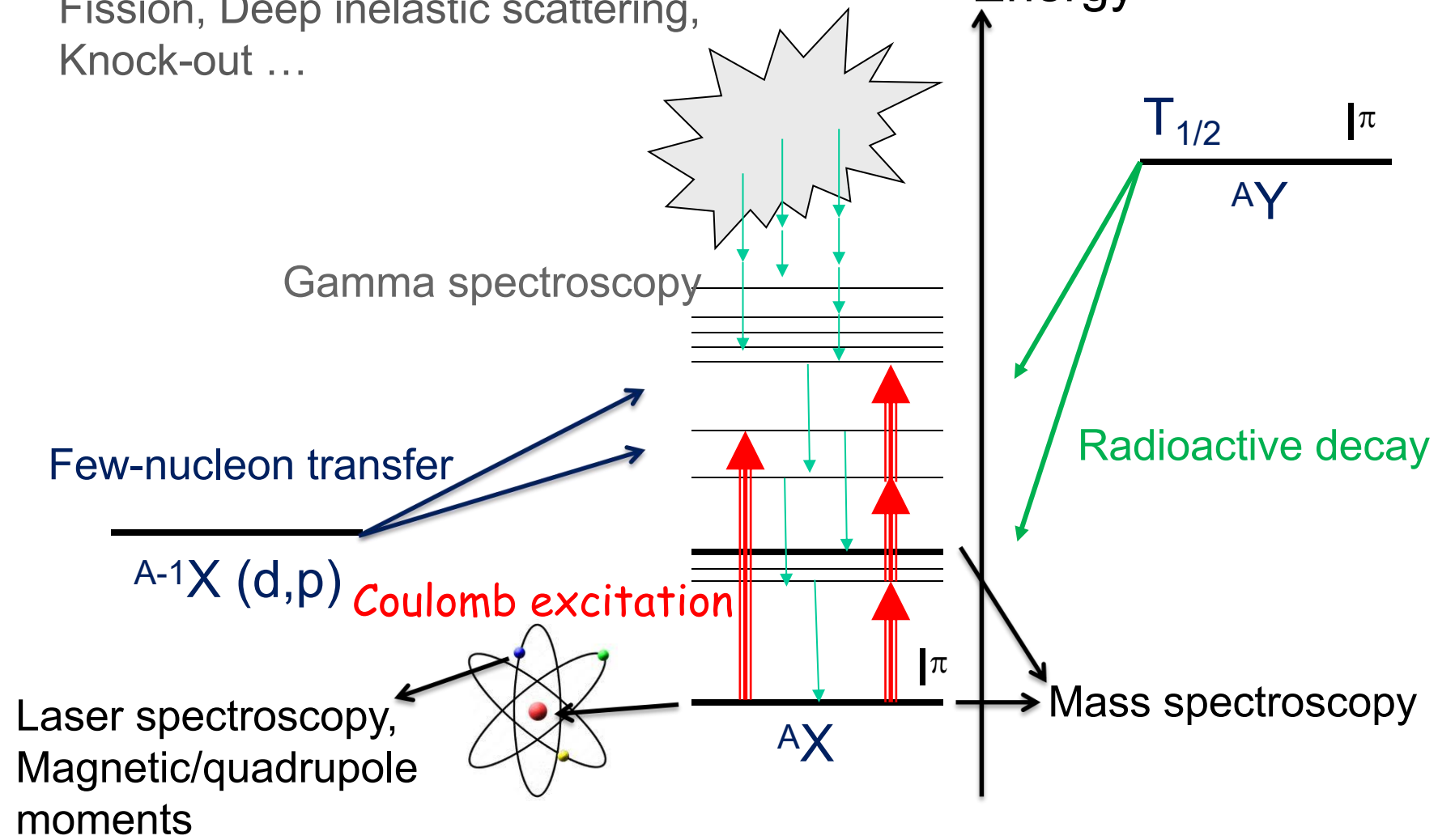
(nice physics with modern experimental nuclear and atomic techniques)



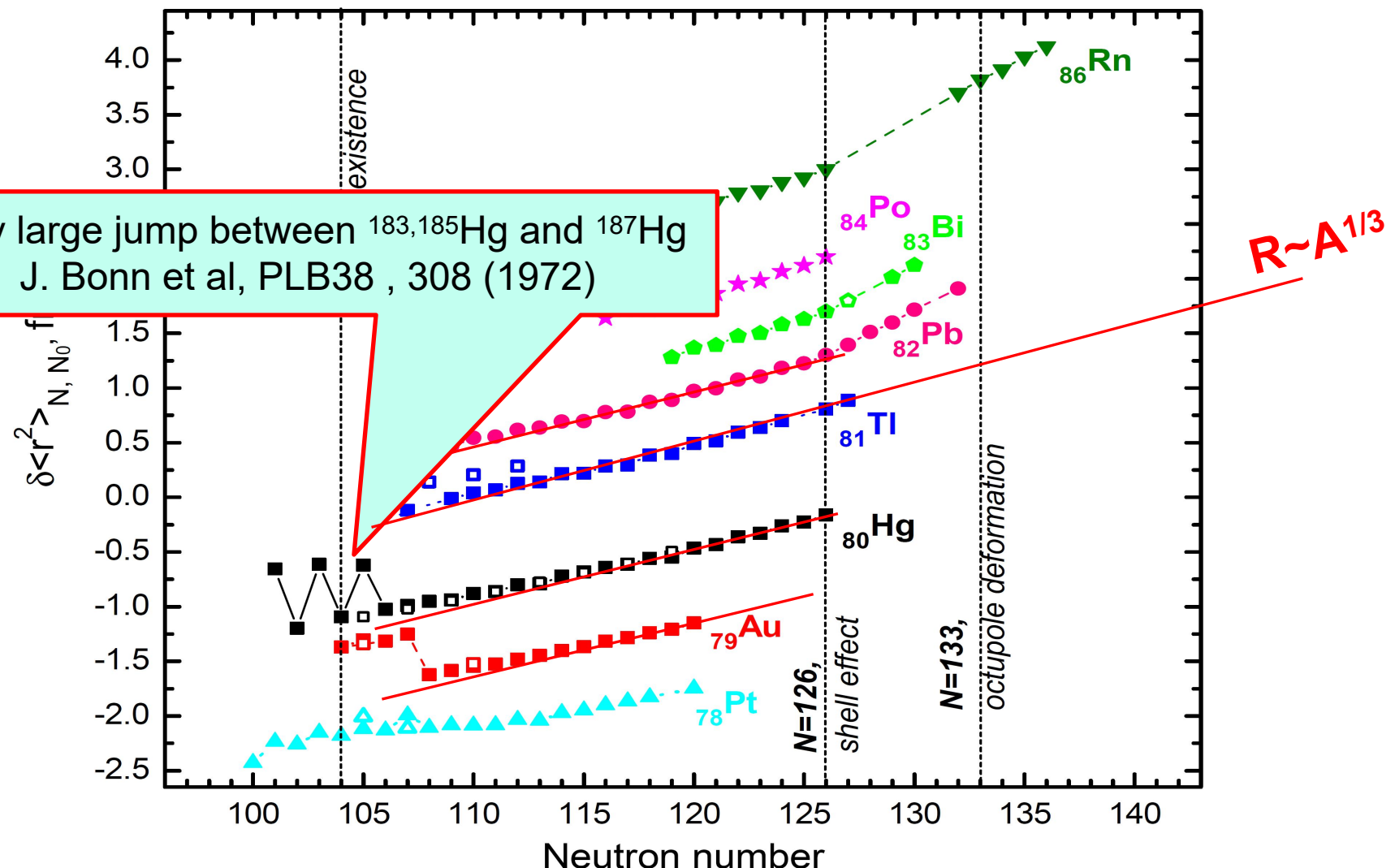
- Shape coexistence around $N \sim 104$ (coexistence of several shapes)
- **Sphericity around $N=126$, kink in radii, high-spin isomers**
- **Octupole effects around $N \sim 132$, inverse odd-even radii staggering**

Experimental Probes

Fusion evaporation, Fragmentation,
Fission, Deep inelastic scattering,
Knock-out ...

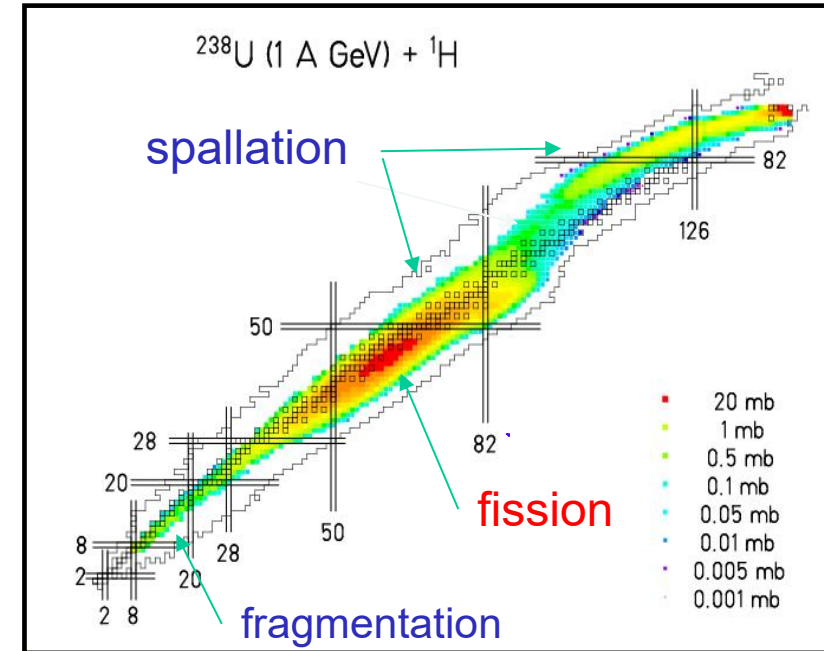
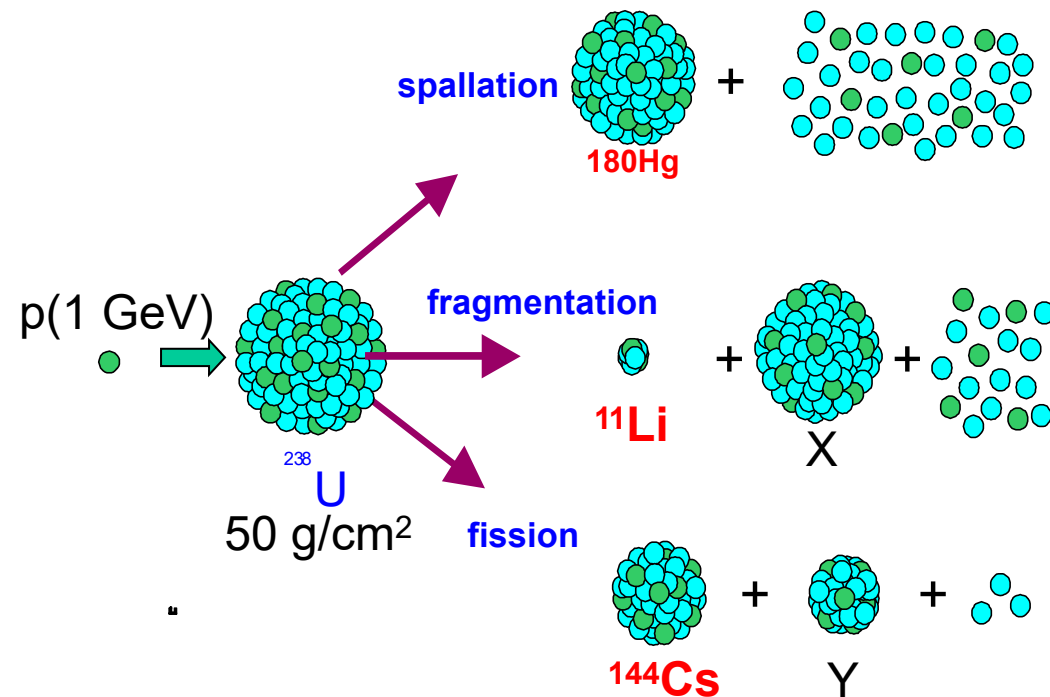


Pre-2003: Charge Radii in the Lead Region



- Shape coexistence around $N \sim 104$
- Sphericity around $N=126$, kink in radii, high-spin isomers
- Octupole effects around $N \sim 132$, inverse odd-even radii staggering

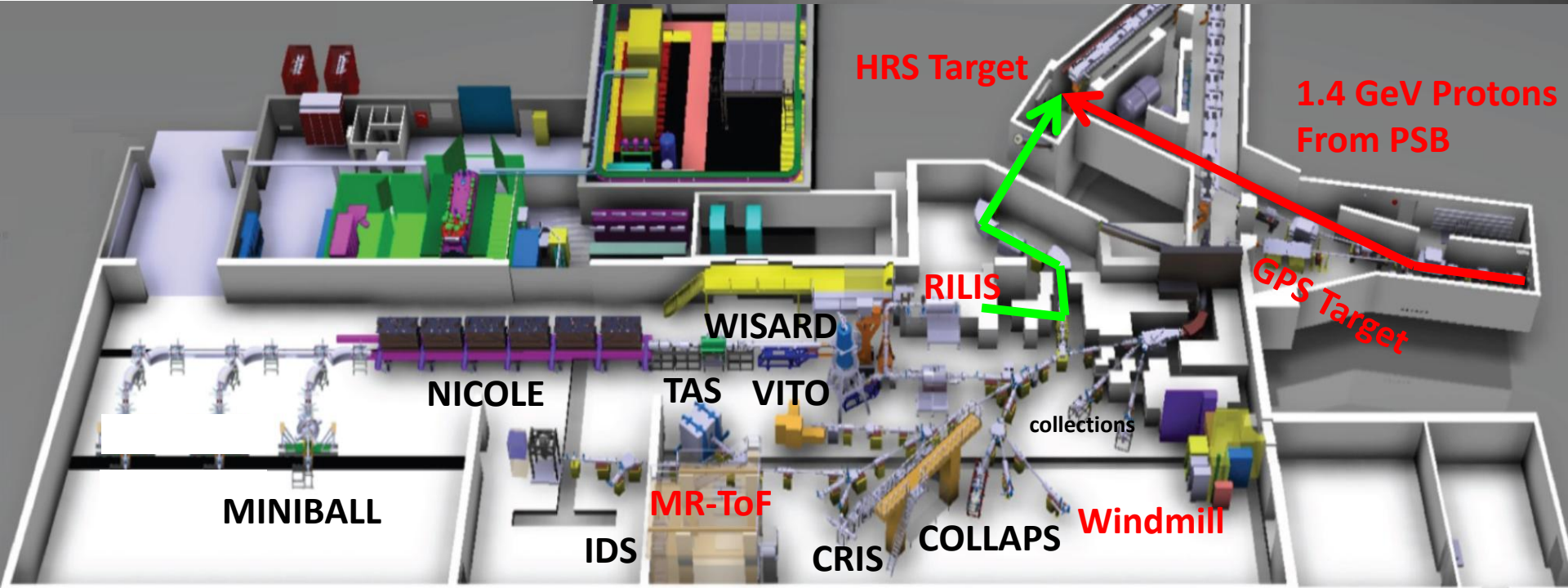
Thick Targets ISOL Method: RIBs Production Reactions at ISOLDE (CERN) induced by p(1 GeV) on a thick Uranium Target



- One can use different (lighter) targets, e.g. La, W to produce lighter elements
- **Chemically-selective** - not all elements can be extracted (e.g. refractory elements are difficult)
- Half-life limitations ($>10\text{-}20 \text{ ms}$, often $>100 \text{ ms}$), limited by diffusion through thick target
- **Hundreds of isotopes produced simultaneously, need a separator!**

Similar method is used at TRIUMF (Vancouver, Canada), they use 500 MeV protons

The ISOLDE facility at CERN



ISOLDE Facility (CERN, Geneva)

(example of a surface-ionization ion source)



ISOLDE Target Unit (with Quartz transfer line)

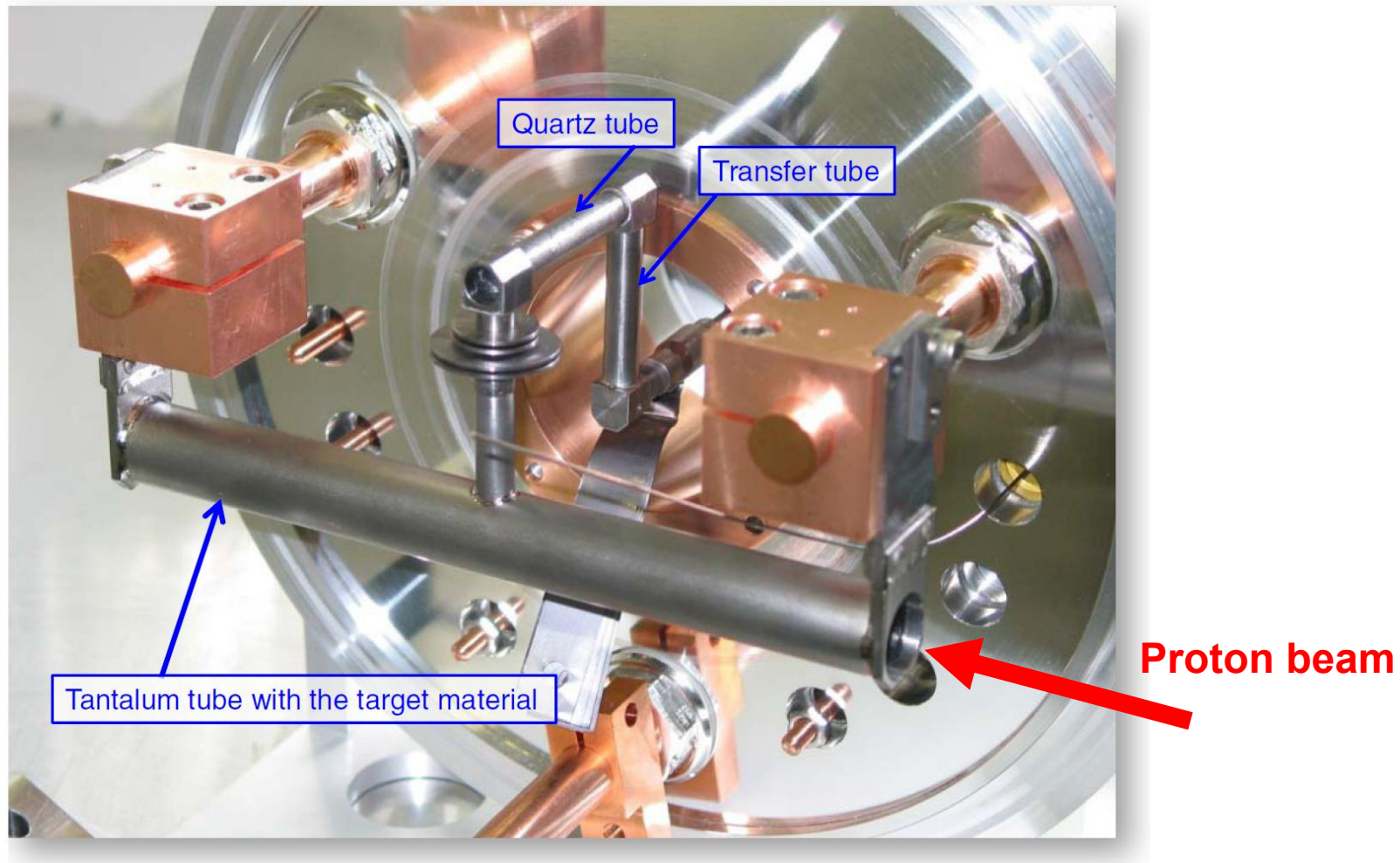
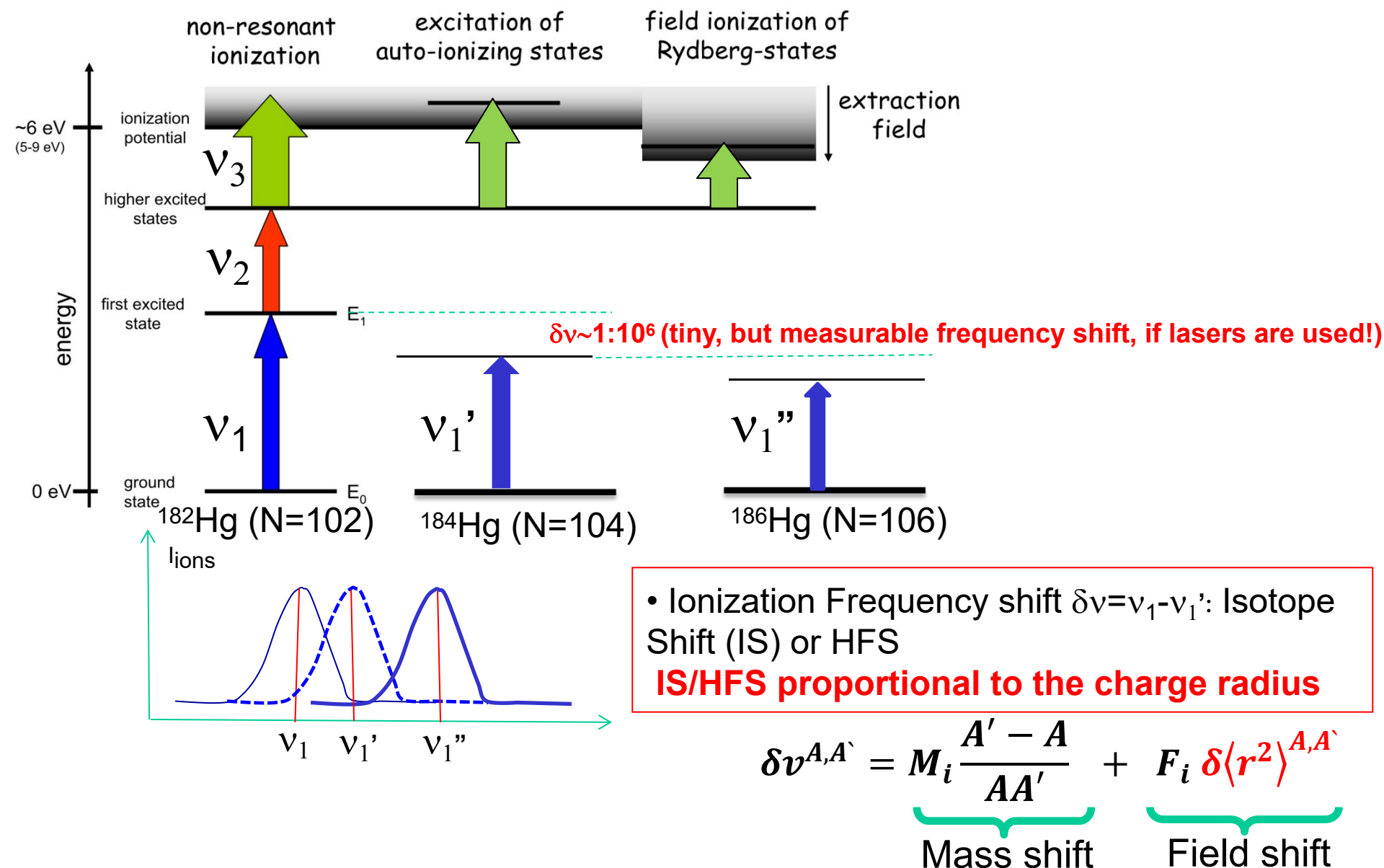


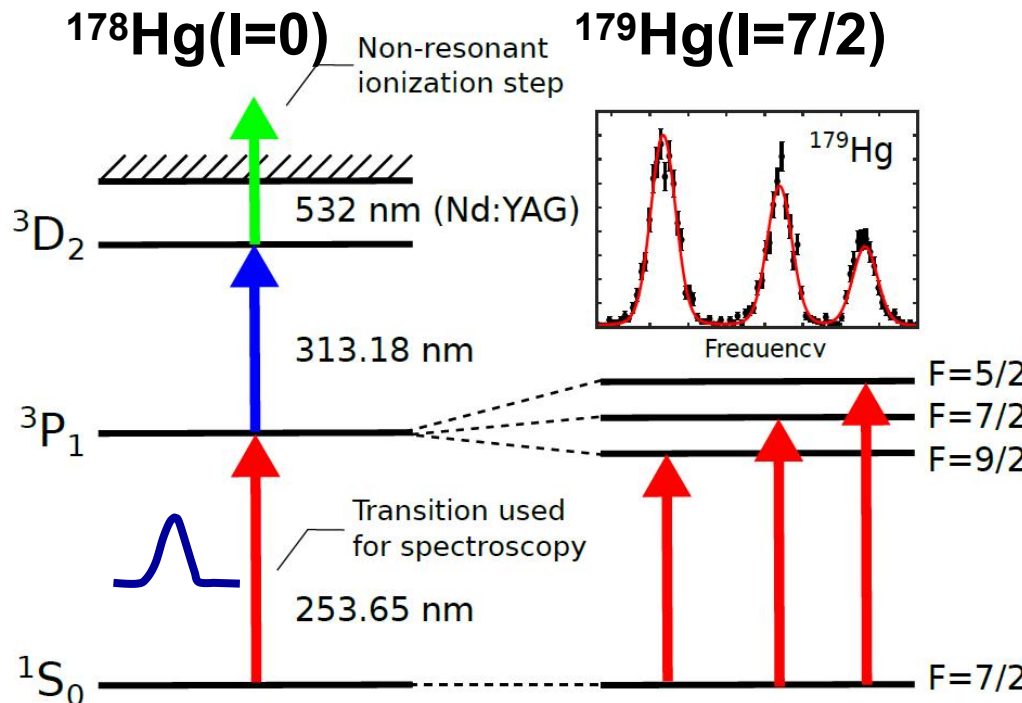
Figure 16. A photo of the ISOLDE target unit. The tantalum target container is ohmically heated. The radioactive atoms are transported to the ion source via the transfer tube. Part of the tube contains a quartz container that absorbs the rubidium atoms. This configuration was used to produce zinc beams using laser resonant ionization. Adapted from [48].

Selective Resonance Laser Spectroscopy of an atom (even-even nuclei)



Resonance Laser Spectroscopy of an odd-*A* nucleus

- A **single peak** in ‘optical/frequency’ spectra for **even-even nuclei**
- More complex in odd-*A* (odd-odd-*A*) cases, need to consider Hyperfine Splitting (HFS), due to coupling of nuclear *I* and electron spin *J*, giving a **total atomic spin $F=I+J$**
- This often results in **many peaks** in the frequency spectrum



$$F_{atom} = I_{nuclear} + J_{electron}$$

$$\Delta F = 0, \pm 1$$

$$\Delta\nu^F = A \frac{C}{2} + B \frac{\frac{3}{4}C(C+1) - I(I+1)J(J+1)}{2(2I-1)(2J-1)IJ}$$

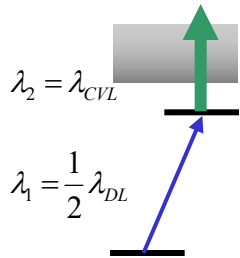
$$A = \frac{\mu_I B_e(0)}{IJ}$$

$$B = eQ_s \frac{\partial^2 V}{\partial^2 z}$$

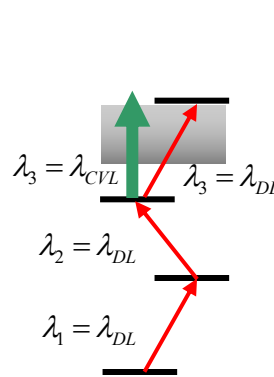
The method allows to deduce magnetic (μ) and quadrupole (Q_s) momenta of the nucleus!

Schemes of Atomic Resonance Ionization used with Cu-Vapor Laser

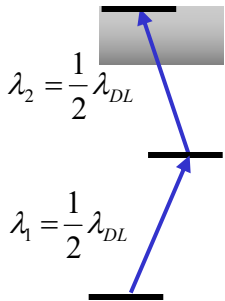
Available lasers: visible light, 2-3 eV photon energy: need multi-step ionisation!



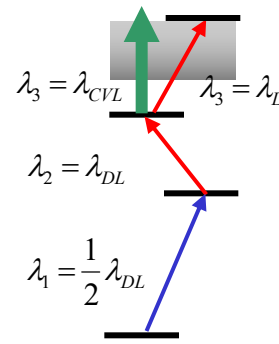
Al (5.99 eV)
Ca (6.11 eV)
Ga (6.00 eV)
In (5.79 eV)
Tl (6.11 eV)



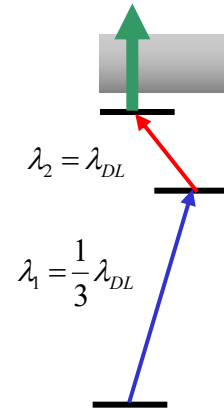
Cu (7.73 eV)



Li (5.39 eV)
Na (5.14 eV)
Sr (5.69 eV)
Ce (5.54 eV)
Nd (5.52 eV)
Sm (5.64 eV)
Eu (5.67 eV)
Gd (6.15 eV)
Tb (5.86 eV)
Ho (6.02 eV)
Tm (6.18 eV)
Yb (6.25 eV)
Lu (5.43 eV)
Actinides... (at Mainz)



Mg (7.65 eV)
Mn (7.43 eV)
Co (7.86 eV)
Ni (7.64 eV)
Cu (7.73 eV)
Y (6.22 eV)
Ag (7.58 eV)
Tc (7.28 eV)
Sn (7.34 eV)
Pb (7.42 eV)
Bi (7.29 eV)

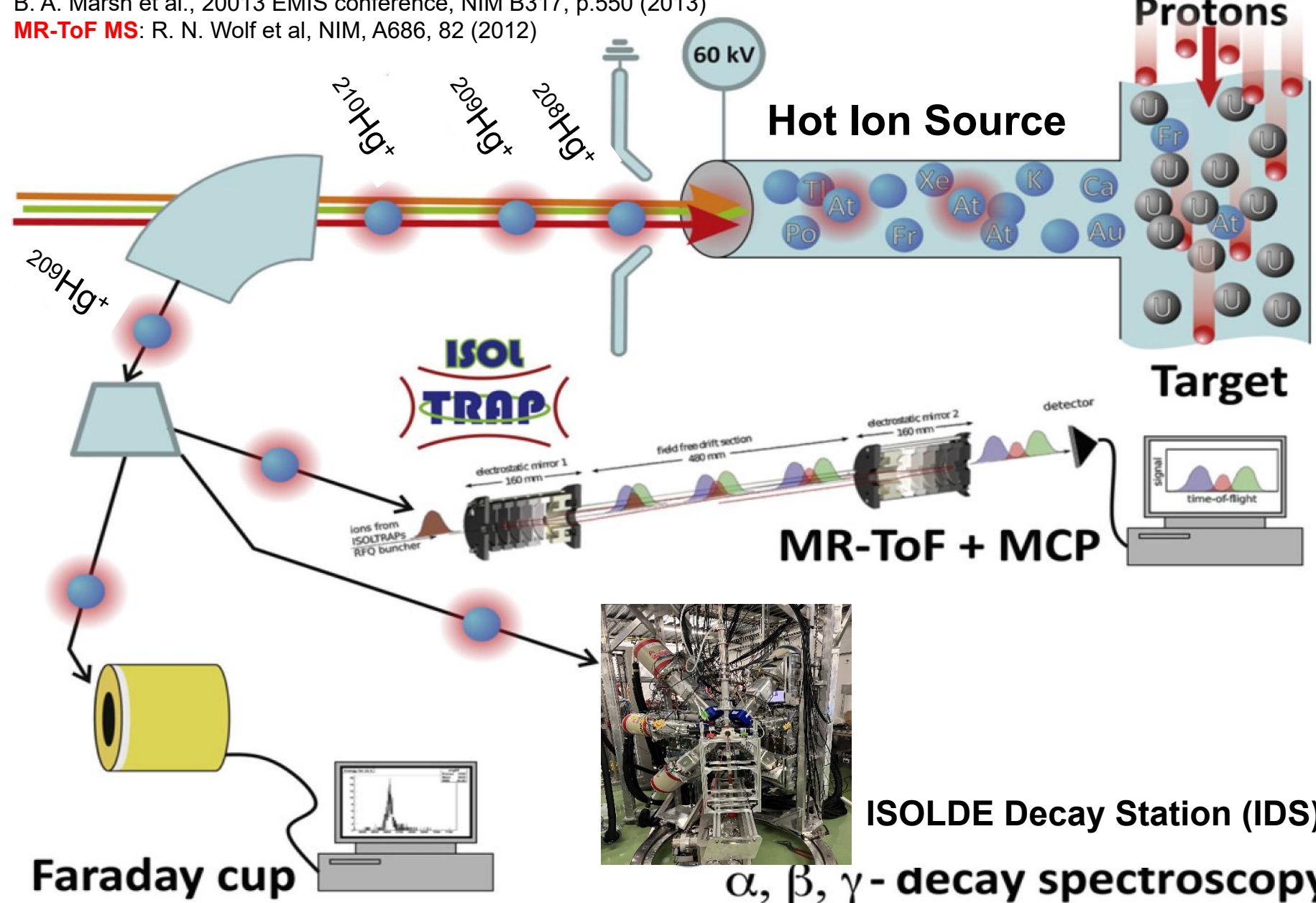


Be (9.32 eV)

Our tools for in-source Laser Spectroscopy at ISOLDE

B. A. Marsh et al., 20013 EMIS conference, NIM B317, p.550 (2013)

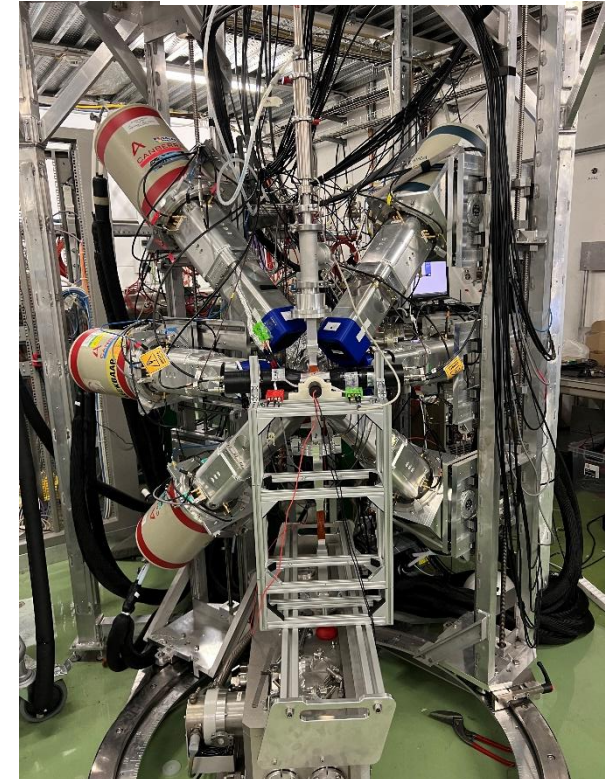
MR-ToF MS: R. N. Wolf et al, NIM, A686, 82 (2012)



ISOLDE Decay Station

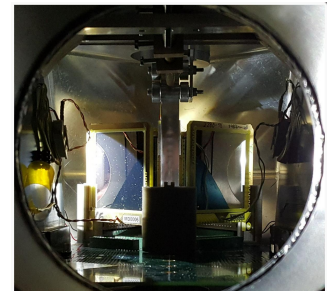
<https://isolde-ids.web.cern.ch/>

- Collaboration of 14 institutes worldwide (Further collaborations are welcome)
- IDS fame can hold up to 15 clovers on 5 gantries



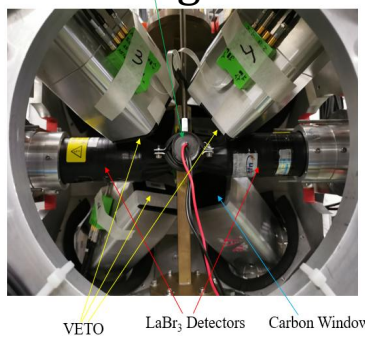
Zoo of IDS detectors

alpha



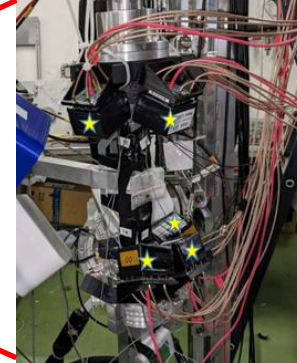
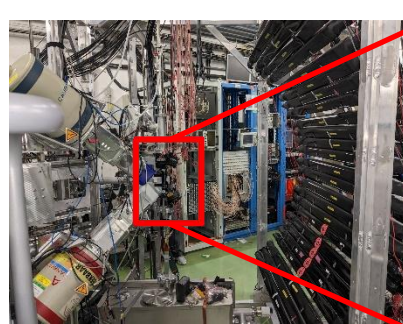
DSSDs and Si
PADs

Beta-gamma

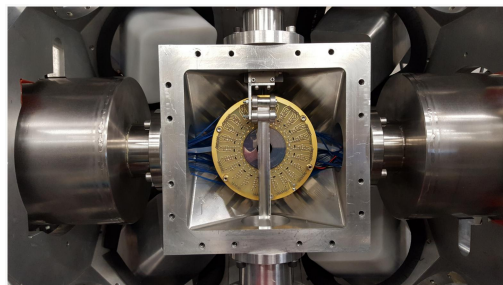


Fast-timing (LaBr₃;
beta scintillator;
clovers)

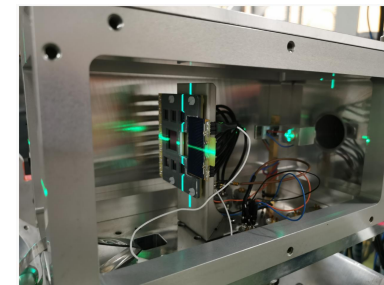
Neutrons



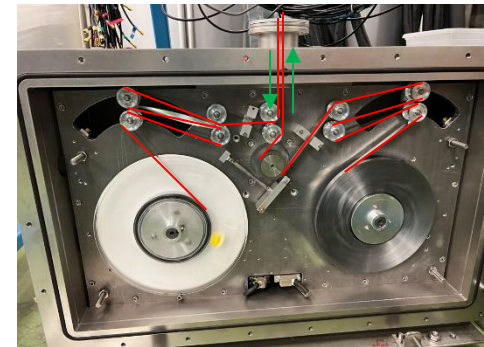
Annular Si with Tape



SPEDE



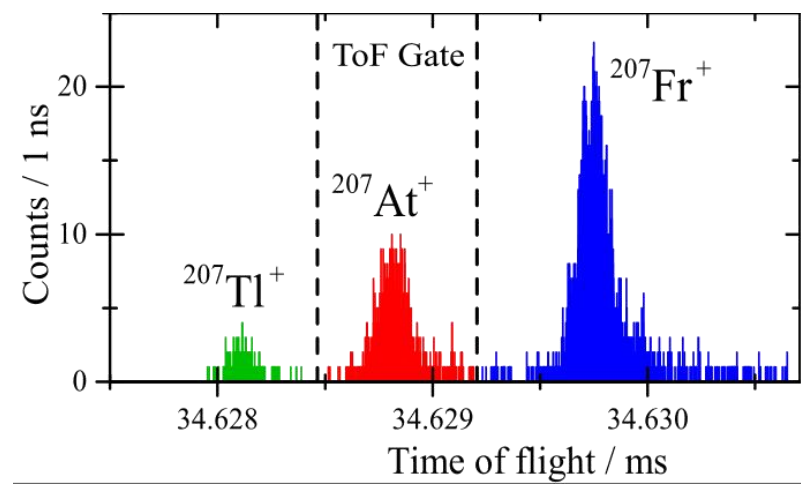
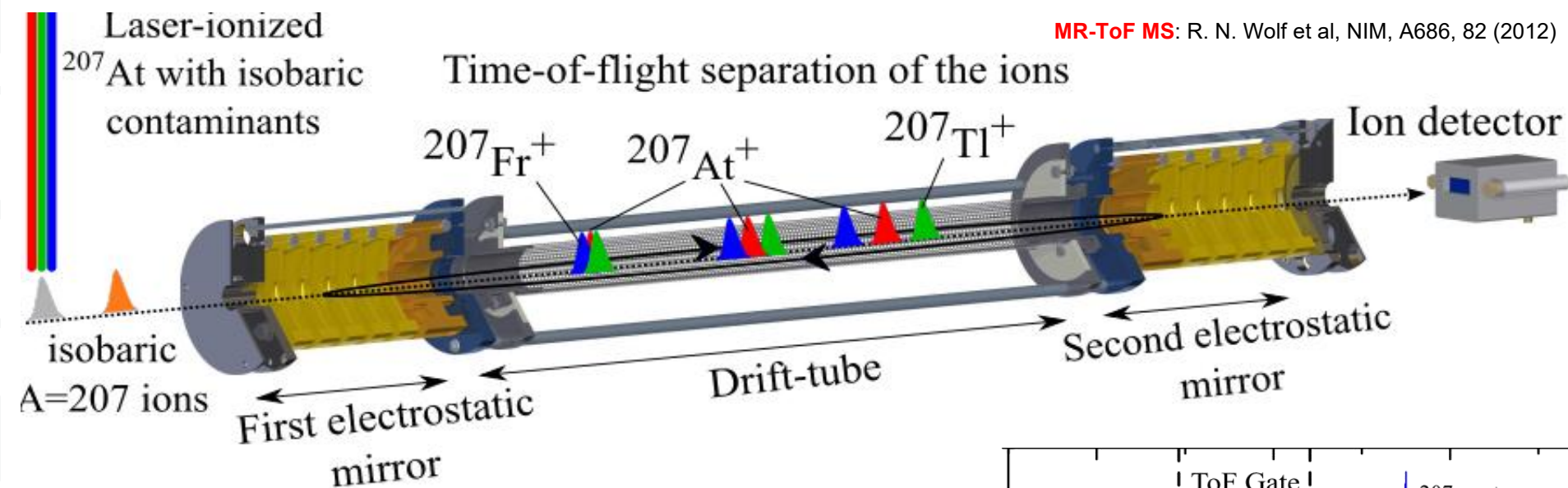
Si pins and Solar cell



Tape station

Multi-Reflection Time-of-Flight (MR-ToF) Spectrometer for HFS studies and mass measurements

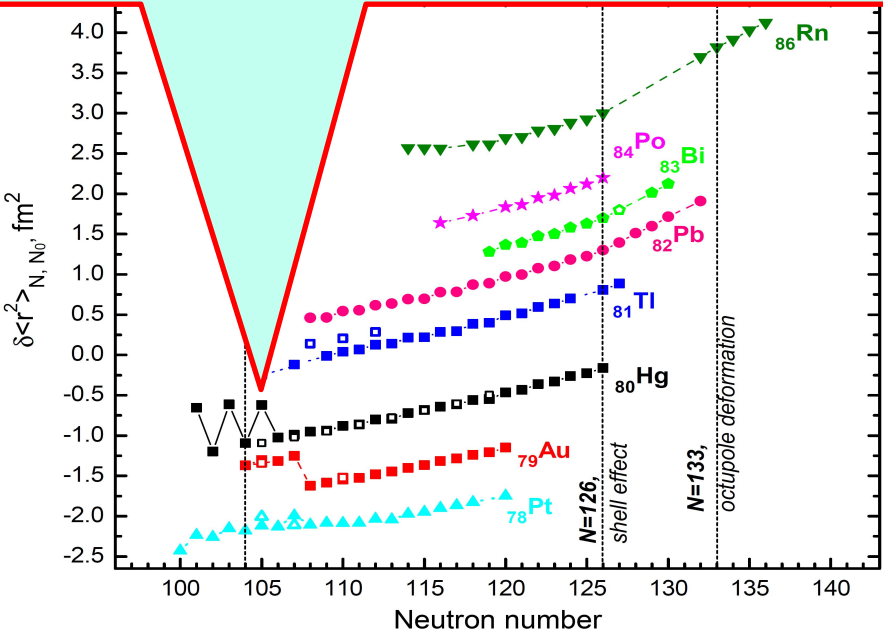
- The IDS technique requires **waiting for the decay** of the isotope. Not practical for long-lived or stable isotopes.
- Alternative – to **use ‘counting’ ions** (instead of waiting for decay)



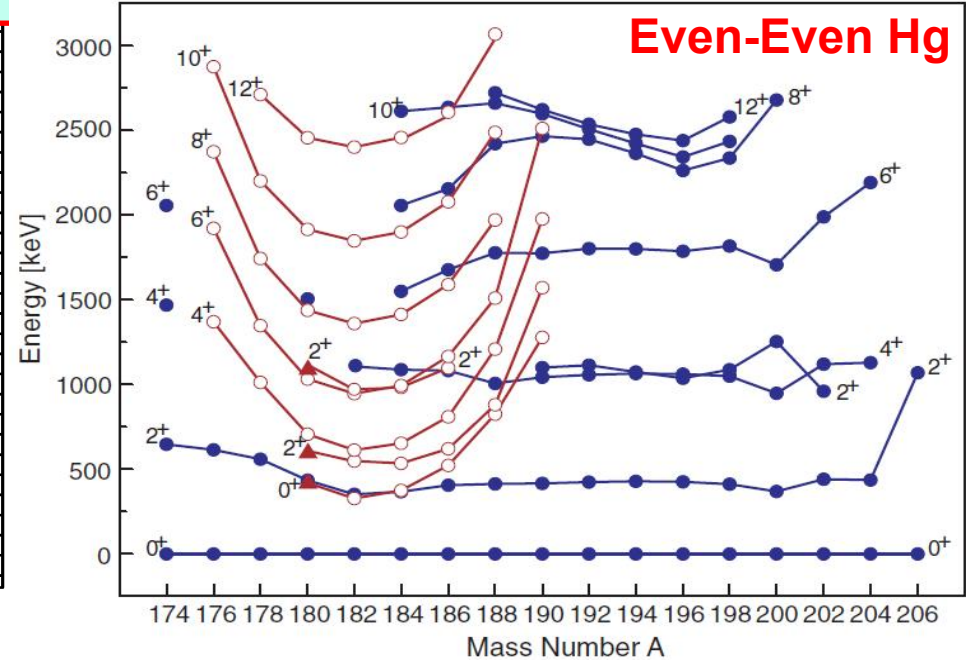
Example for neutron-deficient Hg isotopes (or, what happens after shape staggering in $^{181-185}\text{Hg}$?)

Large IS between $^{183,185}\text{Hg}$ and ^{187}Hg

J. Bonn et al, PLB38, 308 (1972)



R. Julin, K. Helariutta, M. Muikku, J. Phys. G 27 (2001)



Previous Hg radii data (ISOLDE)

$^{183,185,187,199,201}\text{Hg}$: J. Bonn et al, PLB38, 308 (1972)

$^{181-191}\text{Hg}$: J. Bonn et al., ZPhys A 276, 203 (1976)

$^{182-198}\text{Hg}$: G. Ulm Z. Phys. A 325, 247 259 (1986)

Note: gs of $^{182,184,186}\text{Hg}$ – weakly oblate

In-beam Hg data - examples (RDT, plunger, Coulex)

$^{184,186}\text{Hg}$; L.P. Gaffney LP et al. PRC89 024307(2014)

^{172}Hg : M. Sandzelius et al, PRC79, 064315 (2009)

^{175}Hg : D. O'Donnell et al., PRC79, 051304(2009)

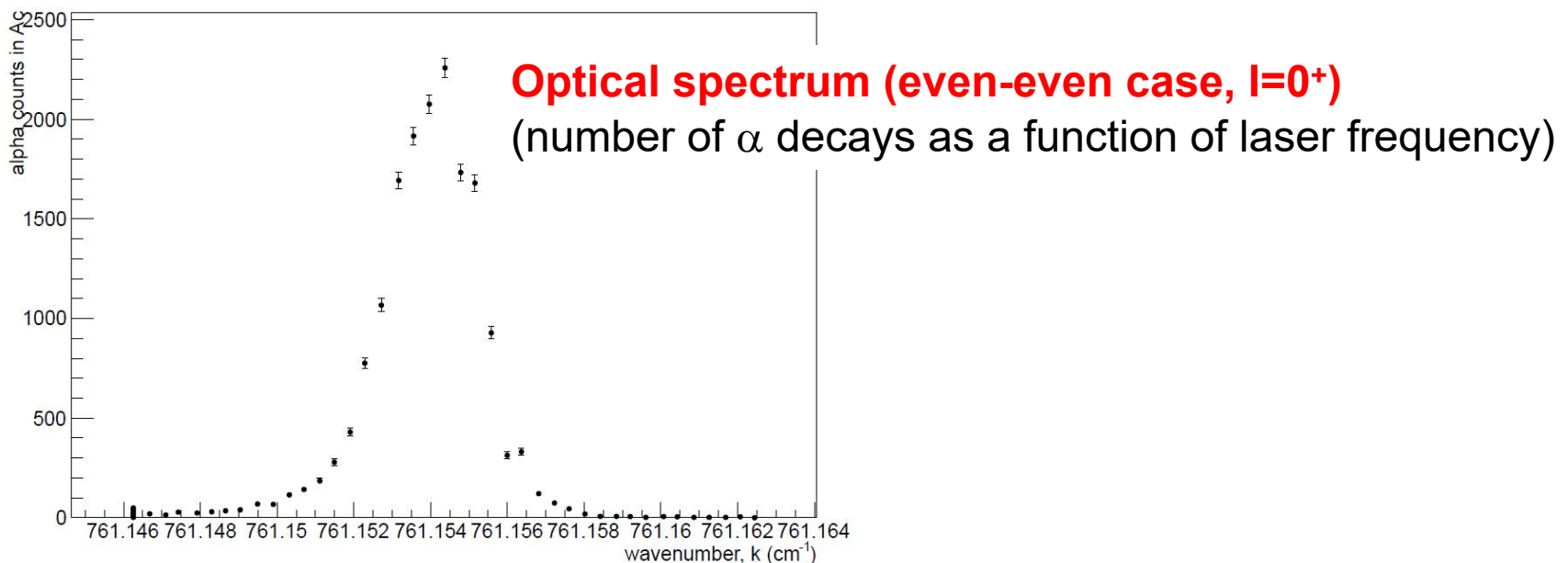
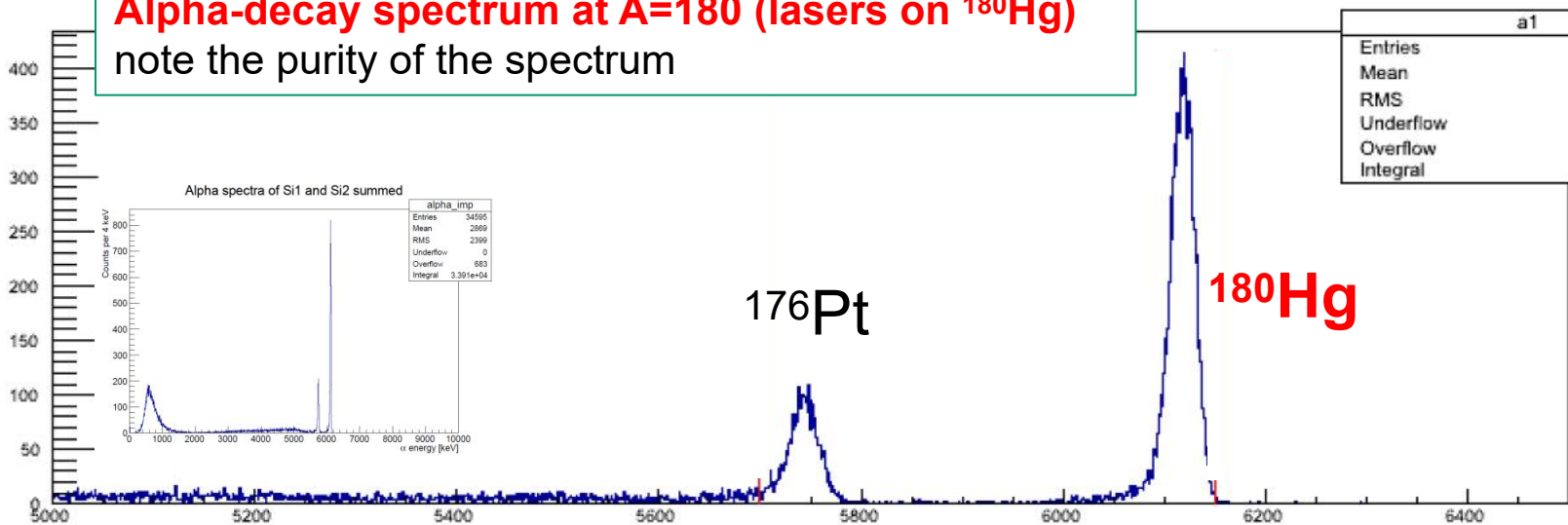
$^{176,178}\text{Hg}$: M. P. Carpenter et al, PRL78, 3650(1997)

^{176}Hg : M. Muikku et al, PRC58, 3033 (1998)

$^{180,182}\text{Hg}$: T. Grahm et al, PRC80, 014324 (2009)

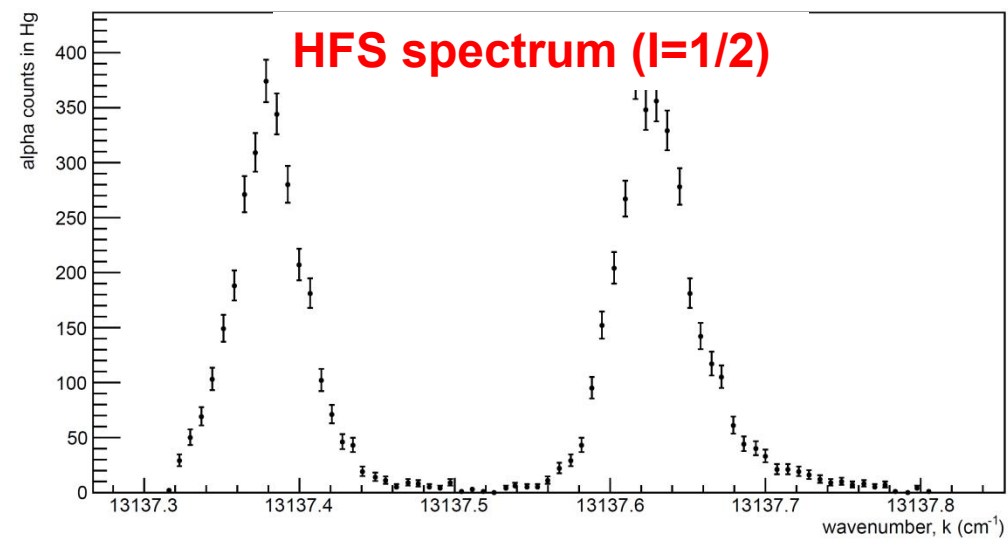
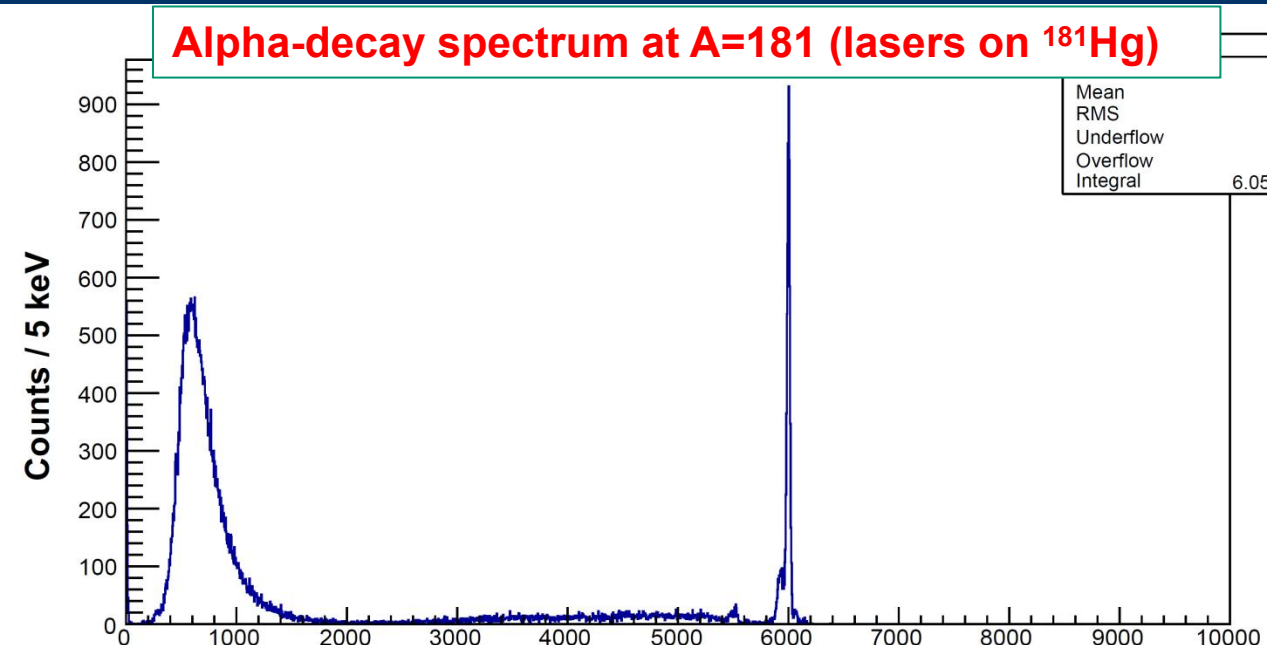
^{180}Hg

Alpha-decay spectrum at A=180 (lasers on ^{180}Hg)
note the purity of the spectrum

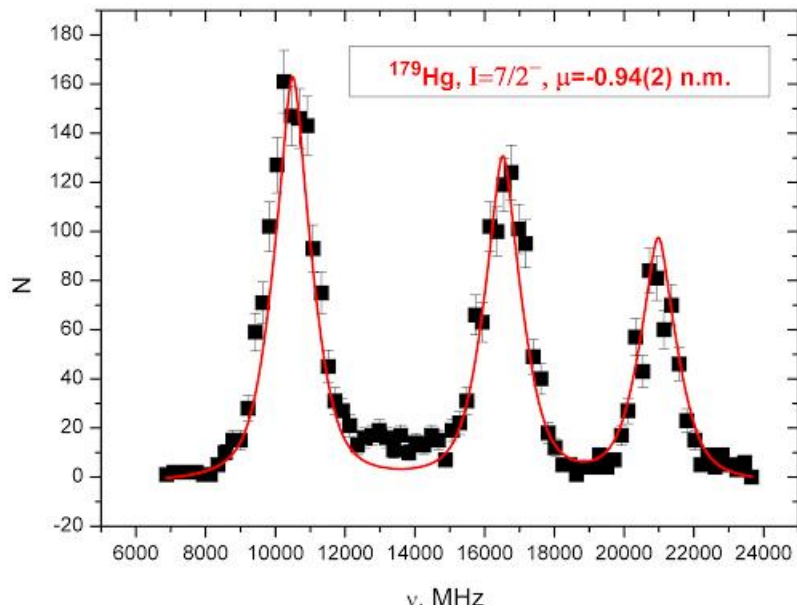


^{181}Hg

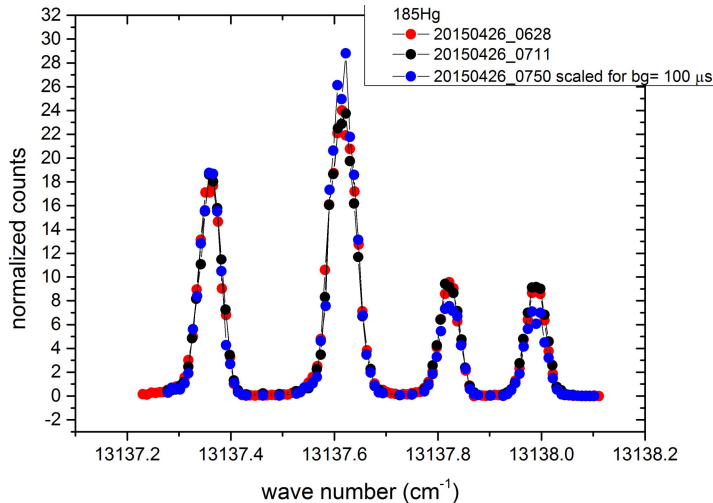
Alpha-decay spectrum at A=181 (lasers on ^{181}Hg)



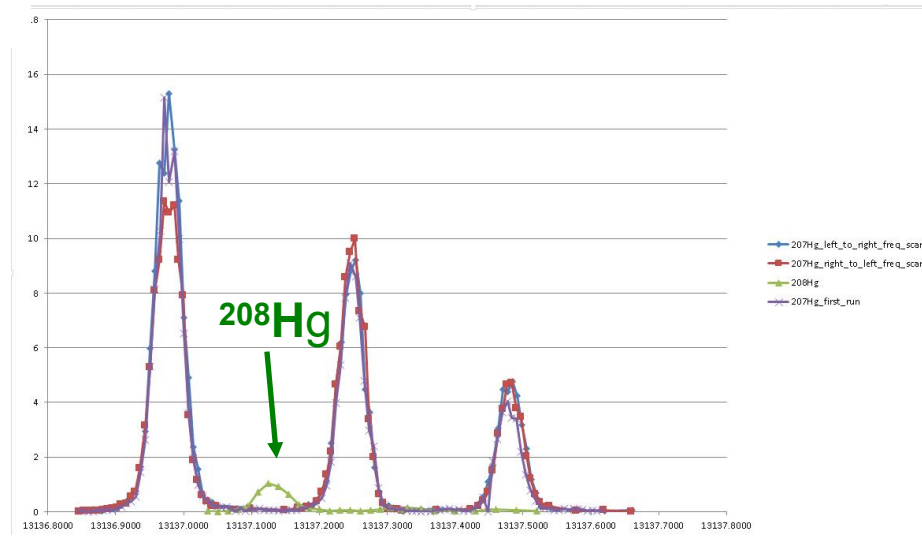
$^{179,185,207,208}\text{Hg}$



^{185}Hg HFS spectrum@MR-ToF, gs+is

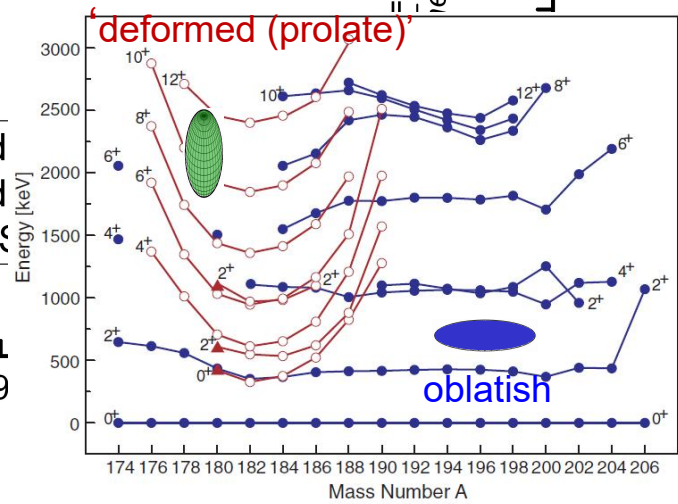
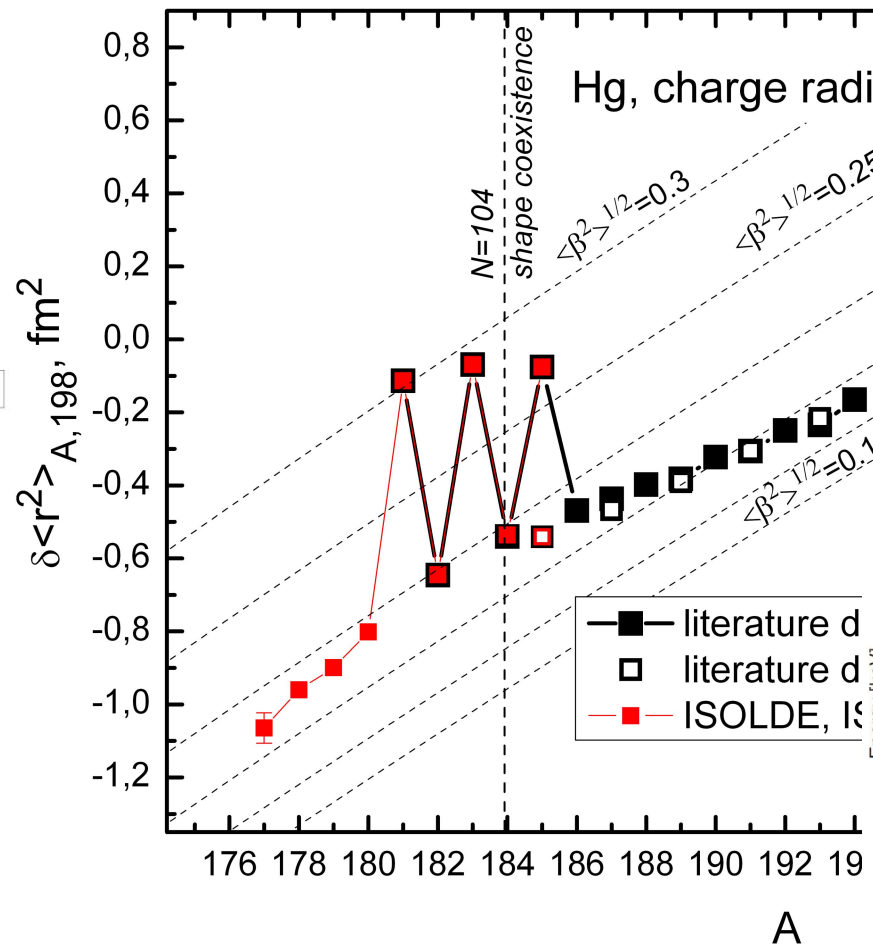
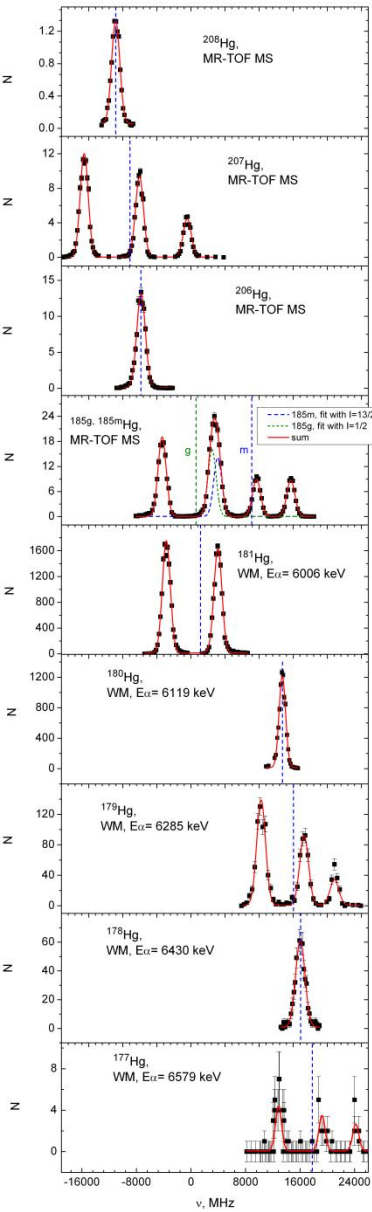


Isotopes with N>126
 ^{207}Hg HFS spectra@MR-ToF, $I=9/2$
 also $^{208}\text{Hg}!$ $I=0$



HFS spectra and Charge radii for Hg isotopes

B.A. Marsh et al., Nature Physics, 1745-2481 (2018)



181,183,185Hg- confirmation of earlier data on staggering for $\frac{1}{2}^-$ gs
177,178,179,180Hg (new) – trend towards sphericity
207,208Hg (new): kink beyond N=126

One for the funding
councils →

B.A. Marsh *et al.*, Nature Physics, 1745-2481 (2018)
Characterization of the shape-staggering effect in mercury nuclei

B.A. Marsh^{1*}, T.Day Goodacre^{1,2,18}, S.Sels^{1,3,18}, Y.Tsunoda⁴, B.Andel^{1,5}, A.N.Andreyev^{6,7}, N.A.Alhubiti², D.Atanasov⁸, A.E.Barzakh⁹, J.Billowes², K.Blaum⁸, T.E.Cocolios^{2,3}, J.G.Cubiss^{1,6}, J.Dobaczewski⁶, G.J.Farooq-Smith^{2,3}, D.V.Fedorov^{1,9}, V.N.Fedosseev¹, K.T.Flanagan², L.P.Gaffney^{1,3,10}, L.Ghys³, M.Huyse³, S.Kreim⁸, D.Lunney¹¹, K.M.Lynch¹, V.Manea⁸, Y.Martinez Palenzuela³, P.L.Molkanov⁹, T.Otsuka^{3,4,12,13,14}, A.Pastore⁶, M.Rosenbusch^{13,15}, R.E.Rossel¹, S.Rothe^{1,2}, L.Schweikhard¹⁵, M.D.Seliverstov⁹, P.Spagniotti¹⁰, C.Van Beveren³, P.Van Duppen³, M.Veinhard¹, E.Verstraelen³, A.Welker¹⁶, K.Wendt¹⁷, F.Wienholtz¹⁵, R.N.Wolf⁸, A.Zadvornaya³ and K.Zuber¹⁶

S. Sels *et al.*, Phys. Rev. C 99, 044306 (2019)

Shape staggering of mid-shell mercury isotopes from in-source laser spectroscopy compared with Density Functional Theory and Monte Carlo Shell Model calculations

S. Sels,^{1,*} T. Day Goodacre,^{2,3} B. A. Marsh,³ A. Pastore,⁴ W. Ryssens,⁵ Y. Tsunoda,⁶ N. Alhubiti,² B. Andel,⁷ A. N. Andreyev,^{4,8} D. Atanasov,⁹ A. E. Barzakh,¹⁰ M. Bender,⁵ J. Billowes,² K. Blaum,⁹ T. E. Cocolios,¹ J. G. Cubiss,⁴ J. Dobaczewski,^{4,11} G. Farooq-Smith,¹ D. V. Fedorov,¹⁰ V. N. Fedosseev,³ K. T. Flanagan,² L. P. Gaffney,^{12,1} L. Ghys,^{13,1} P-H. Heenen,¹⁴ M. Huyse,¹ S. Kreim,⁹ D. Lunney,¹⁵ K. M. Lynch,³ V. Manea,⁹ Y. Martinez Palenzuela,¹ T. M. Medonca,³ P. L. Molkanov,¹⁰ T. Otsuka,^{6,16,1} J. P. Ramos,^{3,17} R. E. Rossel,¹ S. Rothe,³ L. Schweikhard,¹⁹ M. D. Seliverstov,¹⁰ P. Spagniotti,¹² C. Van Beveren,¹ P. Van Duppen,¹ M. Veinhard,³ E. Verstraelen,¹ A. Welker,²⁰ K. Wendt,¹⁸ F. Wienholtz,¹⁹ R.N. Wolf,⁹ and A. Zadvornaya¹

One with the
interesting work in →

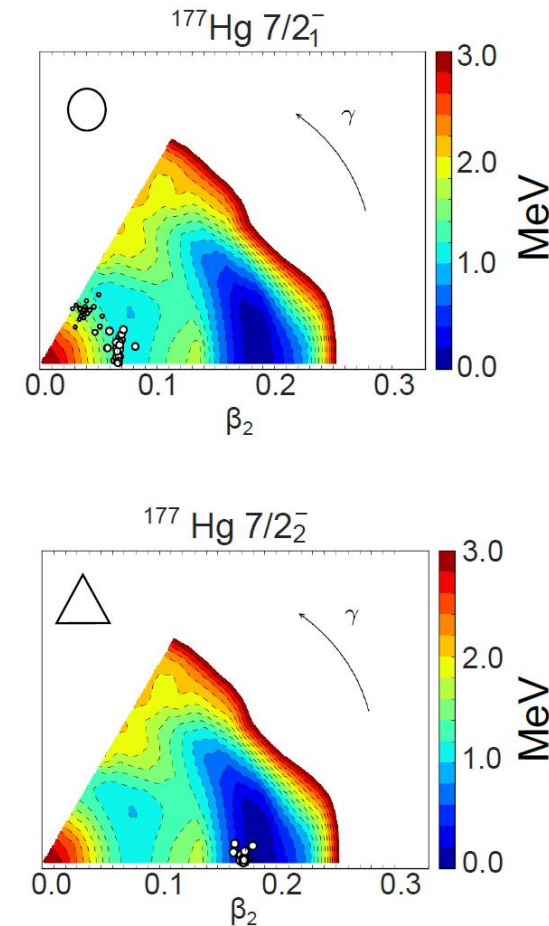
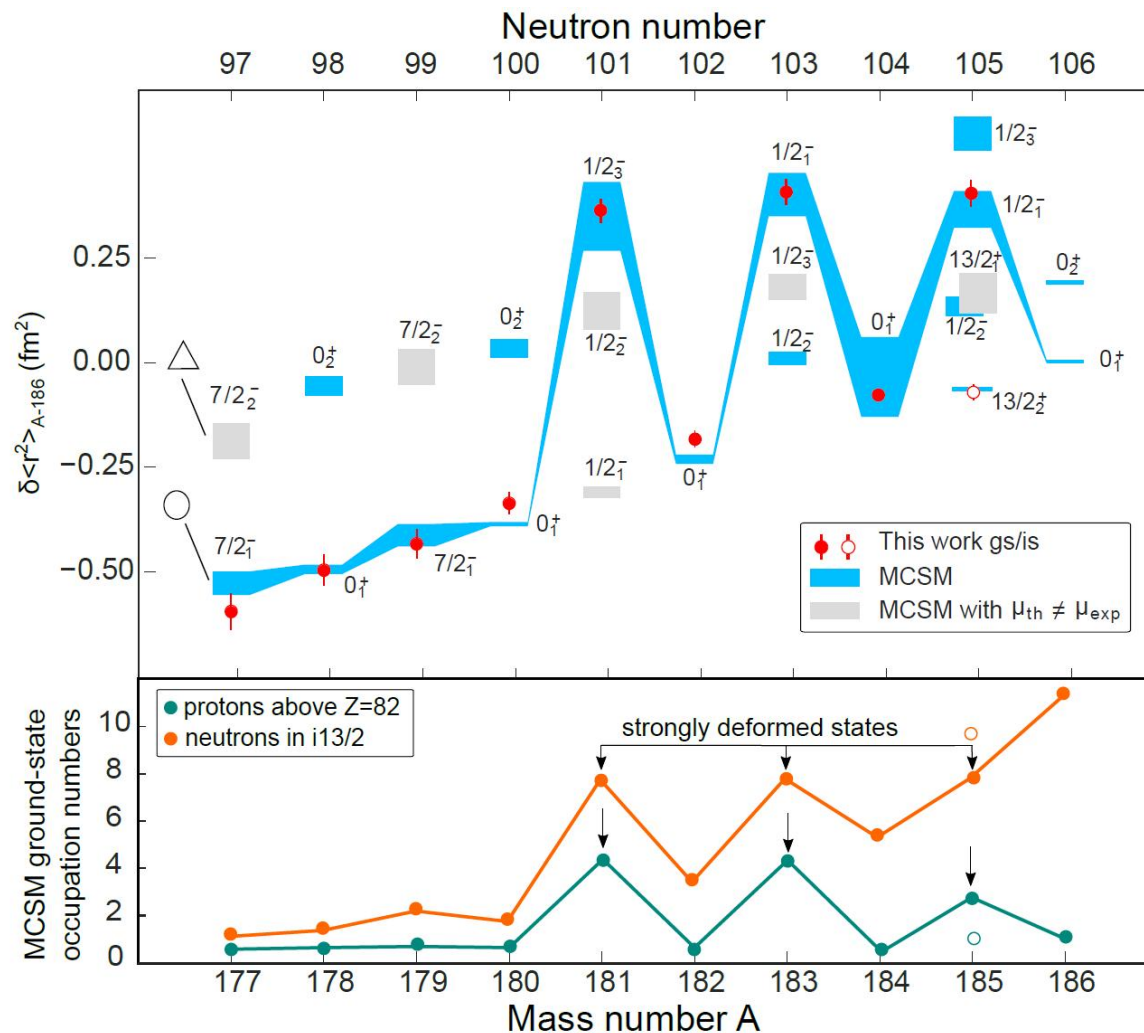
N>126 region : T. Day Goodacre *et al.*, PRL 126, 032502 (2021)
T. Day Goodacre *et al.*, PRC 104, 054322 (2021)

MCSM for Hg isotopes (Y. Tsunoda, T.Otsuka et al)

(B. Marsh et al, Nature Physics, Oct 2018)

Performed by Takaharu Otsuka's team

- Largest calculation of its kind, avoids diagonalization of $>2 \times 10^{42}$ -dimensional H matrix
- Radii are well reproduced.
- Results show an increase of >2 protons promoted into the $h9/2$ intruder state.

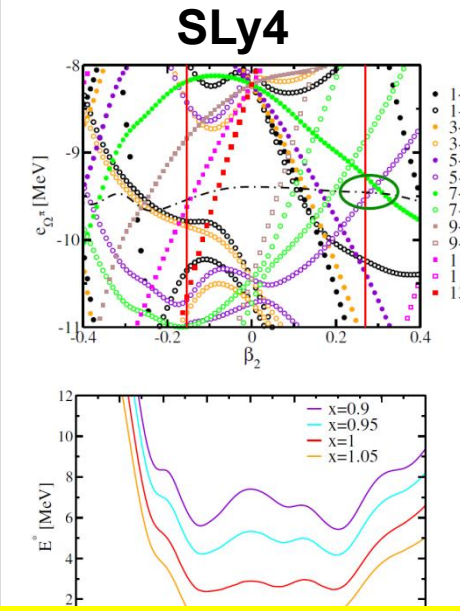
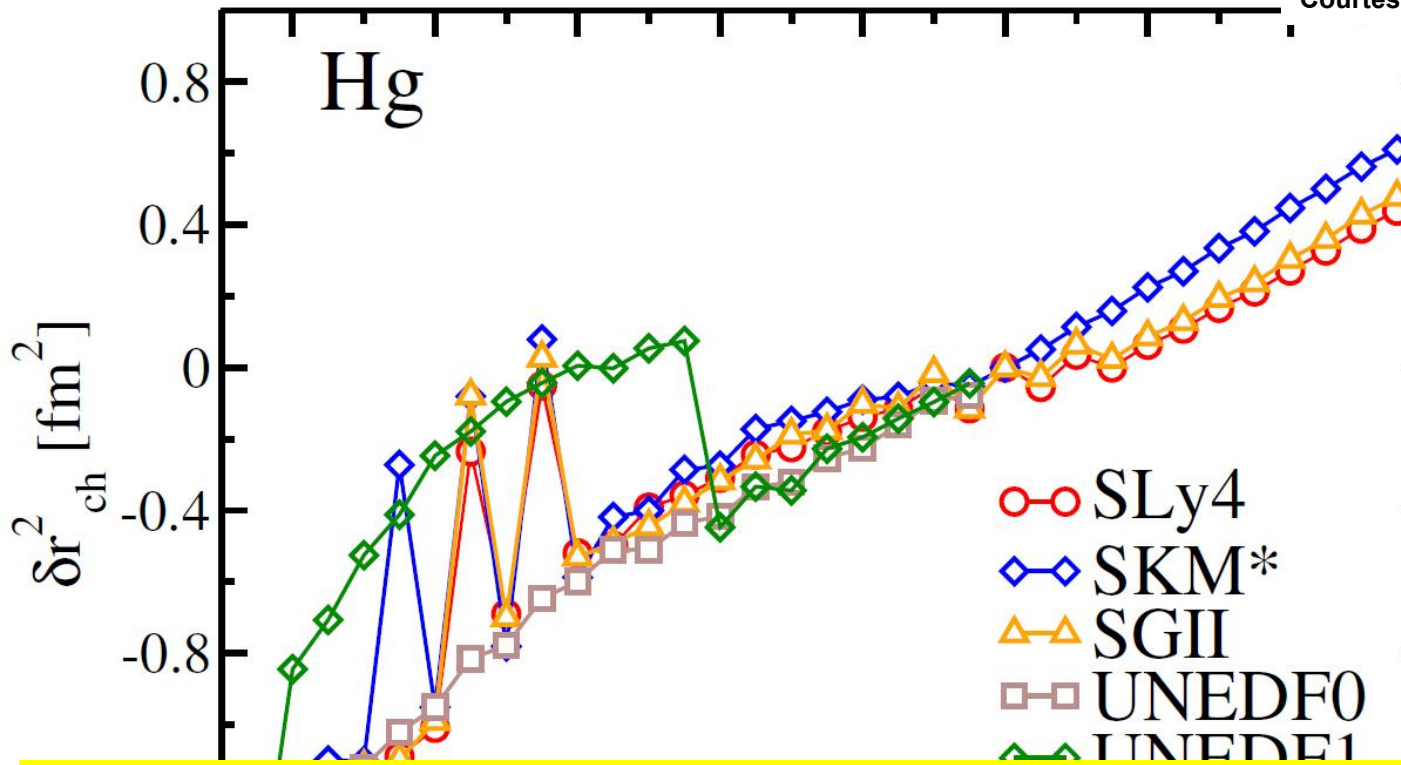


Density Functional Theory (DTF) Potential Energy Calculations (York-Lyon-Brussels Collaboration)

- Extensive Density Functional Theory blocked calculations performed by York-Lyon-Brussels Collaboration (14 parametrizations of Skyrme functional were probed)
- UNEDF0, UNDEF1, UNDED1^{SO}, SLy4, SkM*, SGII
8 parametrizations of SLy5sX
- Variation of pairng strength and other parameters
- Full account in S.Sels et al, PRC, 2019

Charge radii for Hg isotopes (reduced pairing and blocking for odd- A)

Courtesy A. Pastore and J. Dobaczewski (York)

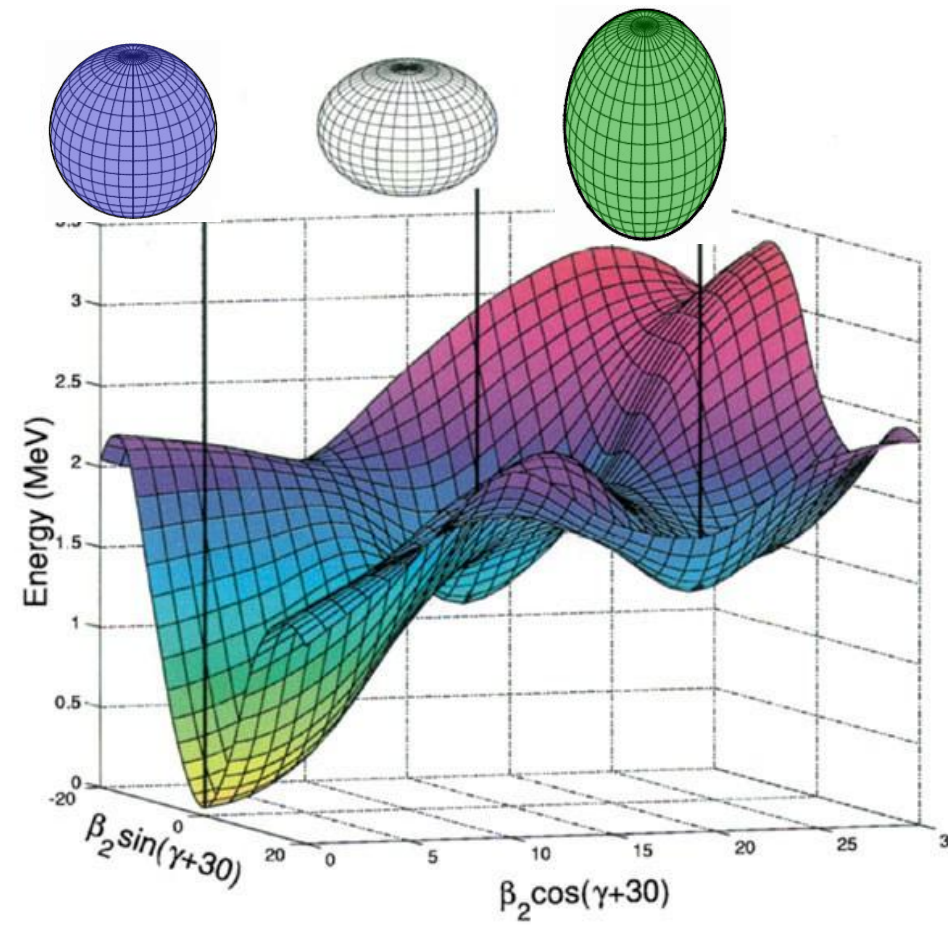


Mean-field theory summary (AP+JD):

- The phenomenon of the radii staggering in Hg is a subtle effect of an interplay between (i) shape coexistence, (ii) pairing strength, and (iii) deformed shell structure
- The presently available functionals **do not allow** for reuniting these three aspects in a consistent way (e.g. spins are not reproduced), although the essential features of the **effect can be reproduced..."**

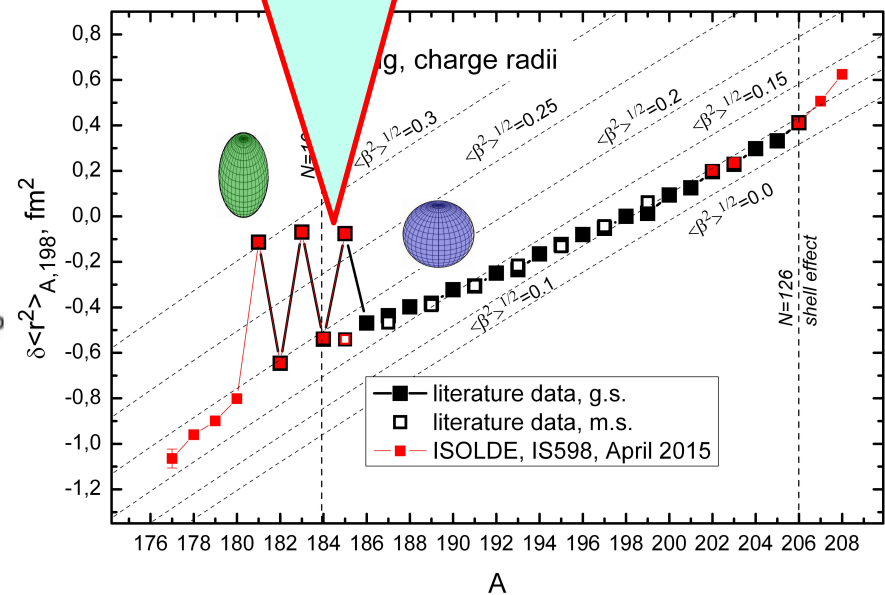
'Schematic explanation': Sphericity vs Deformation around N=104

A.Andreyev et al, Nature 405, 430 (2000)

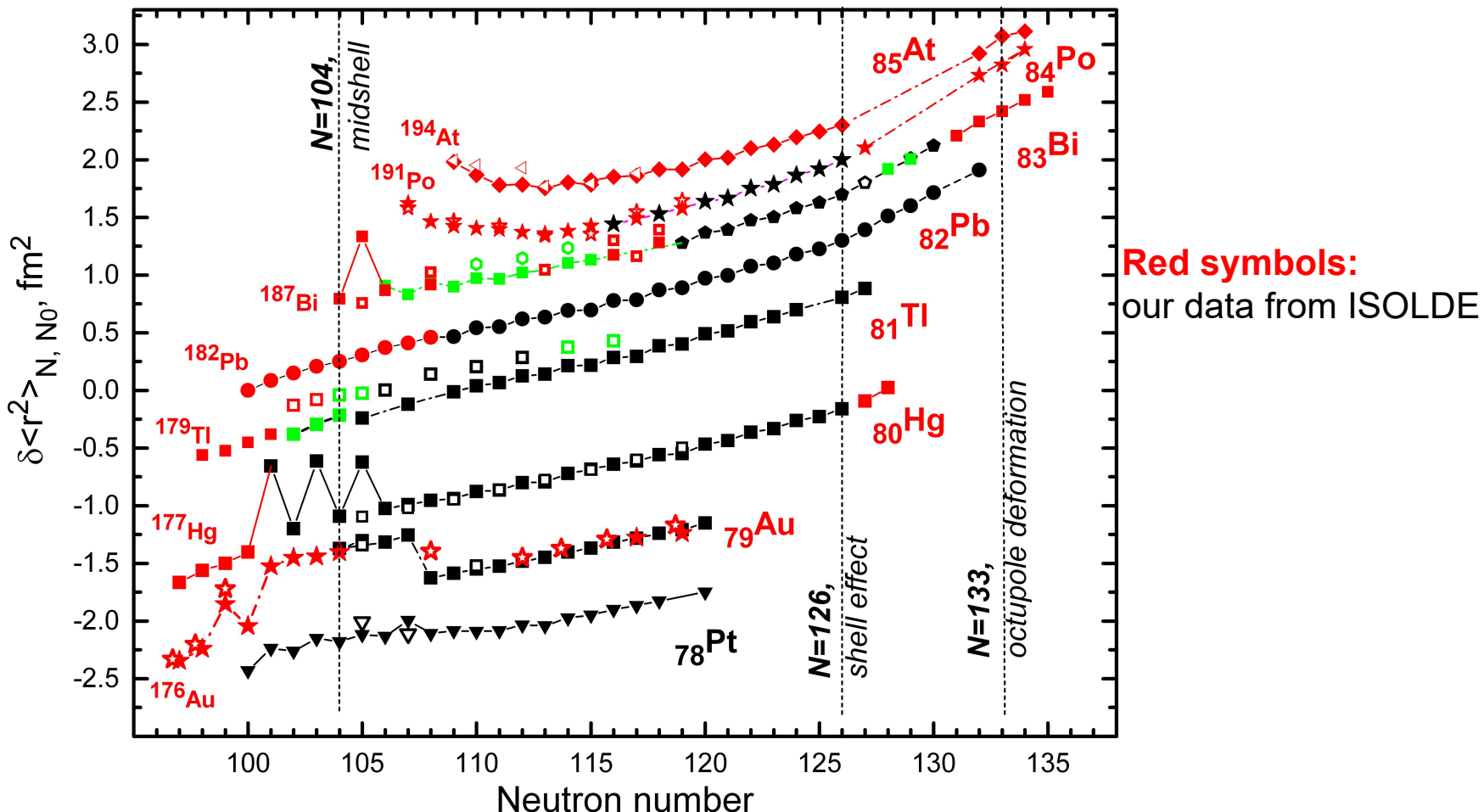


^{186}Pb (Z=82, N=104)

Large IS between $^{183,185}\text{Hg}$ and ^{187}Hg
J. Bonn et al, PLB38, 308 (1972)

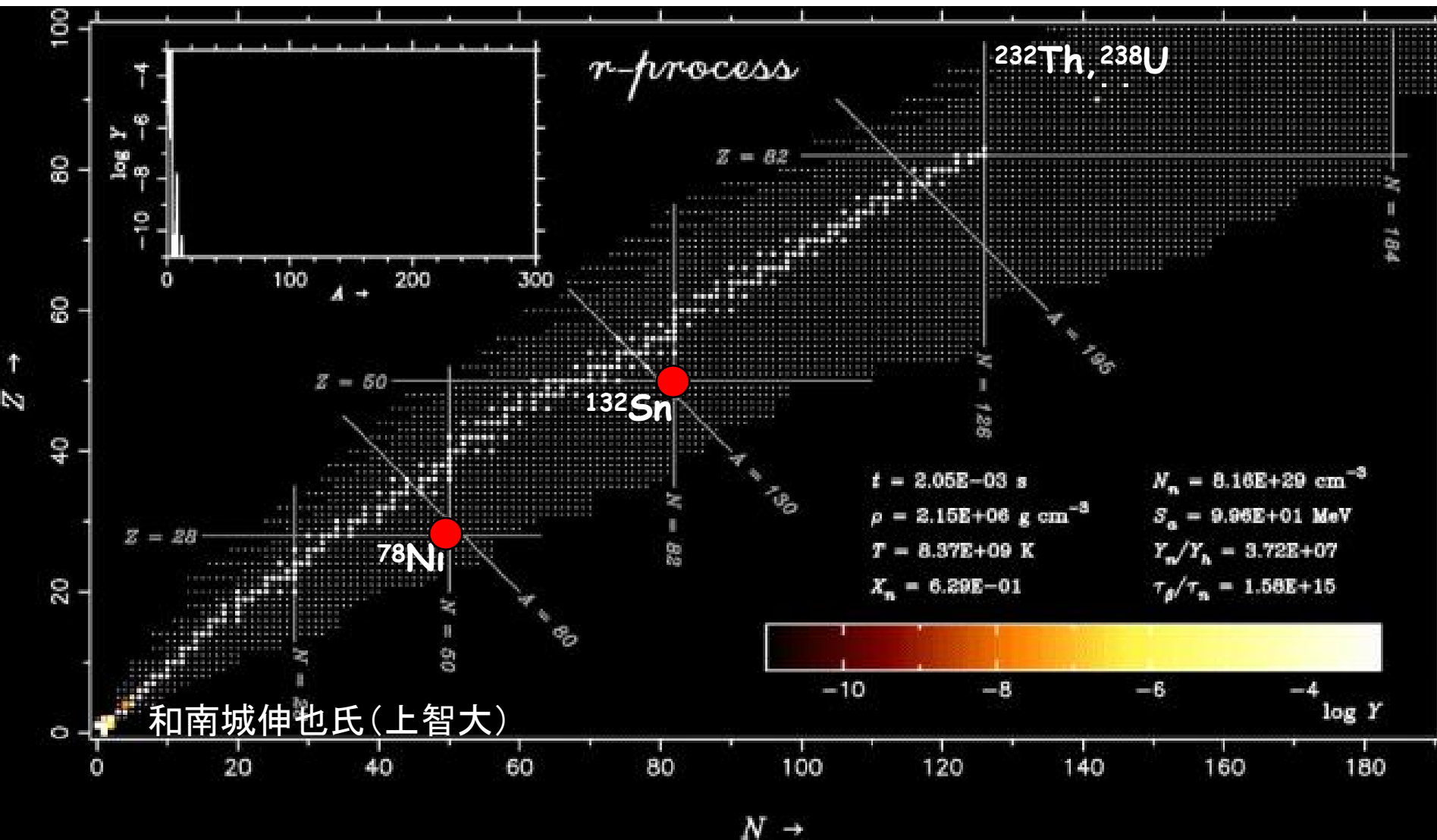


2025' Radii systematics in the Lead region



- IS/HFS/charge radii for >70 isotopes (and isomers) for Au,Hg,Pb,Bi,Po, At
- **Back to sphericity" in the lightest Au and Hg isotopes**
- Magnetic/quadrupole moments will be deduced
- Large amount of by-product nuclear spectroscopic information on parents and their daughters products

R-process network calculations



R-process network calculations require data for very neutron-rich nuclei: half-lives, decay modes, neutron-capture cross sections, fission barriers and mass distributions.

ISOLDE studies of neutron-rich isotopes around N=126

One of the least experimentally explored regions of nuclear chart – “Terra incognita” for nuclear and laser spectroscopy, especially below Z=82

N=126

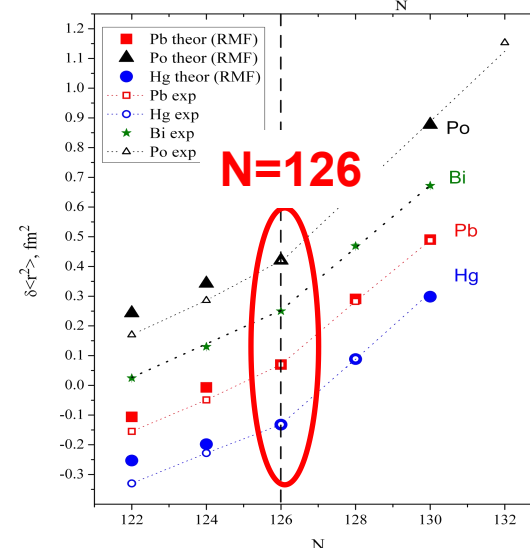
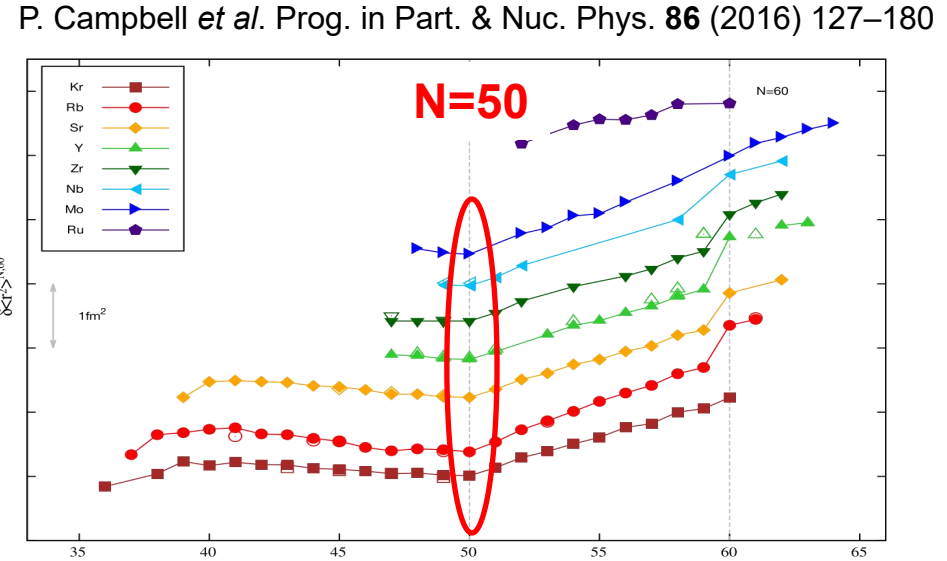
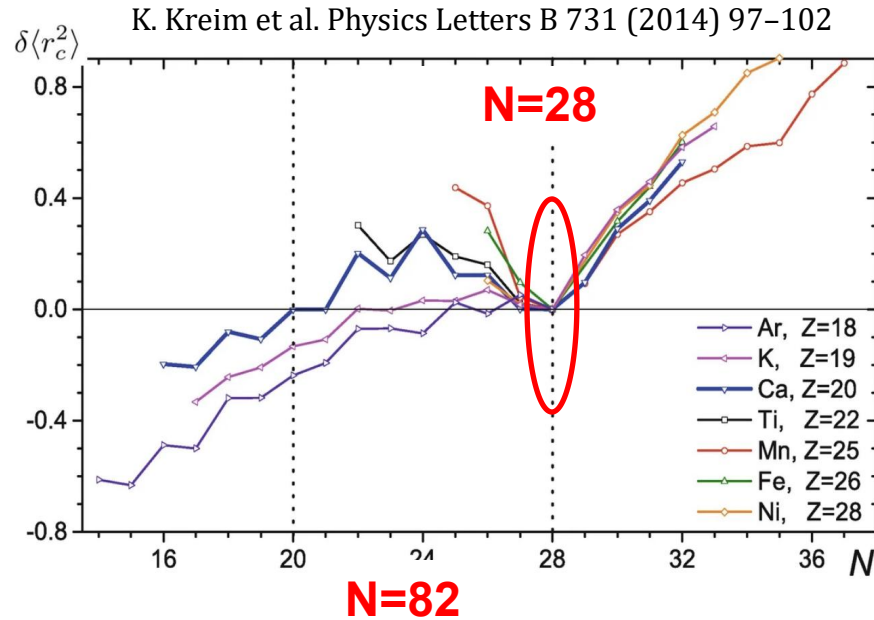
212Fr 20.0 min $\tau = 57.00\%$ $\tau = 43.00\%$	213Fr 34.82 s $\alpha = 99.44\%$ $\epsilon = 0.56\%$	214Fr 5.0 ms $\alpha = 100.00\%$	215Fr 86 ns $\alpha = 100.00\%$	216Fr 700 ns $\alpha = 100.00\%$	217Fr 19 ps $\alpha = 100.00\%$	218Fr 1.0 ms $\alpha = 100.00\%$	219Fr 20 ms $\alpha = 100.00\%$	220Fr 27.4 s $\alpha = 99.65\%$ $\beta^- = 0.35\%$
211Rn 14.6 h $\tau = 72.60\%$ $\tau = 27.40\%$	212Rn 23.9 min $\alpha = 100.00\%$	213Rn 19.5 ms $\alpha = 100.00\%$	214Rn 0.27 μ s $\alpha = 100.00\%$	215Rn 2.30 μ s $\alpha = 100.00\%$	216Rn 45 μ s $\alpha = 100.00\%$	217Rn 0.54 ms $\alpha = 100.00\%$	218Rn 35 ms $\alpha = 100.00\%$	219Rn 3.96 s $\alpha = 100.00\%$
210At 8.1 h $\tau = 99.82\%$ $\alpha = 0.18\%$	211At 7.214 h $\epsilon = 58.20\%$ $\alpha = 41.80\%$	212At 0.314 s $\alpha = 100.00\%$	213At 125 ns $\alpha = 100.00\%$	214At 558 ns $\alpha = 100.00\%$	215At 0.10 ms $\alpha = 100.00\%$	216At 0.30 ms $\alpha = 100.00\%$	217At 32.3 ms $\alpha = 99.99\%$ $\beta^- = 7.0\text{-}3\%$	218At 1.5 s $\alpha = 99.90\%$ $\beta^- = 0.10\%$
209Po 124 y $\tau = 99.55\%$ $\alpha = 0.45\%$	210Po 138.376 d $\alpha = 100.00\%$	211Po 0.516 s $\alpha = 100.00\%$	212Po 0.299 μ s $\alpha = 100.00\%$	213Po — $\alpha = 100.00\%$	214Po — $\alpha = 100.00\%$	215Po 1.781 ms $\alpha = 100.00\%$	216Po 0.145 s $\alpha = 100.00\%$	217Po 1.53 s $\alpha = 100.00\%$
208Bi 3.68E+5 y $\tau = 100.00\%$	209Bi 2.01E19 y 100% $\alpha = 100.00\%$	210Bi 5.012 d $\beta^- = 100.00\%$ $\alpha = 1.3E-4\%$	211Bi 2.14 min $\alpha = 99.72\%$ $\beta^- = 0.28\%$	212Bi 60.55 min $\alpha = 64.06\%$ $\alpha = 35.94\%$	213Bi 45.61 min $\alpha = 97.80\%$ $\alpha = 2.20\%$	214Bi 19.9 min $\alpha = 99.98\%$ $\alpha = 0.02\%$	215Bi 7.6 min $\alpha = 100.00\%$	216Bi 2.2 min $\beta^- \leq 100.00\%$
207Pb STABLE 22.1%	208Pb STABLE 52.4%	209Pb 3.234 h $\beta^- = 100.00\%$ $\alpha = 1.92\text{-}6\%$	210Pb 22.20 y $\beta^- = 100.00\%$ $\alpha = 1.92\text{-}6\%$	211Pb 36.1 min $\beta^- = 100.00\%$	212Pb 10.64 h $\beta^- = 100.00\%$	213Pb 10.2 min $\beta^- = 100.00\%$	214Pb 27.06 min $\beta^- = 100.00\%$	215Pb 147 s $\beta^- = 100.00\%$
206Tl 1.202 min $\alpha = 100.00\%$	207Tl 4.77 min $\beta^- = 100.00\%$	208Tl 3.053 min $\beta^- = 100.00\%$	209Tl 2.162 min $\beta^- = 100.00\%$	210Tl 1.30 min $\beta^- = 100.00\%$	211Tl 88 s $\beta^- = 100.00\%$	212Tl > 300 ns $\beta^- = 100.00\%$	213Tl 101 s $\beta^- = 100.00\%$	214Tl > 300 ns $\beta^- = 100.00\%$
202Hg STABLE 29.86%	203Hg 46.594 d $\beta^- = 100.00\%$	204Hg STABLE 6.87%	205Hg 5.14 min $\beta^- = 100.00\%$	206Hg 4.32 min $\beta^- = 100.00\%$	207Hg 2.9 min $\beta^- = 100.00\%$	208Hg 41 min $\beta^- = 100.00\%$	209Hg 36 s $\beta^- = 100.00\%$	210Hg > 300 ns $\beta^- = 100.00\%$
201Au 26.0 min $\beta^- = 100.00\%$	202Au 28.4 s $\beta^- = 100.00\%$	203Au 60 s $\beta^- = 100.00\%$	204Au 39.8 s $\beta^- = 100.00\%$	205Au 32.5 s $\beta^- = 100.00\%$	206Au 40 s $\beta^- = 100.00\%$	207Au > 300 ns $\beta^- = 100.00\%$	208Au > 300 ns $\beta^- = 100.00\%$	209Au > 300 ns $\beta^- = 100.00\%$
210Au > 300 ns $\beta^- = 100.00\%$	211Au > 300 ns $\beta^- = 100.00\%$	212Au > 300 ns $\beta^- = 100.00\%$	213Au > 300 ns $\beta^- = 100.00\%$	214Au > 300 ns $\beta^- = 100.00\%$	215Au > 300 ns $\beta^- = 100.00\%$	216Au > 300 ns $\beta^- = 100.00\%$	217Au > 300 ns $\beta^- = 100.00\%$	218Au > 300 ns $\beta^- = 100.00\%$

Masses are largely unknown below Z=82 (ISOLDE/ESR-GSI)

202Hg STABLE 29.86%	203Hg 46.594 d $\beta^- = 100.00\%$	204Hg STABLE 6.87%	205Hg 5.14 min $\beta^- = 100.00\%$	206Hg 4.32 min $\beta^- = 100.00\%$	207Hg 2.9 min $\beta^- = 100.00\%$	208Hg 41 min $\beta^- = 100.00\%$	209Hg 36 s $\beta^- = 100.00\%$	210Hg > 300 ns $\beta^- = 100.00\%$	211Hg > 300 ns $\beta^- = 100.00\%$	212Hg > 300 ns $\beta^- = 100.00\%$	213Hg 300 ns $\beta^- = 100.00\%$
201Au 26.0 min $\beta^- = 100.00\%$	202Au 28.4 s $\beta^- = 100.00\%$	203Au 60 s $\beta^- = 100.00\%$	204Au 39.8 s $\beta^- = 100.00\%$	205Au 32.5 s $\beta^- = 100.00\%$	206Au 40 s $\beta^- = 100.00\%$	207Au > 300 ns $\beta^- = 100.00\%$	208Au > 300 ns $\beta^- = 100.00\%$	209Au > 300 ns $\beta^- = 100.00\%$	210Au > 300 ns $\beta^- = 100.00\%$	211Au > 300 ns $\beta^- = 100.00\%$	212Au > 300 ns $\beta^- = 100.00\%$

The N=126 kink in charge radii across the Chart of Nuclei

- Sudden increase of the slope in $\delta\langle r_c^2 \rangle$ when crossing a shell closure
- seen all over nuclear chart



Let's start with some 'classics'

PHYSICAL REVIEW C

VOLUME 43, NUMBER 2

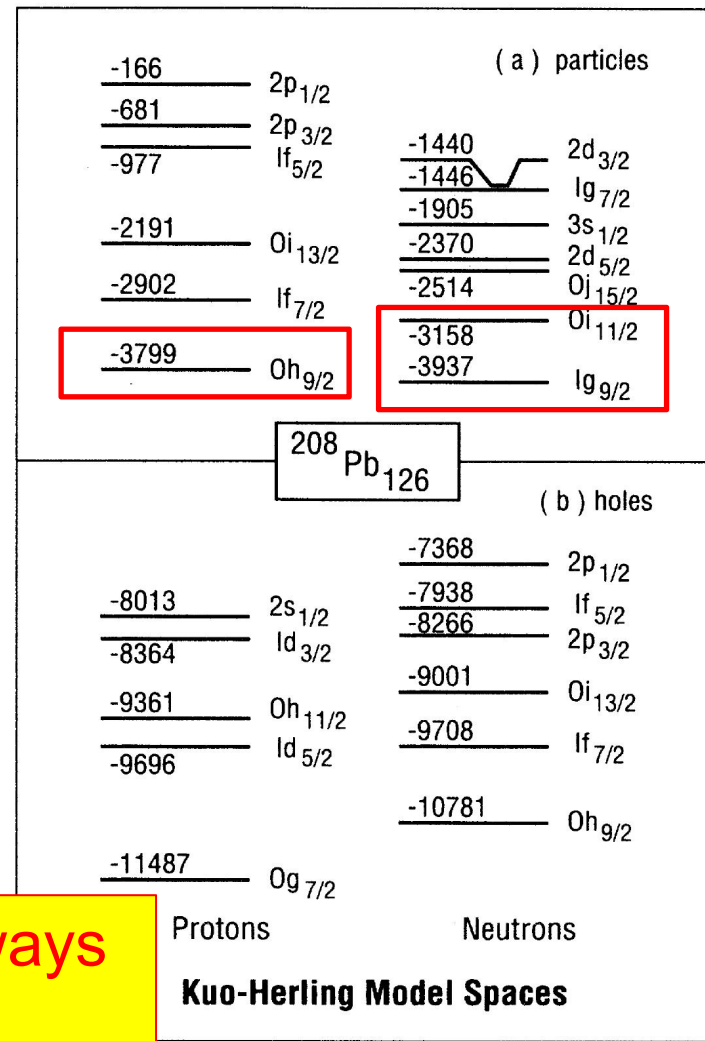
FEBRUARY 1991

Appraisal of the Kuo-Herling shell-model interaction and application to $A=210-212$ nuclei

E. K. Warburton
Brookhaven National Laboratory, Upton, New York 11973

B. A. Brown
*Cyclotron Laboratory and Department of Physics and Astronomy,
Michigan State University, East Lansing, Michigan 48824*
(Received 11 September 1990)

Shell-model calculations are described for $A=204-212$ nuclei. These calculations use the

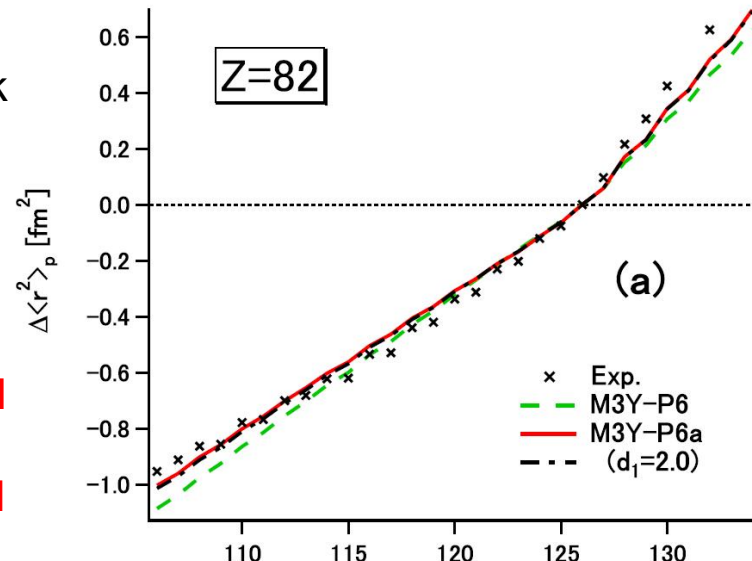


In standard SM, neutron $g_{9/2}$ is always below $i_{11/2}$!

FIG. 1. The Kuo-Herling model spaces for the lead region. Single-particle energies (in keV) are taken from the experimental spectra of $A=207$ and 209 nuclei and are relative to ^{208}Pb .

(In)Famous Kink at N=126 - Theoretical description

- Number of theoretical attempts at describing the kink
P.M. Goddard *et al.*, PRL **110**, 032503 (2013)
H. Nakada & T. Inakura, PRC **91**, 021302(R) (2015)
H. Nakada, PRC **92**, 044307 (2015)
-
- **All invoke a significant occupation of $\nu i_{11/2}$ orbital**
- **Not consistent with the classical shell model and experiment, which require first $g9/2$ to be occupied!**
- E.g. ^{209}Pb and ^{211}Po have magnetic moments consistent with pure $\nu g_{9/2}$ states



H. Nakada, PRC **92**, 044307 (2015)

Role of $1i_{11/2}$ neutron occupancy on the kink around the lead region?

PRL 110, 032503 (2013)

PHYSICAL REVIEW LETTERS

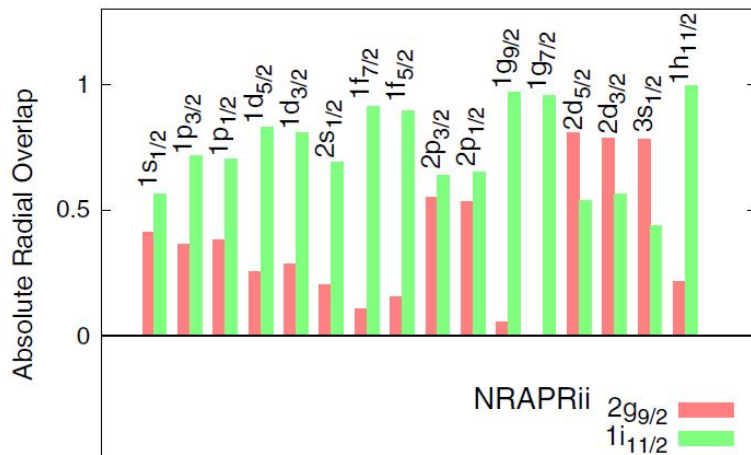
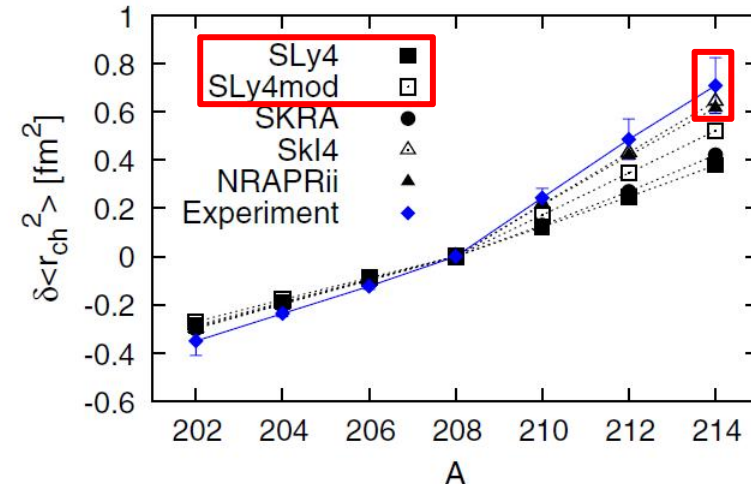
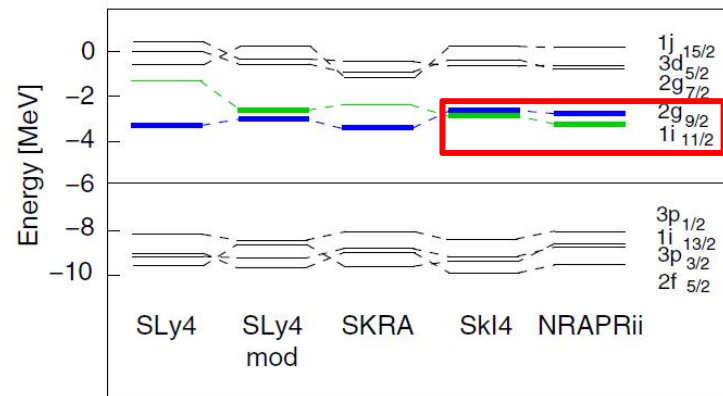
week ending
18 JANUARY 2013

Charge Radius Isotope Shift Across the $N = 126$ Shell Gap

P. M. Goddard, P. D. Stevenson, and A. Rios

Department of Physics, University of Surrey, Guildford GU2 7XH, United Kingdom

(Received 9 October 2012; revised manuscript received 26 November 2012; published 15 January 2013)

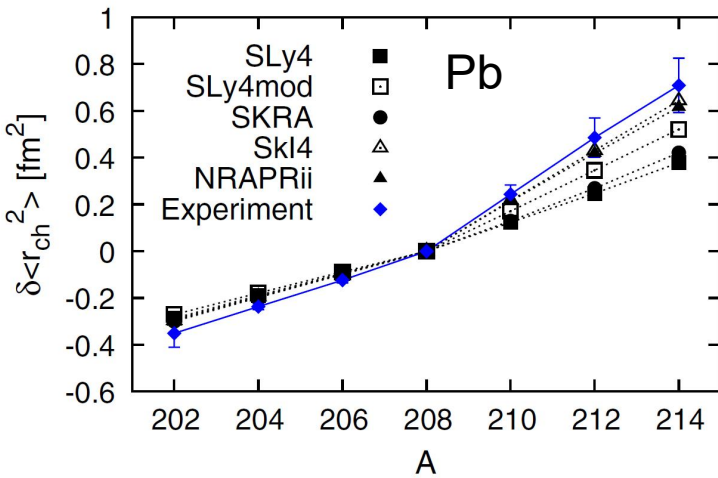
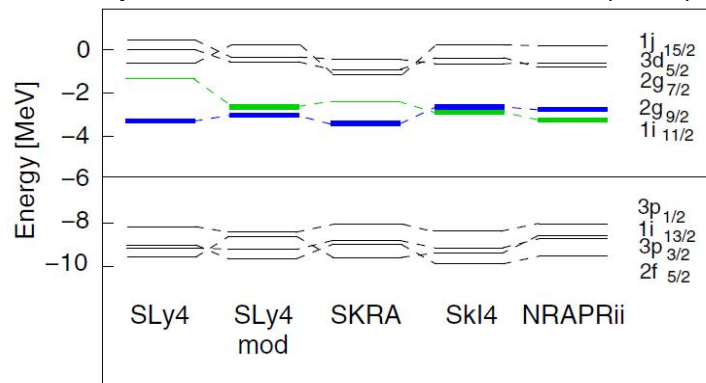


Overlap of $1i_{11/2}$ significantly
 $> 2g_{9/2}$

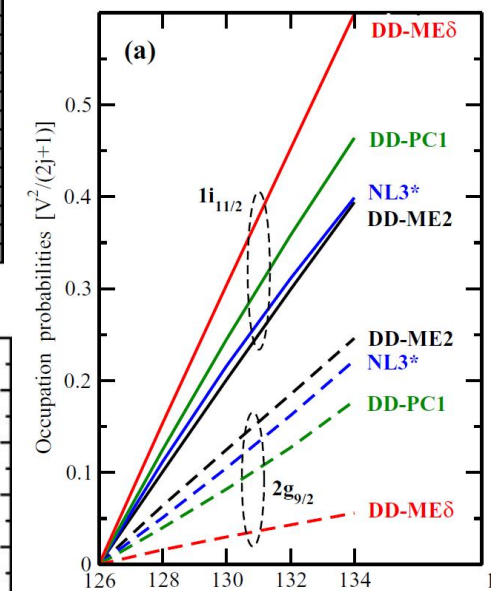
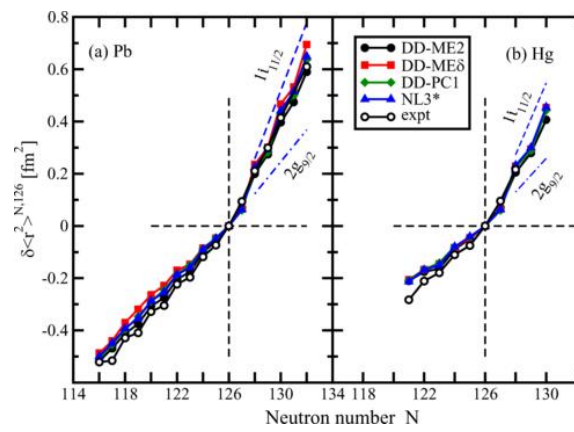
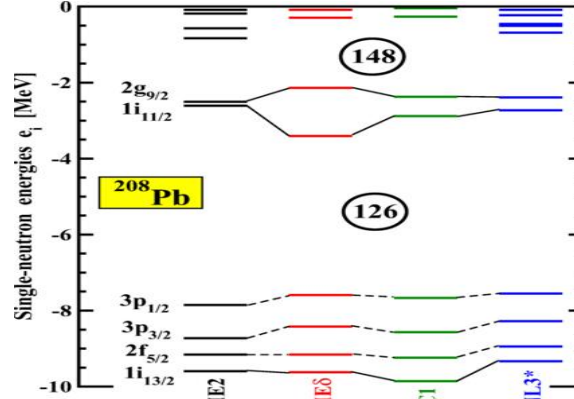
Occupation of the neutron $1h_{11/2}$ orbital provides a better overlap with majority of $n=1$ proton orbitals (via symmetry energy), thus driving them to a larger radius?

Role of 1i11/2 neutron occupancy on the kink around the lead region?

Skyrme, P.M. Goddard et al, PRL110 (2013)



Relativistic, T. Day Goodacre et al, PRL126(2021)&PRC104(2021)

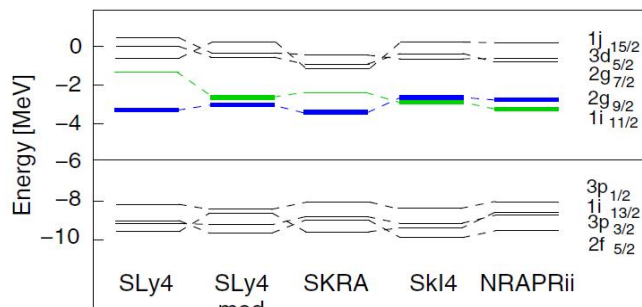


It seems the models in which **the $i_{11/2}$ neutron orbital is below $g_{9/2}$** (or very close to it) reproduce the kink better, due to enhanced population of the $i_{11/2}$ orbital. In particular, this is a common property of relativistic approaches.

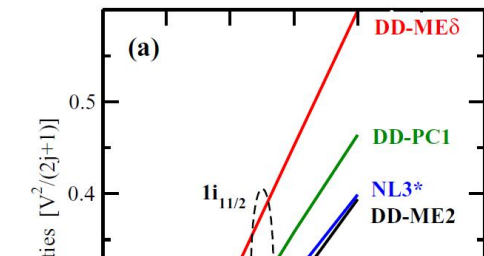
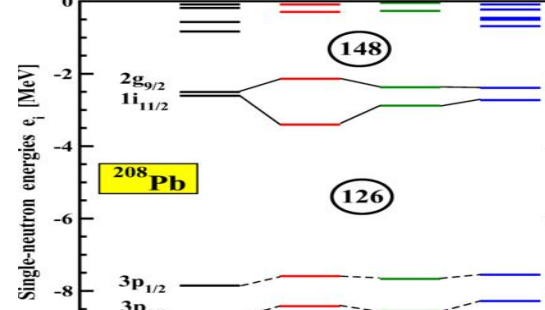
Goal: High-spin isomers $^{212m1,m2,213m}\text{Bi}$ and the N=126 kink problem (successful experiment on 3-9 December 2025)

Properties of the high-spin isomers $^{212m1,m2,213m}\text{Bi}$ and their link to the kink in Bi gs charge radii at N=126:
is the position and occupation of the $i_{11/2}$ neutron orbital a real culprit for the N=126 kink?

Skyrme, P.M. Goddard et al, PRL110 (2013)



Relativistic, T. Day Goodacre et al, PRC104,054322(2021)

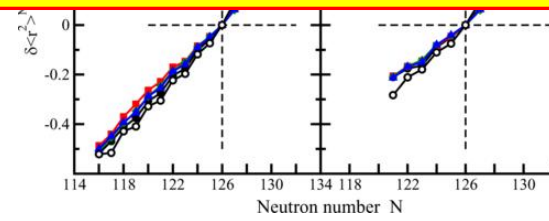
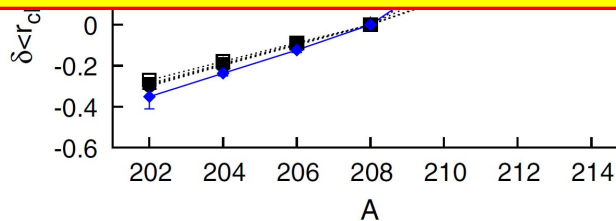


This effect can be probed by charge radii of high-spin isomers in $^{212m2,213m}\text{Bi}$, whose configuration **presumably includes an $i_{11/2}$ neutron**:

$^{212m2}\text{Bi}$ [$\pi h9/2 \times ((vg9/2)^2 \times vi11/2)$]18 $-$,

^{213m}Bi [$\pi h9/2 \times (vg9/2 \times vi11/2)$]25/2 $-$,

relative to their gs's or $^{212m1}\text{Bi}$ [$\pi h9/2 \times vg9/2)$]8 $-$, 9 $-$, which have no $i_{11/2}$ neutrons.

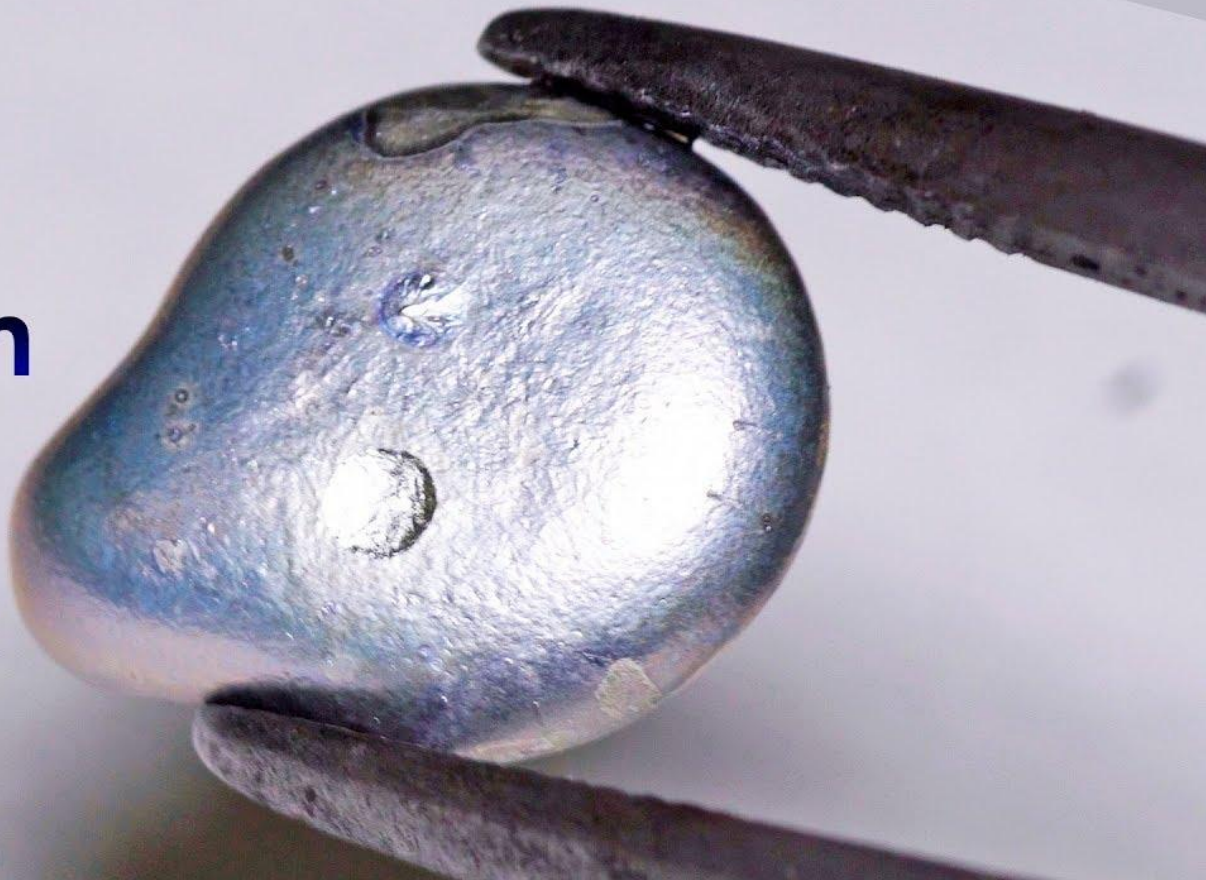


It seems the models in which **the $i_{11/2}$ neutron orbital is below $g9/2$** (or very close to it) reproduce the kink better, due to enhanced population of the $i_{11/2}$ orbital. **This is a common property of relativistic approaches.**

The N=126 kink in charge radii and magnetic moments in the neutron-rich Tl ($Z=81$) isotopes

Tl

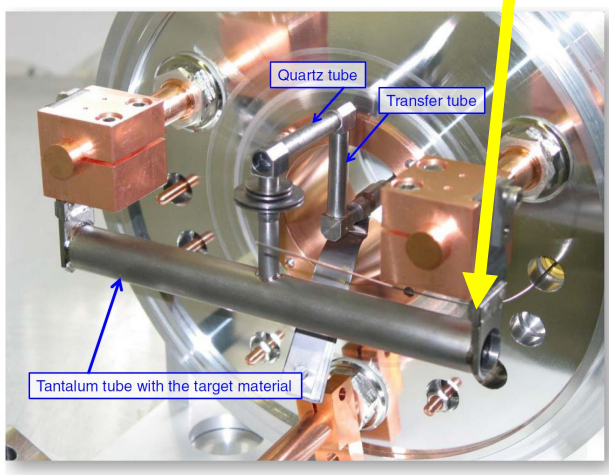
Thallium



The N=126 kink in charge radii of Tl (Z=81) isotopes

Fr Isobaric contamination is our main enemy at masses A=207-212 and A>219!!!

Ohmic heating 2000 degrees



Fr isobaric contaminations!											
Fr-90/90						Fr-208/208			Fr-220/220		
Fr-208Ra	Fr-209Ra	Fr-210Ra	Fr-211Ra	Fr-212Ra	Fr-213Ra	Fr-214Ra	Fr-215Ra	Fr-216Ra	Fr-217Ra	Fr-218Ra	Fr-219Ra
1.3 s $\alpha = 95.00\%$ $\epsilon = 5.00\%$	4.6 s $\alpha = 90.00\%$ $\epsilon = 10.00\%$	3.7 s $\alpha = 96.00\%$ $\epsilon = 4.00\%$	13 s $\alpha = 93.00\%$ $\epsilon = 7.00\%$	13.0 s $\alpha = 85.00\%$ $\epsilon = 15.00\%$	2.73 min $\alpha = 80.00\%$ $\epsilon = 0.06\%$	2.46 s $\alpha = 99.94\%$ $\epsilon < 1.0E-8\%$	1.66 ms $\alpha = 100.00\%$ $\epsilon = 0.00\%$	182 ns $\alpha = 100.00\%$ $\epsilon < 1.0E-8\%$	1.6 s $\alpha = 100.00\%$ $\epsilon = 0.00\%$	25.2 s $\alpha = 100.00\%$ $\epsilon = 0.00\%$	10 ms $\alpha = 100.00\%$ $\epsilon = 0.00\%$
14 s $\alpha = 95.00\%$ $\epsilon = 5.00\%$	59.1 s $\alpha = 89.00\%$ $\epsilon = 11.00\%$	50.5 s $\alpha = 85.00\%$ $\epsilon = 11.00\%$	3.18 min $\alpha = 71.00\%$ $\epsilon = 29.00\%$	3.10 min $\alpha = 80.00\%$ $\epsilon = 13.00\%$	20.8 min $\alpha = 57.00\%$ $\epsilon = 43.00\%$	34.82 s $\alpha = 95.14\%$ $\epsilon = 0.2\%$	5.0 ms $\alpha = 100.00\%$ $\epsilon = 0.00\%$	88 ns $\alpha = 100.00\%$ $\epsilon = 0.00\%$	700 ns $\alpha = 100.00\%$ $\epsilon = 0.00\%$	19 s $\alpha = 100.00\%$ $\epsilon = 0.00\%$	1.0 ms $\alpha = 100.00\%$ $\epsilon = 0.00\%$
5.67 min $\alpha = 62.00\%$ $\epsilon = 38.00\%$	207Rn 5.65 min $\alpha = 62.00\%$ $\epsilon = 38.00\%$	208Rn 24.35 min $\alpha = 62.00\%$ $\epsilon = 38.00\%$	209Rn 5.6 min $\alpha = 62.00\%$ $\epsilon = 38.00\%$	210Rn 2.4 h $\alpha = 8.00\%$ $\epsilon = 17.00\%$	211Rn 6.6 h $\alpha = 96.00\%$ $\epsilon = 4.00\%$	212Rn 23.9 min $\alpha = 100.00\%$ $\epsilon = 0.00\%$	213Rn 9.5 ms $\alpha = 10.00\%$ $\epsilon = 0.00\%$	214Rn 2.1 ms $\alpha = 100.00\%$ $\epsilon = 0.00\%$	215Rn 1.5 ms $\alpha = 100.00\%$ $\epsilon = 0.00\%$	216Rn 45 ms $\alpha = 100.00\%$ $\epsilon = 0.00\%$	217Rn 0.54 ms $\alpha = 100.00\%$ $\epsilon = 0.00\%$
26.9 min $\alpha = 99.00\%$ $\epsilon = 0.00\%$	208At 30.6 min $\alpha = 99.00\%$ $\epsilon = 0.00\%$	207At 41 h $\alpha = 9.00\%$ $\epsilon = 8.00\%$	208At 1.63 h $\alpha = 99.45\%$ $\epsilon = 0.55\%$	209At 5.42 h $\alpha = 8.1 h$	210At 8.1 h $\alpha = 99.22\%$ $\epsilon = 0.18\%$	211At 214 h $\alpha = 100.00\%$ $\epsilon = 0.00\%$	212At 0.314 s $\alpha = 100.00\%$ $\epsilon = 0.00\%$	213At 0.104 s $\alpha = 100.00\%$ $\epsilon = 0.00\%$	214At 0.30 ms $\alpha = 100.00\%$ $\epsilon = 0.00\%$	215At 0.323 ms $\alpha = 100.00\%$ $\epsilon = 0.00\%$	216At 1.5 s $\alpha = 100.00\%$ $\epsilon = 0.00\%$
3.519 h $\alpha = 99.23\%$ $\epsilon = 0.67\%$	204Po 1.74 h $\alpha = 99.86\%$ $\epsilon = 0.04\%$	205Po 8.8 d $\alpha = 94.53\%$ $\epsilon = 5.45\%$	206Po 5.80 h $\alpha = 99.45\%$ $\epsilon = 0.5\%$	207Po 2.898 y $\alpha = 99.00\%$ $\epsilon = 4.0E-3\%$	208Po 124 y $\alpha = 100.00\%$ $\epsilon = 0.00\%$	209Po 138.376 d $\alpha = 100.00\%$ $\epsilon = 0.00\%$	210Po 0.516 s $\alpha = 100.00\%$ $\epsilon = 0.00\%$	211Po 0.299 μs $\alpha = 100.00\%$ $\epsilon = 0.00\%$	212Po 0.299 μs $\alpha = 100.00\%$ $\epsilon = 0.00\%$	213Po 0.145 s $\alpha = 100.00\%$ $\epsilon = 0.00\%$	214Po 1.781 ms $\alpha = 100.00\%$ $\epsilon = 0.00\%$
11.76 h $\alpha = 100.00\%$ $\epsilon = 0.00\%$	204Bi 11.22 h $\alpha = 100.00\%$ $\epsilon = 0.00\%$	205Bi 15.31 d $\alpha = 100.00\%$ $\epsilon = 0.00\%$	206Bi 6.243 d $\alpha = 100.00\%$ $\epsilon = 0.00\%$	207Bi 1.55 y $\alpha = 100.00\%$ $\epsilon = 0.00\%$	208Bi 3.68E+5 y $\alpha = 100.00\%$ $\epsilon = 0.00\%$	209Bi 1.01E+9 y $\alpha = 100.00\%$ $\epsilon = 0.00\%$	210Bi 5.012 d $\alpha = 100.00\%$ $\epsilon = 1.3E-4\%$	211Bi 0.14 min $\alpha = 100.00\%$ $\epsilon = 0.00\%$	212Bi 60.55 min $\alpha = 72\%$ $\epsilon = 64.00\%$	213Bi 22.20 y $\alpha = 100.00\%$ $\epsilon = 35.94\%$	214Bi 19.9 min $\alpha = 100.00\%$ $\epsilon = 0.00\%$
52.5E+3 y $\alpha = 100.00\%$ $\epsilon = 100.00\%$	203Pb 51.92 h $\alpha = 100.00\%$ $\epsilon = 100.00\%$	204Pb 5.1E+17 y $\alpha = 100.00\%$ $\epsilon = 100.00\%$	205Pb 1.73E+7 y $\alpha = 100.00\%$ $\epsilon = 100.00\%$	206Pb STABLE 24.1%	207Pb STABLE 1.1%	208Pb STABLE 52.4%	209Pb 2.234 h $\alpha = 100.00\%$ $\epsilon = 0.00\%$	210Pb 2.220 y $\alpha = 100.00\%$ $\epsilon = 0.00\%$	211Pb 46.1 min $\alpha = 100.00\%$ $\epsilon = 0.00\%$	212Pb 16.64 h $\alpha = 100.00\%$ $\epsilon = 0.00\%$	213Pb 10.2 min $\alpha = 100.00\%$ $\epsilon = 0.00\%$
20.111 3.042E11 d $\alpha = 100.00\%$ $\epsilon = 100.00\%$	203Tl 12.21 min $\alpha = 100.00\%$ $\epsilon = 100.00\%$	204Tl 3.753 s $\beta = 97.05\%$ $\epsilon = 2.92\%$	205Tl STABLE 70.48%	206Tl 4.202 min $\beta = 100.00\%$ $\epsilon = 0.00\%$	207Tl 0.17 min $\beta = 100.00\%$ $\epsilon = 0.00\%$	208Tl 3.053 min $\beta = 100.00\%$ $\epsilon = 0.00\%$	209Tl 0.15 min $\beta = 100.00\%$ $\epsilon = 0.00\%$	210Tl 0.15 min $\beta = 100.00\%$ $\epsilon = 0.00\%$	211Tl 88 s $\beta = 100.00\%$ $\epsilon = 0.00\%$	> 300 s $\beta = 100.00\%$ $\epsilon = 0.00\%$	101 s $\beta = 100.00\%$ $\epsilon = 0.00\%$
200Hg 23.10% $\beta = 100.00\%$ $\epsilon = 100.00\%$	201Hg 100.00% $\beta = 100.00\%$ $\epsilon = 100.00\%$	202Hg 24.594 d $\beta = 100.00\%$ $\epsilon = 100.00\%$	203Hg 36.9 d $\beta = 100.00\%$ $\epsilon = 100.00\%$	204Hg 5.14 min $\beta = 100.00\%$ $\epsilon = 100.00\%$	205Hg 8.32 min $\beta = 100.00\%$ $\epsilon = 100.00\%$	206Hg 2.9 min $\beta = 100.00\%$ $\epsilon = 100.00\%$	207Hg 41 min $\beta = 100.00\%$ $\epsilon = 100.00\%$	208Hg 36 s $\beta = 100.00\%$ $\epsilon = 100.00\%$	209Hg 36 s $\beta = 100.00\%$ $\epsilon = 100.00\%$	> 300 ns $\beta = 100.00\%$ $\epsilon = 100.00\%$	> 300 ns $\beta = 100.00\%$ $\epsilon = 100.00\%$
197Au 100% $\beta = 100.00\%$ $\epsilon = 100.00\%$	198Au 2.6941 d $\beta = 100.00\%$ $\epsilon = 100.00\%$	199Au 3.139 d $\beta = 100.00\%$ $\epsilon = 100.00\%$	200Au 48.4 min $\beta = 100.00\%$ $\epsilon = 100.00\%$	201Au 25.0 min $\beta = 100.00\%$ $\epsilon = 100.00\%$	202Au 28.4 s $\beta = 100.00\%$ $\epsilon = 100.00\%$	203Au 60 s $\beta = 100.00\%$ $\epsilon = 100.00\%$	204Au 39.8 s $\beta = 100.00\%$ $\epsilon = 100.00\%$	205Au 32.5 s $\beta = 100.00\%$ $\epsilon = 100.00\%$	206Au 40 s $\beta = 100.00\%$ $\epsilon = 100.00\%$	207Au 300 ns $\beta = 100.00\%$ $\epsilon = 100.00\%$	208Au > 300 ns $\beta = 100.00\%$ $\epsilon = 100.00\%$
221Ra 28 s $\beta = 100.00\%$ $\epsilon = 100.00\%$	222Ra 27.4 s $\beta = 99.65\%$ $\epsilon = 0.35\%$	223Ra 28.0 ms $\beta = 100.00\%$ $\epsilon = 0.00\%$	224Ra 27.4 s $\beta = 100.00\%$ $\epsilon = 0.00\%$	225Ra 28.6 s $\beta = 100.00\%$ $\epsilon = 0.00\%$	226Ra 28.0 ms $\beta = 100.00\%$ $\epsilon = 0.00\%$	227Ra 28.0 ms $\beta = 100.00\%$ $\epsilon = 0.00\%$	228Ra 28.0 ms $\beta = 100.00\%$ $\epsilon = 0.00\%$	229Ra 28.0 ms $\beta = 100.00\%$ $\epsilon = 0.00\%$	230Ra 28.0 ms $\beta = 100.00\%$ $\epsilon = 0.00\%$	231Ra 3.96 s $\beta = 100.00\%$ $\epsilon = 0.00\%$	232Ra 55.6 s $\beta = 100.00\%$ $\epsilon = 0.00\%$

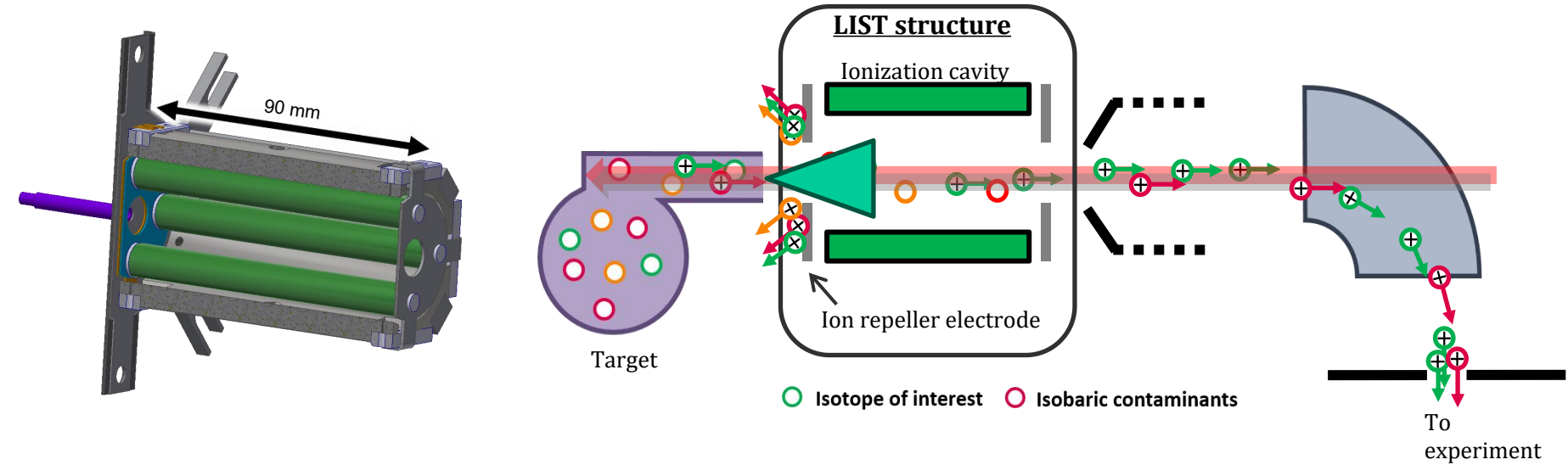
	$\alpha = 100.00\%$	$\alpha = 100.00\%$	$\alpha = 100.00\%$
3Rn 5 ms	$\alpha = 100.00\%$	$\alpha = 100.00\%$	$\alpha = 100.00\%$
2T _{1/2} 1.3 ms	$\alpha = 100.00\%$	$\alpha = 100.00\%$	$\alpha = 100.00\%$
15Rn 1.0 μs	$\alpha = 100.00\%$	$\alpha = 100.00\%$	$\alpha = 100.00\%$
216Rn 45 μs	$\alpha = 100.00\%$	$\alpha = 100.00\%$	$\alpha = 100.00\%$
α_{241} 314 s	$\alpha = 100.00\%$	$\alpha = 100.00\%$	$\alpha = 100.00\%$
α_{210} 16.0 ms	$\alpha = 100.00\%$	$\alpha = 100.00\%$	$\alpha = 100.00\%$
212Po 0.299 μs	$\alpha = 100.00\%$	$\alpha = 100.00\%$	$\alpha = 100.00\%$
211Po 11.6 s	$\alpha = 100.00\%$	$\alpha = 100.00\%$	$\alpha = 100.00\%$
211Bi 112 d	$\alpha = 100.00\%$	$\alpha = 100.00\%$	$\alpha = 100.00\%$
212Bi 14 min	$\alpha = 100.00\%$	$\alpha = 100.00\%$	$\alpha = 100.00\%$
212Bi 60.55 min	$\alpha = 100.00\%$	$\alpha = 100.00\%$	$\alpha = 100.00\%$
210Pb 22.3 days	$\alpha = 100.00\%$	$\alpha = 100.00\%$	$\alpha = 100.00\%$
211Pb 17.0 hours	$\alpha = 100.00\%$	$\alpha = 100.00\%$	$\alpha = 100.00\%$
212Pb 10.6 hours	$\alpha = 100.00\%$	$\alpha = 100.00\%$	$\alpha = 100.00\%$

Isotope	^{209}Fr	^{209}Tl
Yield (/ μC)	2.5×10^7	3.2×10^2

Mass Number	207	208	209
Half-life of Fr	14.8s	58.6s	50s
Half-life of Tl	4.77m	3.05m	2.16m

The Laser Ion Source and Trap (LIST) at ISOLDE

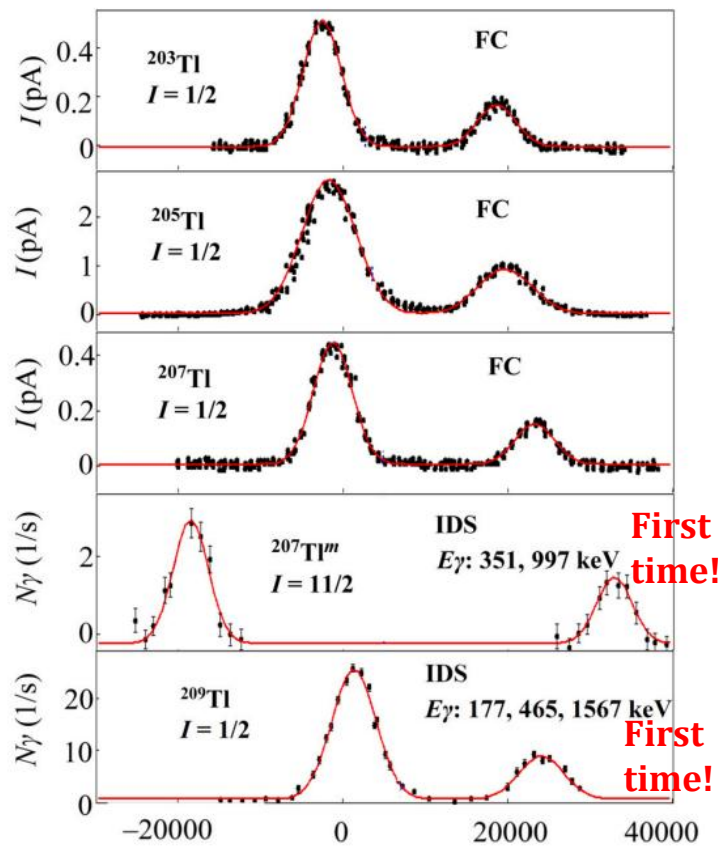
(efficient suppression of surface-ionized species, e.g. alkalii)



- **Spatial separation:** hot cavity \leftrightarrow laser ionization volume
- **Suppression of surface ionized species**
- **Pure laser ionization** inside RF quadrupole structure

- Suppress the ions produced via surface ionization (by a factor of ~ 10000)
- Only lose the isotope of interest (by a factor of 10-15)

HFS/IS, charge radii for neutron-rich Tl isotopes (Z. Yue , A.A. et al., PRC, 2024)



Physics Letters B
Volume 849, February 2024, 138452

Letter
Magnetic moments of thallium isotopes in the vicinity of magic $N=126$

Z. Yue^a , A.N. Andreyev^{a,b}, A.E. Barzakh^c, I.N. Borzov^c, J.G. Cubiss^a, A. Algora^d, M. Ai^{b,e}, M. Balogh^f, S. Bara^g, R.A. Bark^h, C. Bernard^{b,g}, M.J.G. Borgeⁱ, D. Brugara^f, K. Chrysalidis^b, T.E. Cocolios^g, H. De Witte^g, Z. Favier^b, L.M. Fraile^j, H.O.U. Fynbo^k, A. Gottardo^f, ...W. Wojtaczka^g

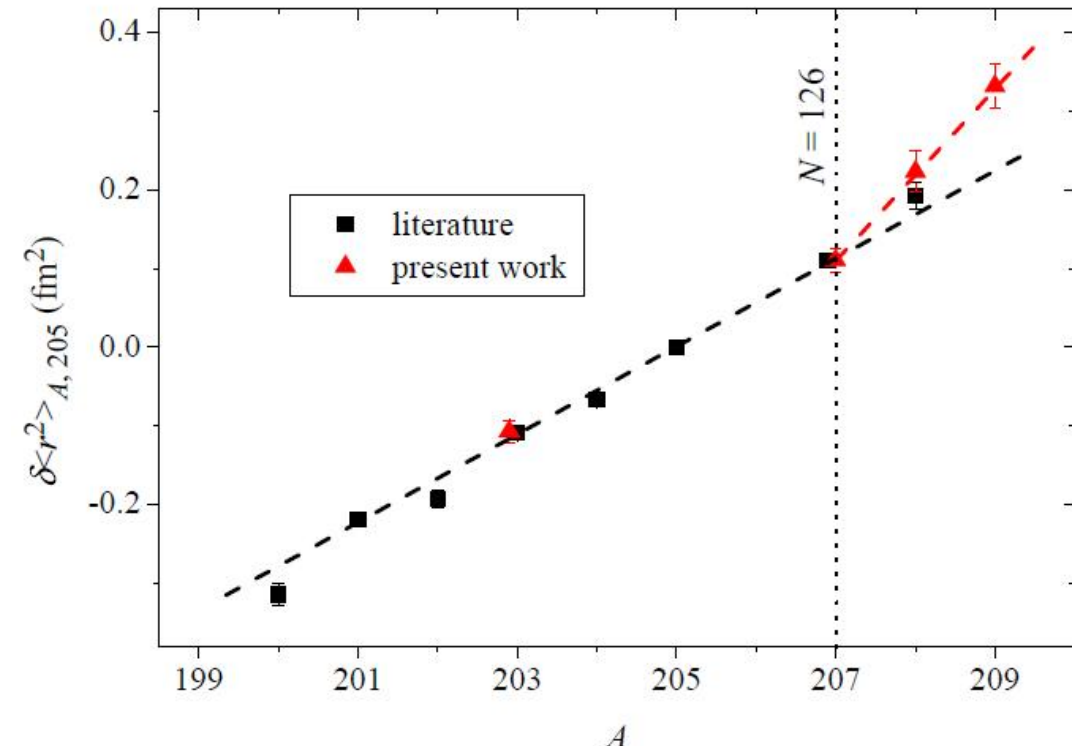


Table 1

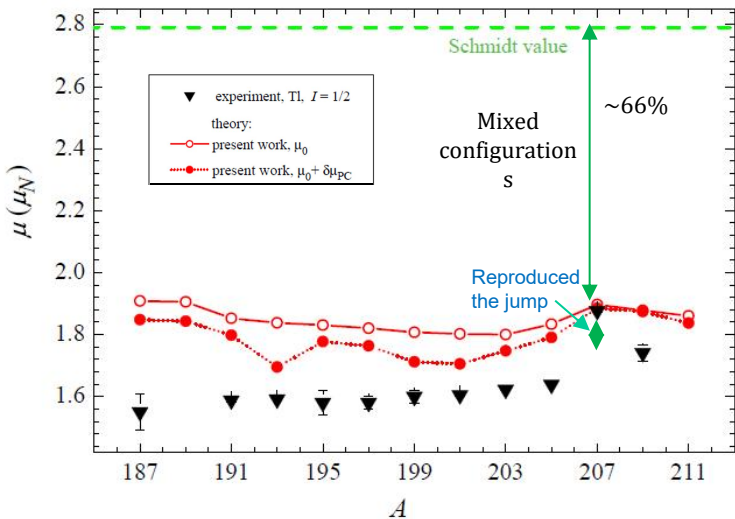
Measured yields for thallium isotopes using the LIST. Uncertainties are estimated as 30%.

Nucleus	Ions/ μC
$^{207}\text{Tl}^g$	5.5×10^6
$^{207}\text{Tl}'^m$	3.4×10^1
^{208}Tl	1.5×10^4
^{209}Tl	3.2×10^2

210Tl should be possible, but difficult to move heavier at ISOLDE, rate and contaminations issues.
(RIBF can reach to 215Tl, see PRL 2024 from RIBF)

Magnetic dipole moments for neutron-rich Tl isotopes

(Z. Yue et al., PLB849, 2024)



- Theory of finite-Fermi systems (TFFS)
- Phonon coupling → jump at N = 126
- Calculated μ for ^{207}gTl matches nicely with experimental data

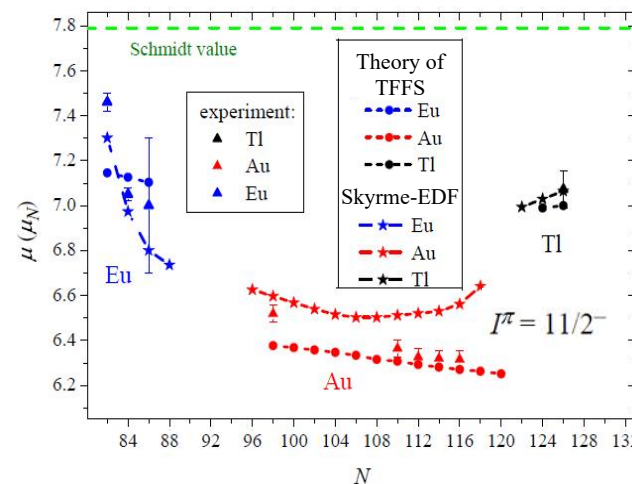
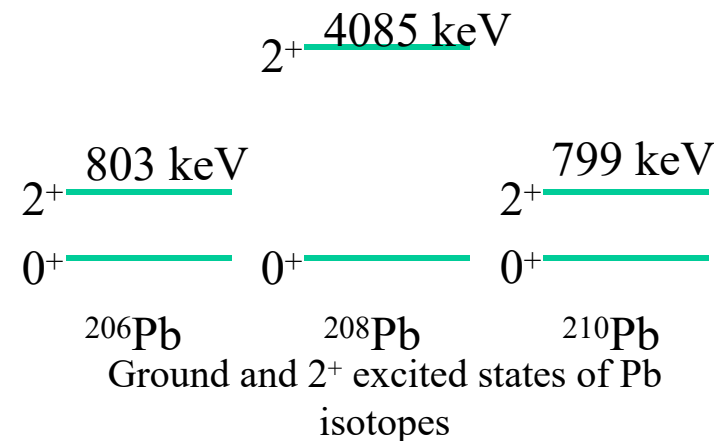


Physics Letters B
Volume 849, February 2024, 138452



Letter
Magnetic moments of thallium isotopes in the vicinity of magic $N=126$

Z. Yue^a , A.N. Andreyev^a , A.E. Barzakh^c, I.N. Borzov^c, J.G. Cubiss^a, A. Algora^d, M. Au^b , M. Bologh^f, S. Bara^g, R.A. Bark^h, C. Bernera^b , M.J.G. Borgeⁱ, D. Brugnara^f, K. Chrysalidis^b, T.F. Cocolios^g, H. De Witte^g, Z. Favier^b, L.M. Fraileⁱ, H.O.U. Fynbo^k, A. Gottardo^f , W. Wojtaczka^g



J. Bonnard, J. Dobaczewski, et al,
Phys. Lett. B 843 (2023) 138014,

Good agreement in describing the Eu and Tl 11/2- isomers

Neutron-rich Hg isotopes at ISOLDE



Hg Physics motivation - configurations, log ft, T_{1/2}, (P_n)

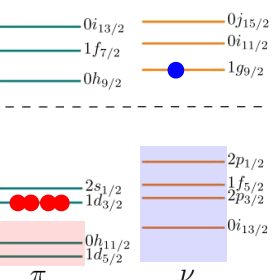
- Competition between allowed and first forbidden β decays due to single particle orbits near Fermi surface
- T_{1/2}, log ft, P_n place constraints on models used for r-process network calculations
- Little available data primarily from in-beam and isomer-decay studies
 - β decay schemes of $^{210,211}\text{Hg}$ unknown
 - Conflicting results for ^{209}Hg decay
- Hyperfine structure + isotope shift measurements will provide radii and moments data
- **Strong theoretical effort**- large scale shell model calculations log ft for FF decays

PHYSICAL REVIEW LETTERS 125, 192501 (2020)

Competition between Allowed and First-Forbidden β Decay: The Case of $^{208}\text{Hg} \rightarrow ^{208}\text{Tl}$

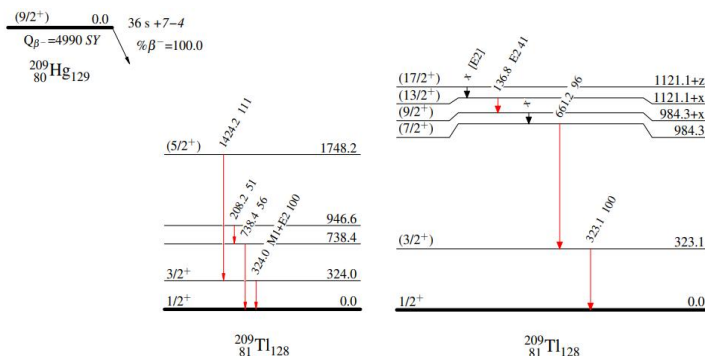
R.J. Carroll,¹ Zs. Podolyák,^{1,2} T. Berry,¹ H. Grawe,³ T. Alexander,¹ A.N. Andreyev,^{4,22} S. Ansari,⁵ M.J.G. Borge,⁶ M. Brunet,¹ J.R. Creswell,⁷ L.M. Fraile,⁸ C. Fähnle,⁹ H.O.U. Fynbo,¹⁰ E.R. Gamla,¹¹ W. Gelletly,¹ R.-B. Gerst,⁵ M. Gherghescu,³ A. Gresham,⁷ D.T. Gremmels,^{12,13} I. I. Hartnacke, Bremann,⁷ M. Hutsu,¹⁴ Q.M. India,¹⁵ D. S. Indian,⁷

In this context the nuclei in the $N = 126$ region are of particular interest [8] because first-forbidden (FF) β decays successfully compete [9–15] with allowed Gamow-Teller (GT) and Fermi decays, and this impacts on the calculations of r-process nucleosynthesis abundances [16]. However, the calculation of FF β decay is notoriously difficult and subject to debate.



Isotope	T _{1/2} Lanzhou	T _{1/2} GSI	T _{1/2} ISOLDE
^{208}Hg	41^{+5}_{-4} min [1]	132.2 ± 50.0 s [3]	135 ± 10 s [4]
^{209}Hg	35^{+9}_{-6} s [2]	6.3 ± 1.1 s [3]	–
^{210}Hg	–	–	–
^{211}Hg	–	–	–

[1] L. Zhang *et al.*, CPL **14**, 507 (1997); [2] Zhang Li *et al.*, PRC **58**, 156 (1998); [3] R. Caballero-Folch *et al.*, PRC **95**, 064322 (2017); [4] R. J. Carroll *et al.* PRL **125**, 192501 (2020).



Lanzhou, decay
Zhang Li *et al.*, PRC **58**, 156 (1998)

GSI, isomer
N. Al-Dahan *et al.*, PRC **80**, 061302(R) (2009).

Hg Physics motivation - masses

- So far, only measured up to ^{208}Hg – values in AME for more neutron-rich cases extrapolated from systematic trends (large uncertainties).
- Study trend in S_{2n} beyond $N=126$ in $Z<82$ region, use ΔS_{2n} to probe weakening of $N=126$ closure
- Explore interaction strength between last proton and neutron, δV_{pn} , in poorly studied region $\frac{1}{4}[\{B(Z, N) - B(Z - 2, N)\} - \{B(Z - 2, N) - B(Z - 2, N - 2)\}]$
- Derived mass excess important for restricting nuclear mass models - input for r -process network calculations.
 - Requires ~50 keV precision [J. Clark *et al.*, EPJA **59**, 204 (2023)]

PRL **94**, 092501 (2005) PHYSICAL REVIEW LETTERS week ending 11 MARCH 2005

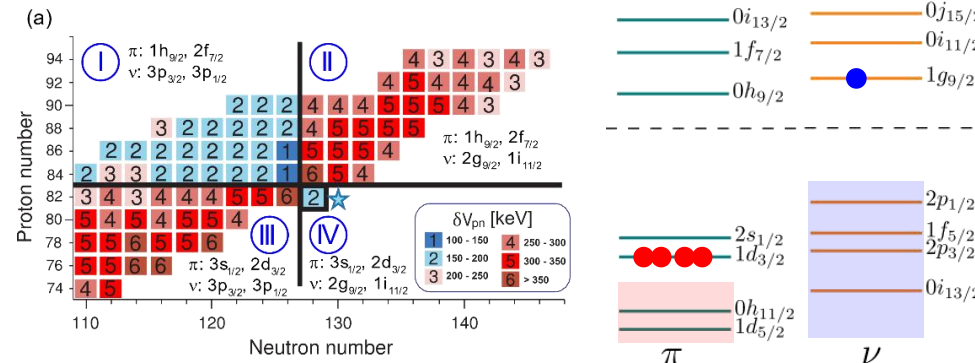
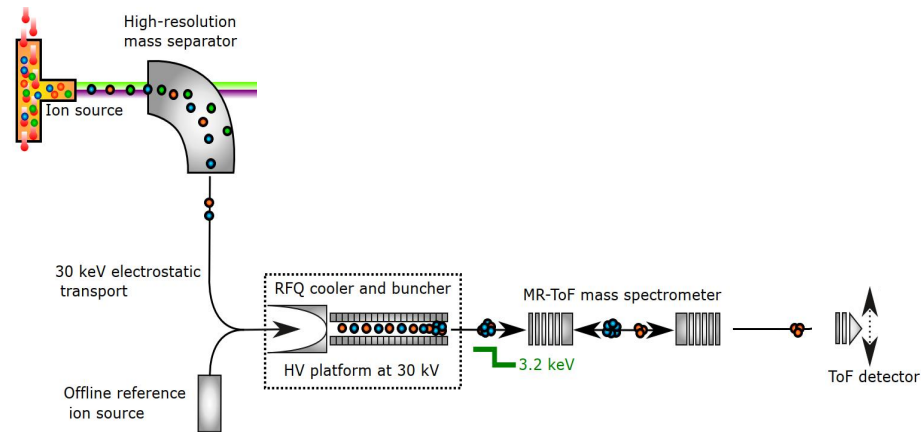
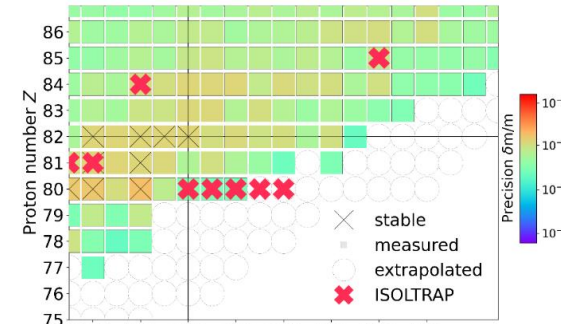
Proton-Neutron Interactions and the New Atomic Masses

R. B. Cakirli,^{1,2} D. S. Brenner,^{1,3} R. F. Casten,¹ and E. A. Millman¹

PRL **102**, 122503 (2009) PHYSICAL REVIEW LETTERS week ending 27 MARCH 2009

Schottky Mass Measurement of the ^{208}Hg Isotope: Implication for the Proton-Neutron Interaction Strength around Doubly Magic ^{208}Pb

L. Chen,^{1,2} Yu. A. Litvinov,^{1,*} W. R. Plab,^{1,2} K. Beckert,¹ P. Beller,¹ F. Bosch,¹ D. Boutin,² L. Caceres,¹ R. B. Cakirli,^{3,4} T. Chomaz,^{5,6} E. Casten,^{4,6} P. Chakrabarty,⁷ D. M. Cullen,^{8,11} T. Cullen,⁹ P. Esbensen,¹⁰ H. Gelman,^{1,2} I. Gaitan,¹



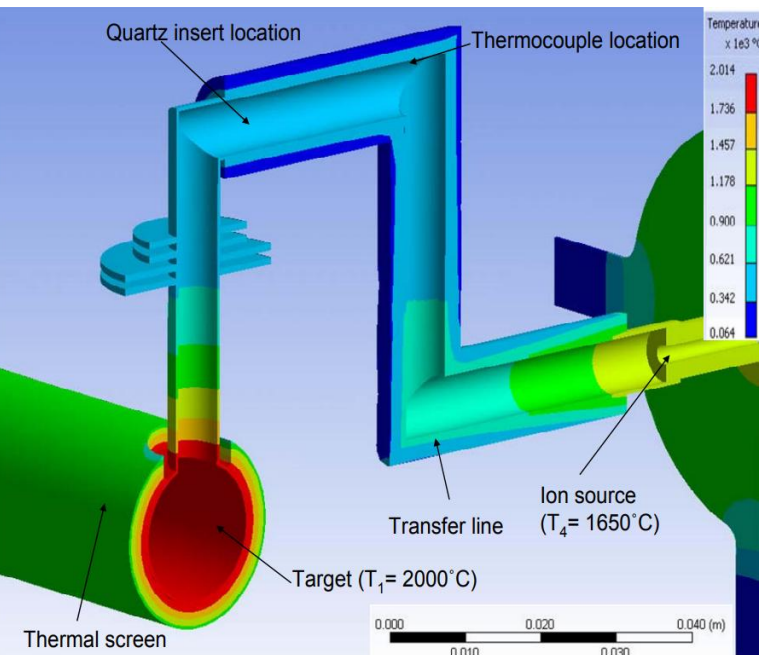
LOI244 - test for neutron-rich Hg's 6 shifts, quartz transfer line

A.Andreyev et al, LoI244



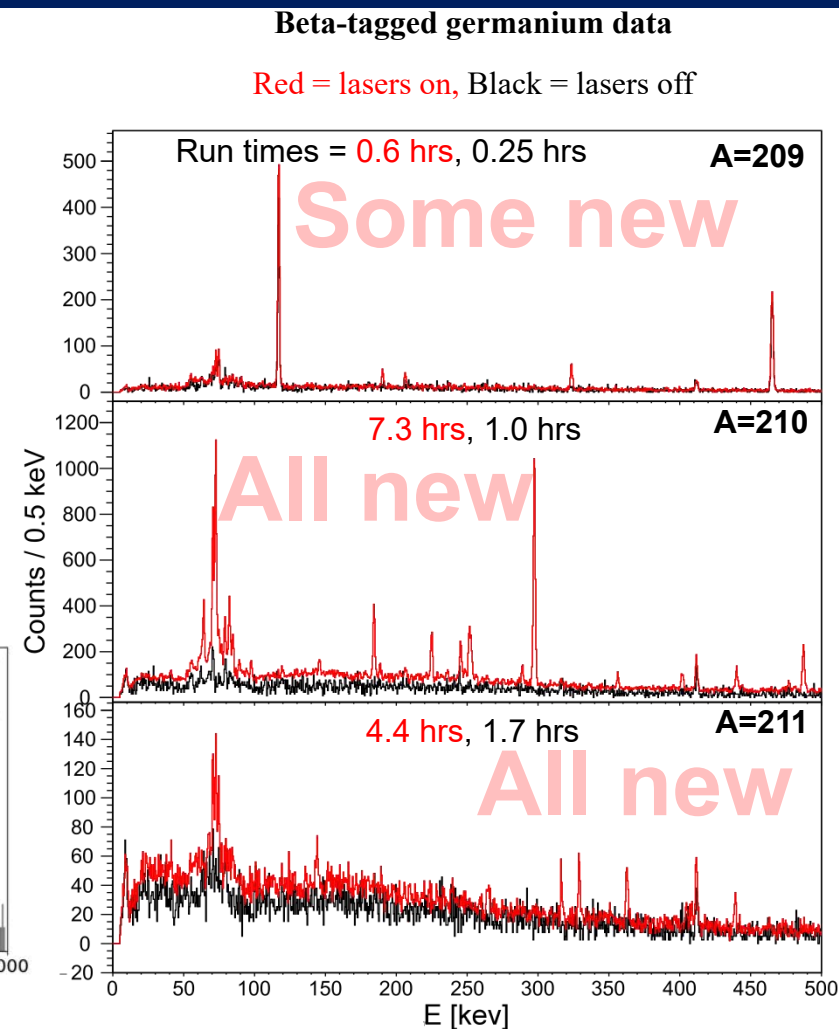
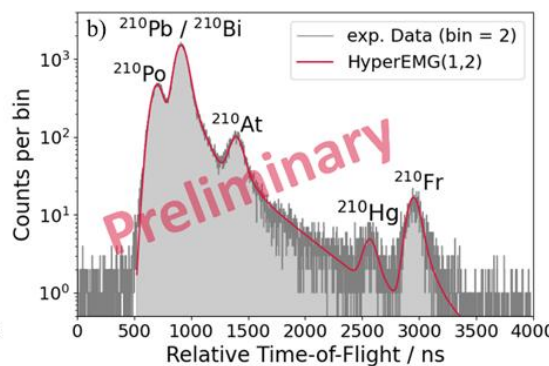
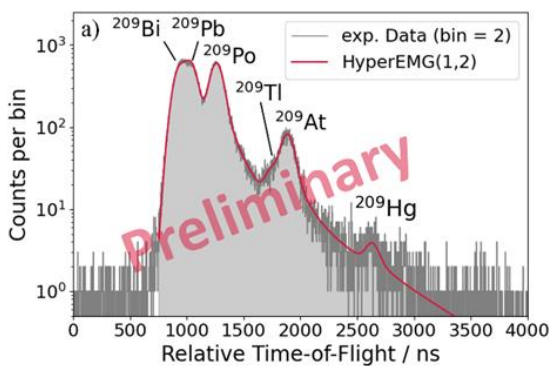
Very strong contamination from isobaric surface-ionized Fr

We use cold quartz transfer line



LOI244 - test for neutron-rich Hg's 6 shifts, quartz transfer line

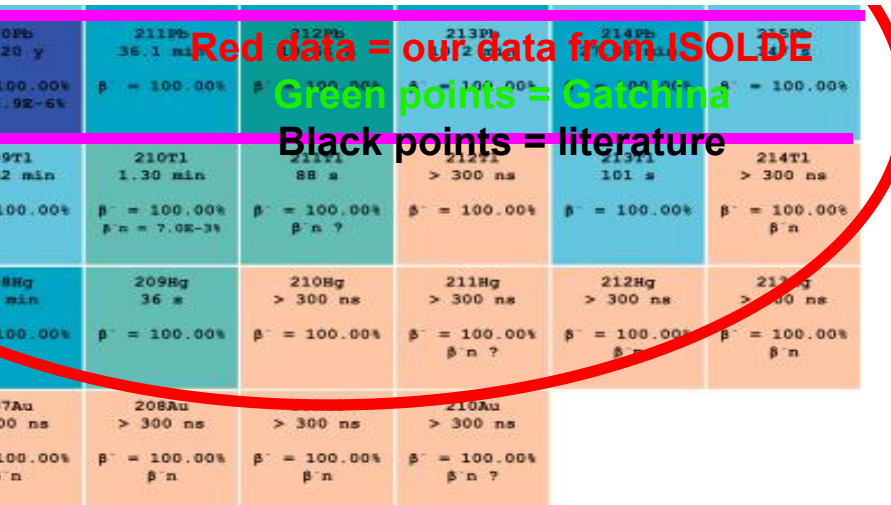
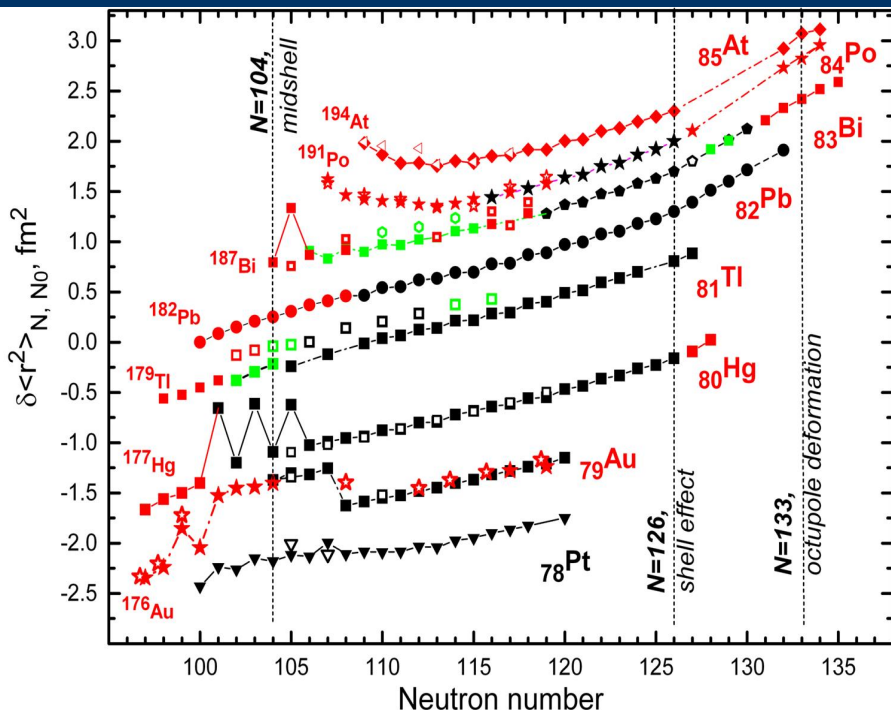
- Decay measurements $^{209-211}\text{Hg}$ – **Brand new results!**
 - No evidence of contaminants – suppressed or too long-lived
 - Clear difference in lasers on/off data – presence of laser ionised Hg
 - High enough rates for dedicated laser and decay studies
 - Preliminary data indicates previous decay schemes for ^{209}Hg is not correct
- Mass spectra for $^{209,210}\text{Hg}$ with MR-ToF – **First ever measurements!**
 - Recorded ~7 ions per shot.
 - Data contain systematic shifts due to space-charge effects – unquantifiable effect in this dataset
 - Quartz line used for experiment before – observed contamination possibly due to some saturation of the line



Isotope	Yield estimate from LoI244 [ions/ μC]	Decay	Mass	Laser
^{209}Hg	4(1)	●	●	●
^{210}Hg	4(1)	●	●	●
^{211}Hg	0.5(1)	●	Will try	Will try
^{212}Hg	n/a	Will try	Will try	Will try

Summary

- Neutron-rich Tl-Bi nuclei are one of the least experimentally explored regions of nuclear chart – “Terra incognita” for nuclear and laser spectroscopy
- However, several techniques are still available to access this region, in particular fragmentation reactions at ISOLDE, GSI-FRS and RIBF-RIKEN.
- Complementary data can be obtained, such as radii/momenta (ISOLDE), short-lived isomers (GSI/RIKEN), beta-gamma, fast timing...

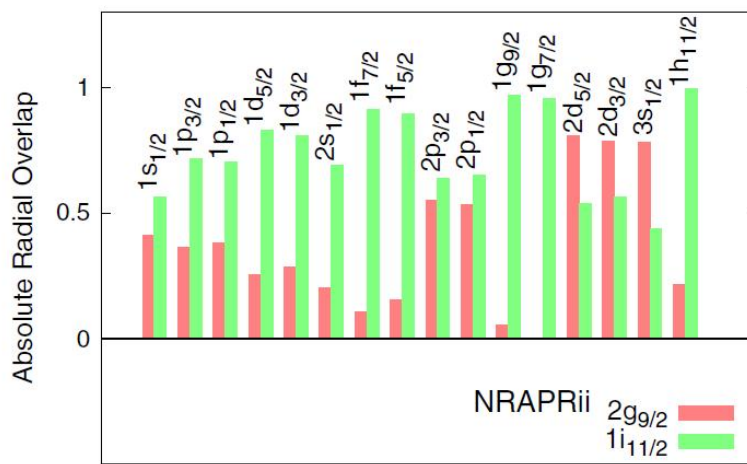
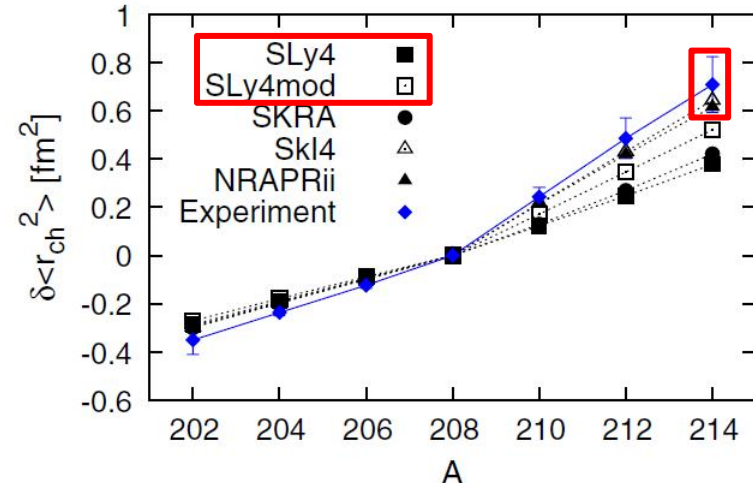
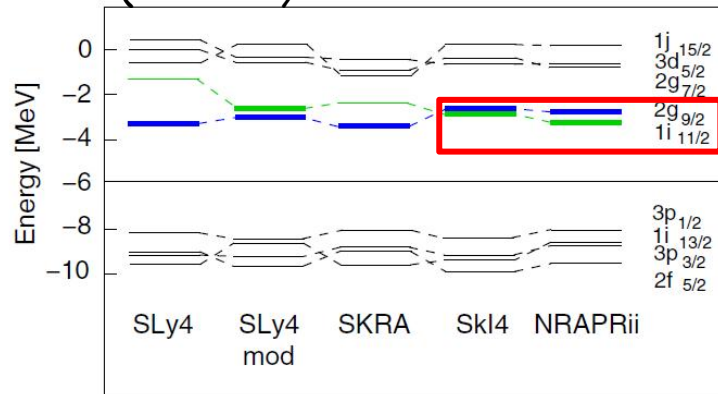


²⁰⁸ Tl	26.0 min	²⁰⁹ Tl	28.4 s	²¹⁰ Tl	60 s	²⁰⁸ Au	39.8 s	²⁰⁹ Au	32.5 s	²¹⁰ Au	> 100 ns	²⁰⁷ Au	> 100 ns	²⁰⁸ Au	40	²⁰⁹ Au	100.00%	²¹⁰ Au	100.00%	²¹¹ Au	100.00%	²¹² Au	100.00%	²¹³ Au	100.00%	²¹⁴ Au	100.00%
	β^- = 100.00%		β^- n ?		β^- n ?		β^- = 100.00%		β^- n ?		β^- = 100.00%		β^- n ?		β^- = 100.00%												

Thank you!

Role of $1i_{11/2}$ neutron occupancy on the kink around the lead region?

P. M. Goddard et al. PRL 110,
032503 (2013)

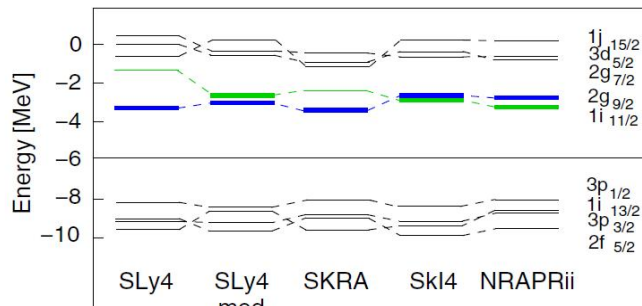


Overlap of $1i_{11/2}$ significantly
 $> 2g_{9/2}$

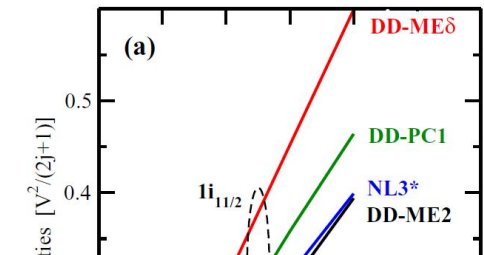
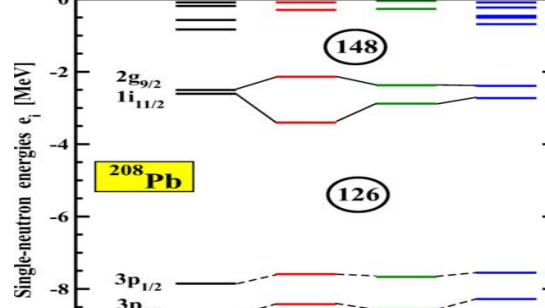
Goal: High-spin isomers $^{212m1,m2,213m}\text{Bi}$ and the N=126 kink problem

Properties of the high-spin isomers $^{212m1,m2,213m}\text{Bi}$ and their link to the kink in Bi gs charge radii at N=126:
is the position and occupation of the $i_{11/2}$ neutron orbital a real culprit for the N=126 kink?

Skyrme, P.M. Goddard et al, PRL110 (2013)



Relativistic, T. Day Goodacre et al, PRC104,054322(2021)

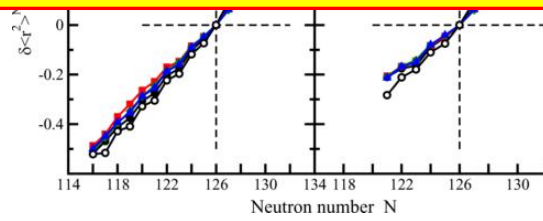
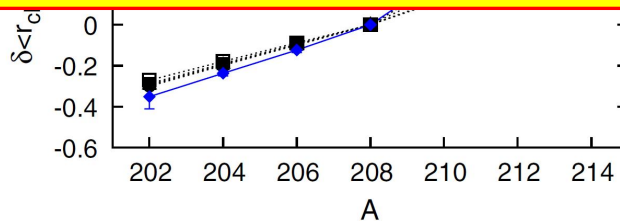


This effect can be probed by charge radii of high-spin isomers in $^{212m2,213m}\text{Bi}$, whose configuration **presumably includes an $i_{11/2}$ neutron**:

$^{212m2}\text{Bi}$ [$\pi h9/2 \times ((vg9/2)^2 \times vi11/2)$]18 $-$,

^{213m}Bi [$\pi h9/2 \times (vg9/2 \times vi11/2)$]25/2 $-$,

relative to their gs's or $^{212m1}\text{Bi}$ [$\pi h9/2 \times vg9/2)$]8 $-$, 9 $-$, which have no $i_{11/2}$ neutrons.



It seems the models in which **the $i_{11/2}$ neutron orbital is below g9/2** (or very close to it) reproduce the kink better, due to enhanced population of the $i_{11/2}$ orbital. **This is a common property of relativistic approaches.**

212g,m1,m2Bi (N=129)

E(level) [†]	J ^π	T _{1/2}	XREF	Comments
0.0	1 ⁽⁻⁾	60.55 min 6	AB	%β ⁻ =64.06 6; %α=35.94 6 Q=+0.1 4; μ=+0.32 4 μ: from laser resonance fluorescence spectroscopy (1997Ki15). Other: 0.41 5 from static low-temperature nuclear orientation (1997Ki15). Q: from laser resonance fluorescence spectroscopy (1997Ki15,2000Pe30,2001Bi23,2016St14). Isotope shifts: 1997Ki15, 2000Pe30. J ^π : log ft from 0 ⁺ suggests J=0 or 1; αγ(θ) rules out J=0 (1986Ma17); π=− from shell model. T _{1/2} : weighted average of 60.480 min 52 (1914Le01) and 60.600 min 43 (1961Ap03). Other: 60.5 min (1949Me54,1948Gh01). %α: weighted average of 36.00 3 (1965Wa09), 35.81 4 (1962Be09), and 35.96 6 (1960Sc07). configuration=(π1h _{9/2})(ν2g _{9/2}).
239 30	(8 ⁻ ,9 ⁻)	25.0 min 2	C	%β ⁻ =33 1; %β ⁻ α=30 1; %α=67 1 E(level): from Schottky mass spectrometry (2013Ch12). Other: 250 from Eα=6.34 MeV to ²⁰⁸ Tl g.s. (1978Ba44). J ^π : J ^π =(9 ⁻) suggested by comparison with ²¹⁰ Bi. Possible configuration=(²¹⁰ Bi 9 ⁻)(ν2g _{9/2}) ⁺² 0 ⁺ (1978Ba44). J ^π =(8 ⁻) suggested by log ft value for β ⁻ decay to J ^π =8 ⁻ state in ²¹² Po (1991Wa18). T _{1/2} : from 1984Es01. Others: 28 min 1 (1980Le27), 25 min 1 (1978Ba44). %α,%β ⁻ : from 1a(25 min ²¹² Bi)/1a(²¹² Po) (1984Es01), see ²¹² Bi β ⁻ decay (25.0 min) data set. %β ⁻ α: from 1a(²¹² Po excited states) (see ²¹² Bi β ⁻ decay (25.0 min) data set).
1478 38	(18 ⁻)	7.0 min 3		%β ⁻ <25; %IT>75 E(level): from Schottky mass spectrometry (2013Ch12). J ^π : from β ⁻ decay to (18 ⁺) level in ²¹² Po, comparison to shell model calculations (2013Ch12, 1991Wa18). T _{1/2} : neutron atom half-life from 1984Es01. Others: 7 min 1 (1980Le27), 9 min 1 (1978Ba44). For highly-charged atoms (charge states of 80 ^{+,81^{+, and 82⁺), T_{1/2} > 30 min (2013Ch12). %IT,%β⁻: only a β⁻ delayed 11.65 MeV α (from 45.1 s ²¹²Po) with T_{1/2}=7.0 m has been observed. Taking log ft for this transition as 5.1 (lower limit for allowed β⁻ transition) and Elevel=1478 keV, the %IT branch must be >75%, as deduced by the evaluators.}}

212gBi

configuration=(π1h_{9/2})(ν2g_{9/2}).

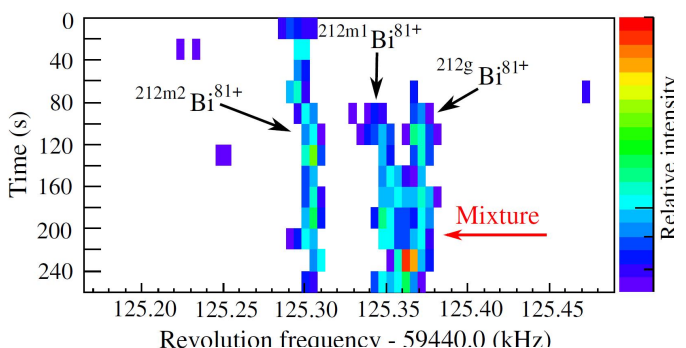
$$((^{210}\text{B} \ 9^-)(\nu 2g_{9/2})^{+2}0^+) \ (1978\text{Ba44}).$$

1478 38 (18⁻) 7.0 min 3

212m2Bi

%β⁻<25; %IT>75
E(level): from Schottky mass spectrometry (2013Ch12).
J^π: from β⁻ decay to (18⁺) level in ²¹²Po, comparison to shell model calculations (2013Ch12, 1991Wa18).
T_{1/2}: neutron atom half-life from 1984Es01. Others: 7 min 1 (1980Le27), 9 min 1 (1978Ba44). For highly-charged atoms (charge states of 80<sup>+,81<sup>+, and 82⁺), T_{1/2} > 30 min (2013Ch12).
%IT,%β⁻: only a β⁻ delayed 11.65 MeV α (from 45.1 s ²¹²Po) with T_{1/2}=7.0 m has been observed. Taking log ft for this transition as 5.1 (lower limit for allowed β⁻ transition) and Elevel=1478 keV, the %IT branch must be >75%, as deduced by the evaluators.</sup></sup>

212m2Bi [πh9/2×((vg9/2)²×vi11/2)]18⁻ ???



L. Chen et al., PRL 110, 122502 (2013)

213g,mBi (N=130)

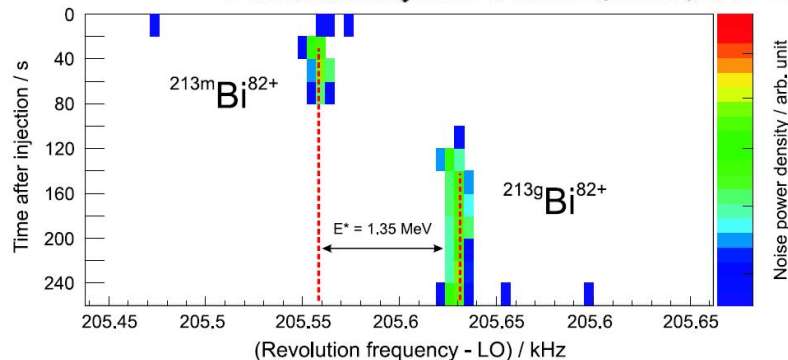
E(level) [†]	J ^π	T _{1/2}	XREF	Comments
0.0	9/2 ⁻	45.59 min 6	ABC	%α=2.140 10; %β ⁻ =97.860 10 μ=+3.699 7 Q=−0.83 5 Isotope shift: δ<r ² >(213Bi, ²⁰⁹ Bi)=0.422 fm ² 29 (2018Ba03). Other: 0.416 fm ² 1 (2013An02).
1353 21	C			J ^π (213At)=9/2 ⁻ based on ²²¹ Fr(J ^π)=5/2 ⁻ α decay → 218 level (J ^π)=5/2 ⁻ and → E2 γ to g.s. of 217At (1972Dz14, 1977Vy02). Also supported by the HFS and μ measurements (2019Ba22).

213gBi

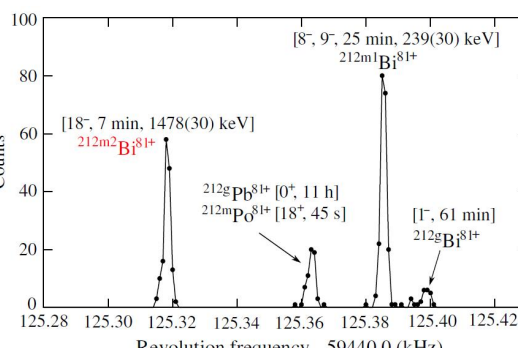
Configuration: $\pi (h_{9/2}^{+1})$.

213mBi

L. Chen et al., Nuclear Physics A 882 (2012) 71–89

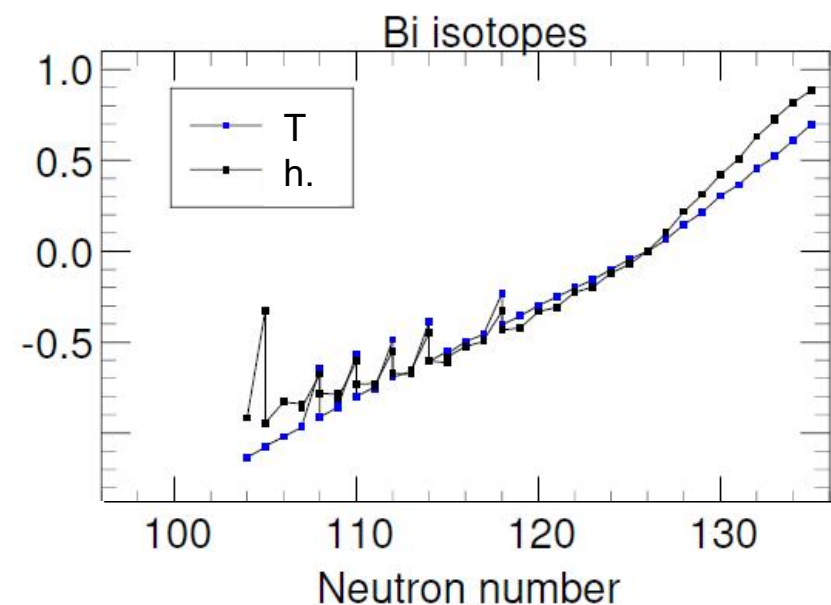
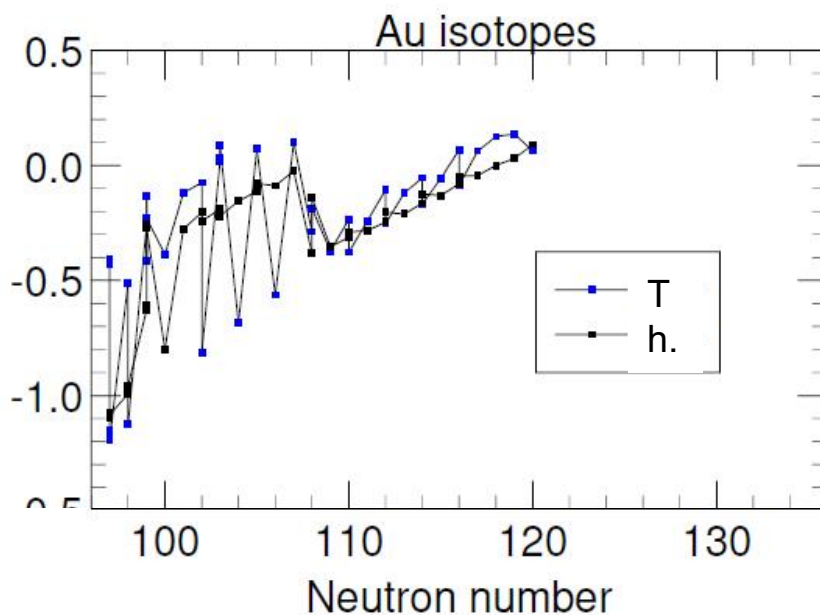


213mBi [πh9/2× (vg9/2×vi11/2)]25/2⁻ ???



HFB calcs.: odd-A and odd-odd nuclei

- Odd-A, and particularly odd-odd nuclei are a challenge for theory
- HFB using D1M-Gogny (S. Goriely *et al.*, PRL **102**, 242501 (2009).).
- Begin by selecting states with correct spin, and calculating ground state.

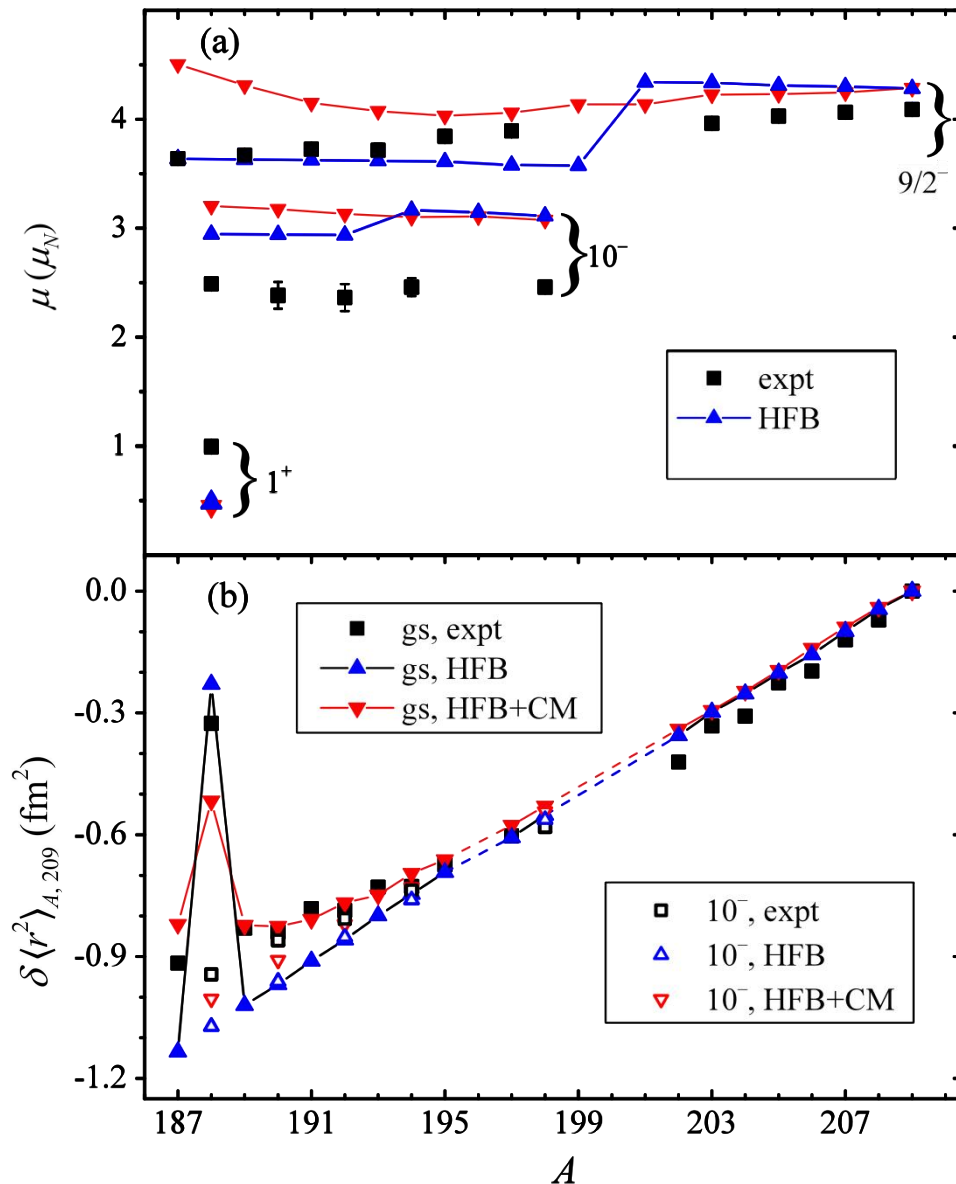
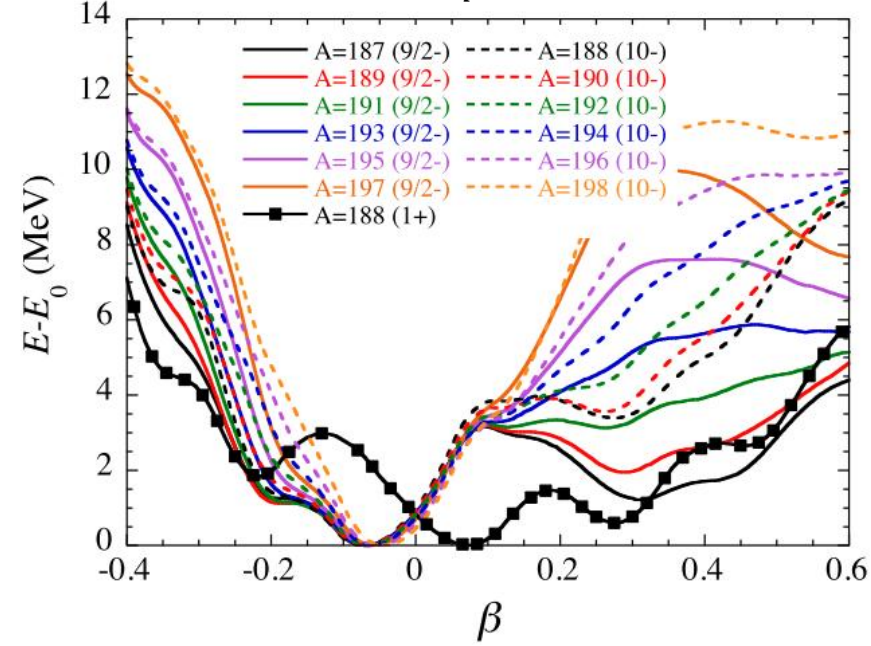


HFB for Bismuth

A.E. Barzakh *et al.*, PRL **127**, 192501 (2021)
 S. Péru *et al.*, PRC **104**, 024328 (2021)

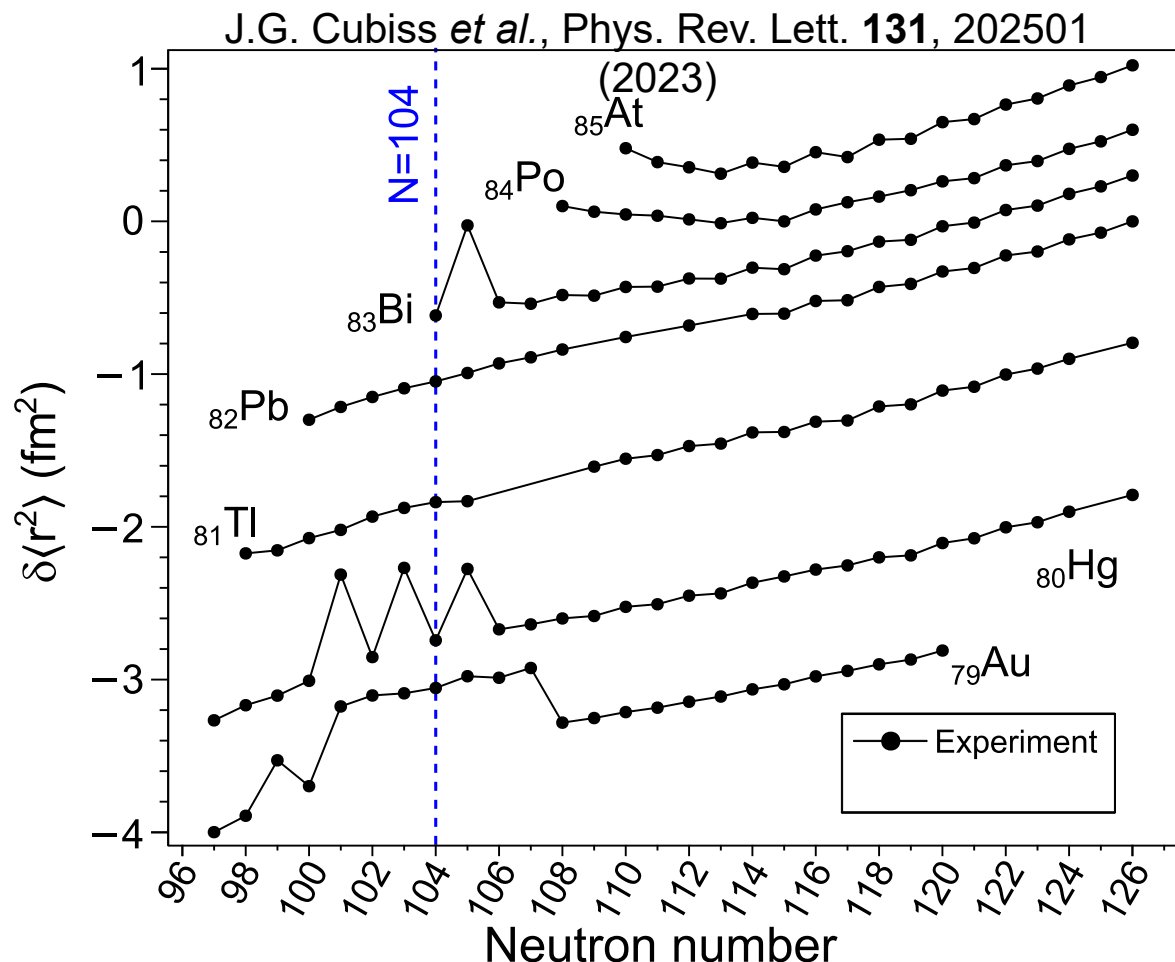
- Candidate states were selected by:
Correct spin, agreement with $\mu, < 1$ MeV
- Configuration mixing** across deformation surface introduced:

$$\langle \mathcal{O} \rangle = \frac{\int_q \mathcal{O} \exp(-E/T) dq}{\int_q \exp(-E/T) dq}$$



Charge-radii across the lead region, from Au to At (Z=79 to 85)

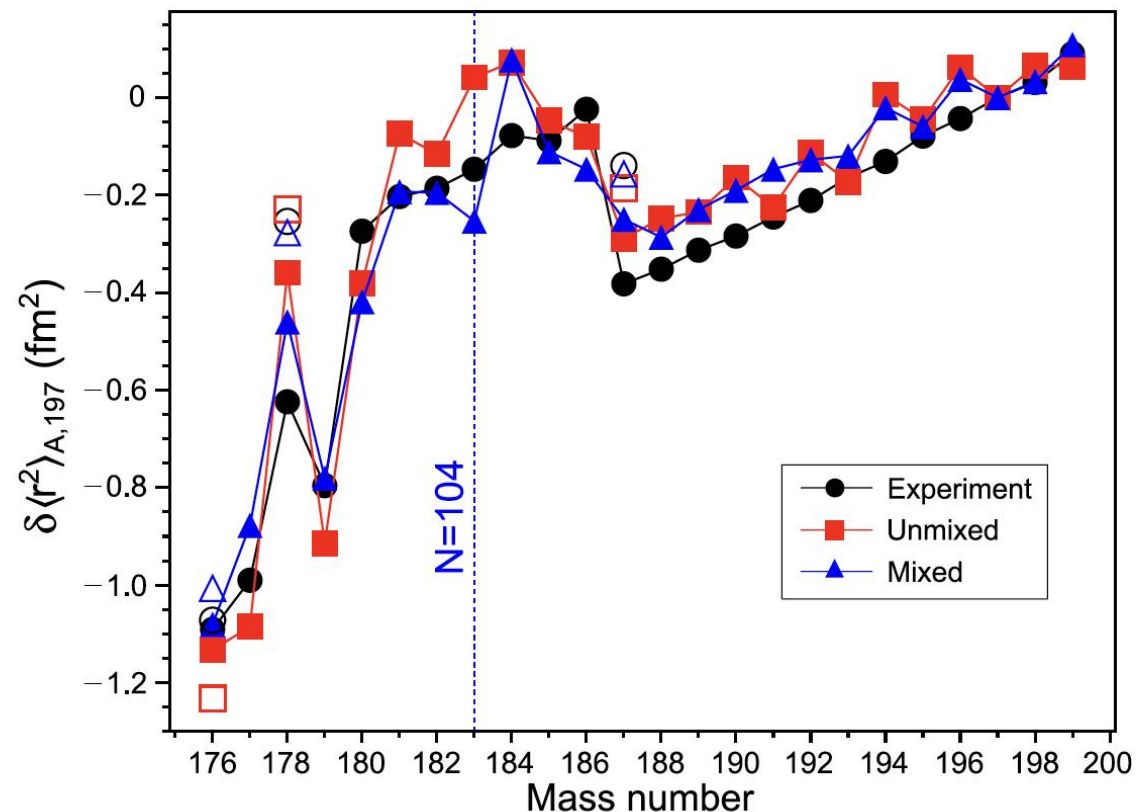
- Try applying same approach to proton-rich ground states of all chains we have measured ($Z=79$ - 85 , ≈ 160 isotopes)
- All results here include mixing, using same statistical approach



Charge-radii across the lead region, from Au to At (Z=79 to 85)

- Try applying same approach to proton-rich ground states of all chains we have measured (Z=79-85, ≈ 160 isotopes)
- All results here include mixing using same statistical approach

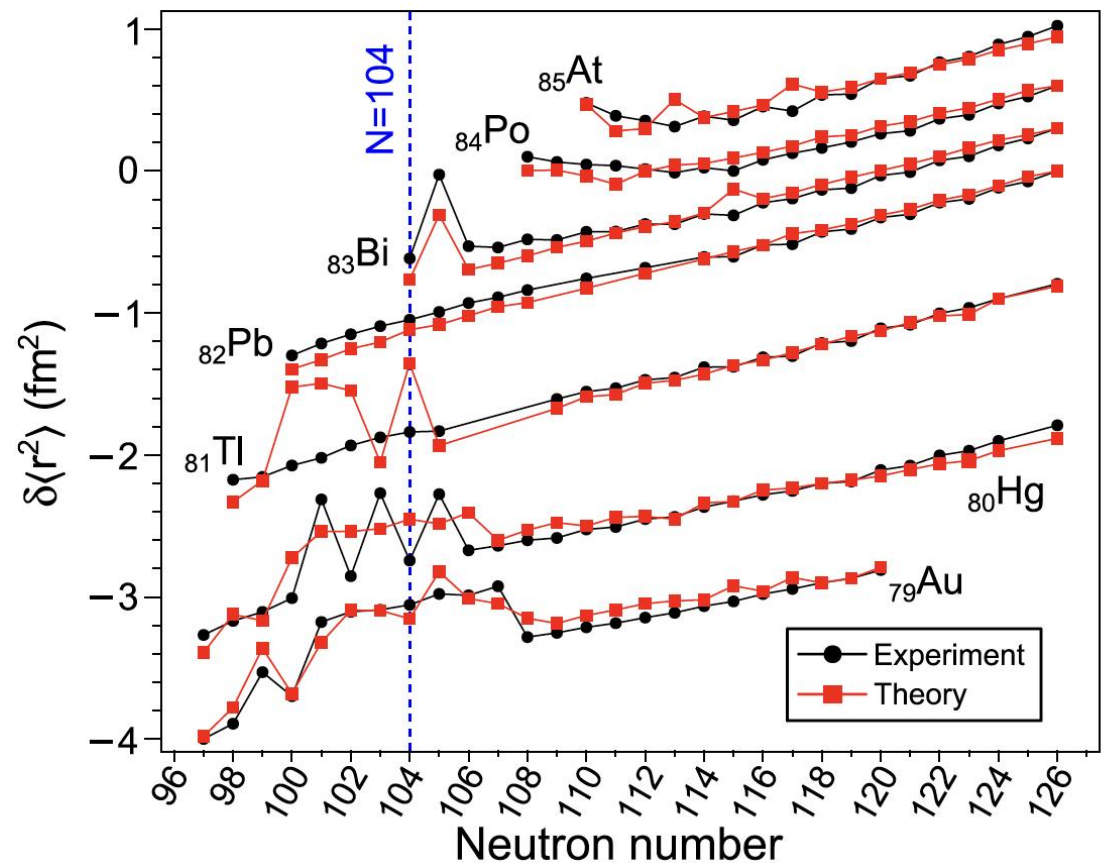
J.G. Cubiss *et al.*, Phys. Rev. Lett. **131**, 202501 (2023)



Charge-radii across the lead region, from Au to At (Z=79 to 85)

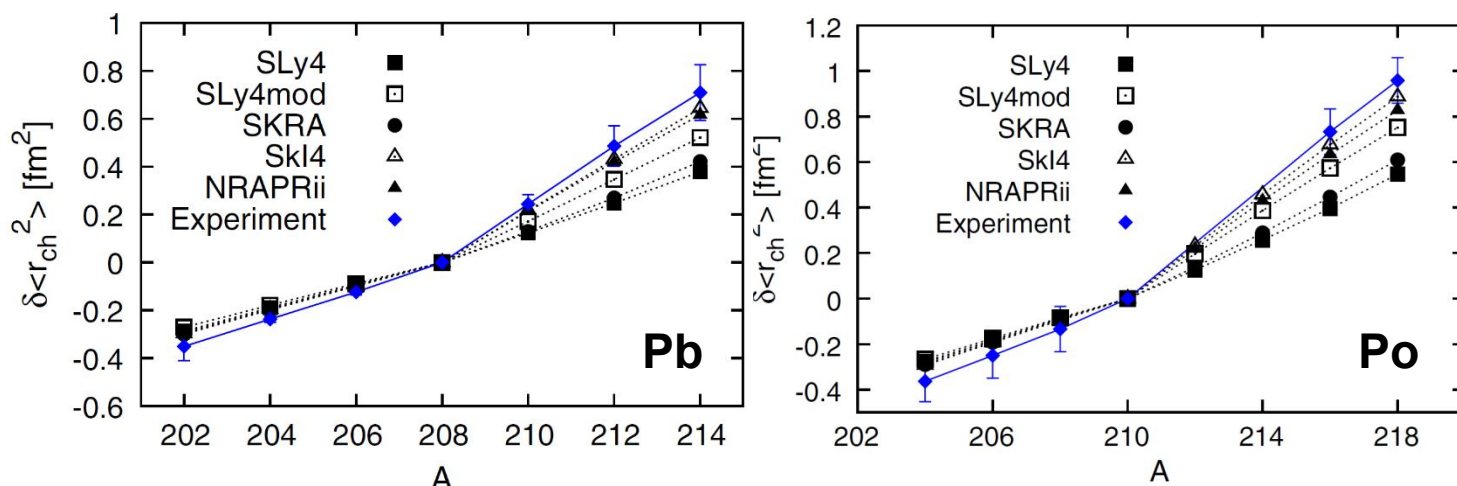
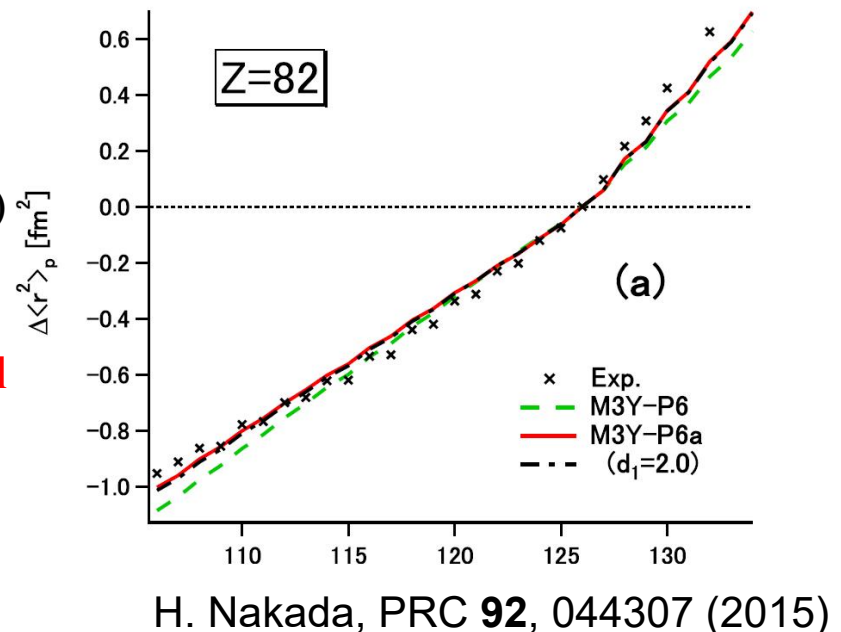
- Try applying same approach to proton-rich ground states of all chains we have measured ($Z=79$ - 85 , ≈ 160 isotopes)
- All results here include mixing, using same statistical approach

J.G. Cubiss *et al.*, Phys. Rev. Lett. **131**, 202501 (2023)



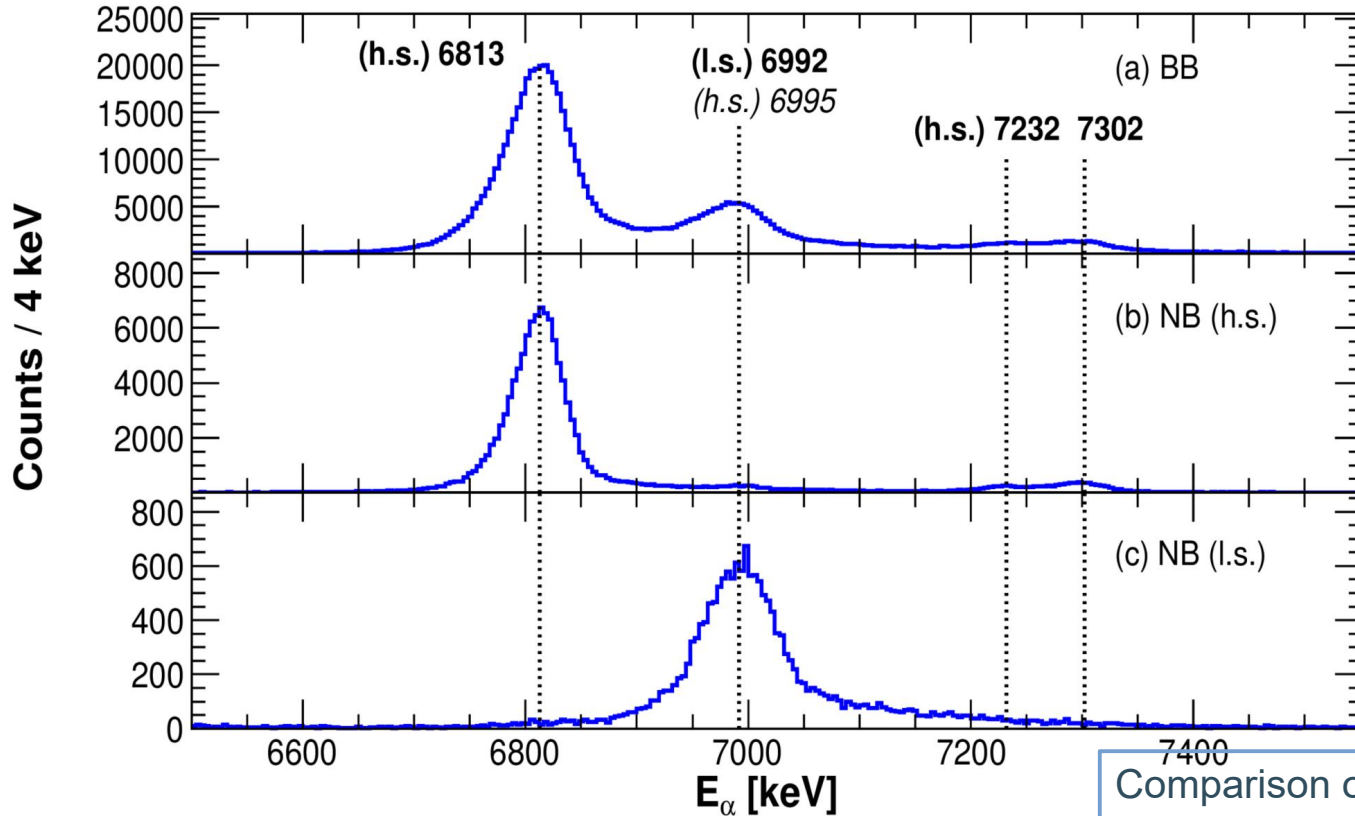
The Kink at N=126 - (some of) theoretical description

- Number of theoretical attempts at describing this:
 P.M. Goddard *et al.*, PRL **110**, 032503 (2013)
 H. Nakada & T. Inakura, PRC **91**, 021302(R) (2015)
 H. Nakada, PRC **92**, 044307 (2015)
- All invoke a significant occupation of $\nu i_{11/2}$ orbital**
- Not consistent with experiment!
 ^{209}Pb and ^{211}Po have magnetic moments consistent with pure $\nu g_{9/2}$ states



P.M. Goddard *et al.*, PRL **110**, 032503 (2013)

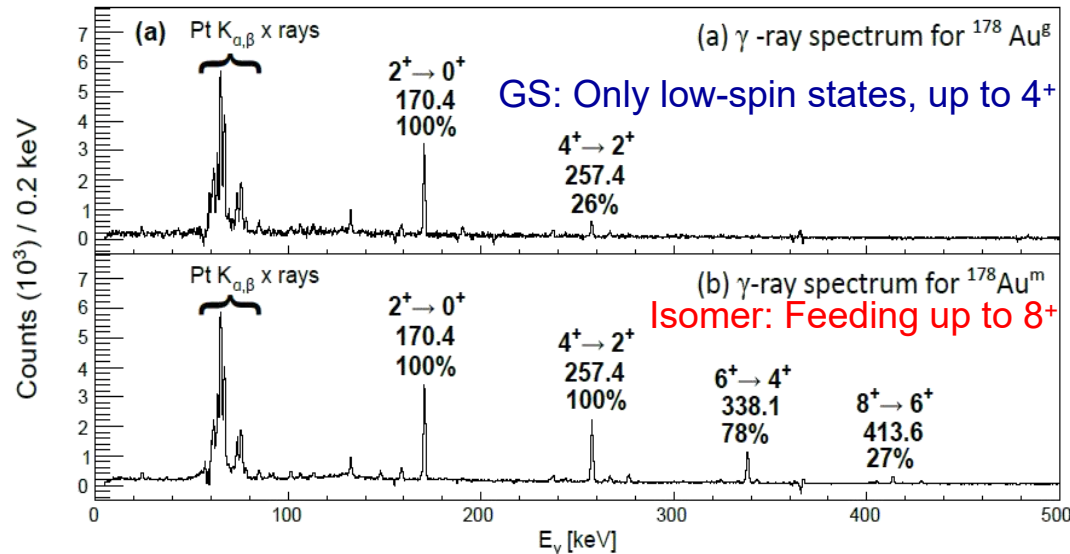
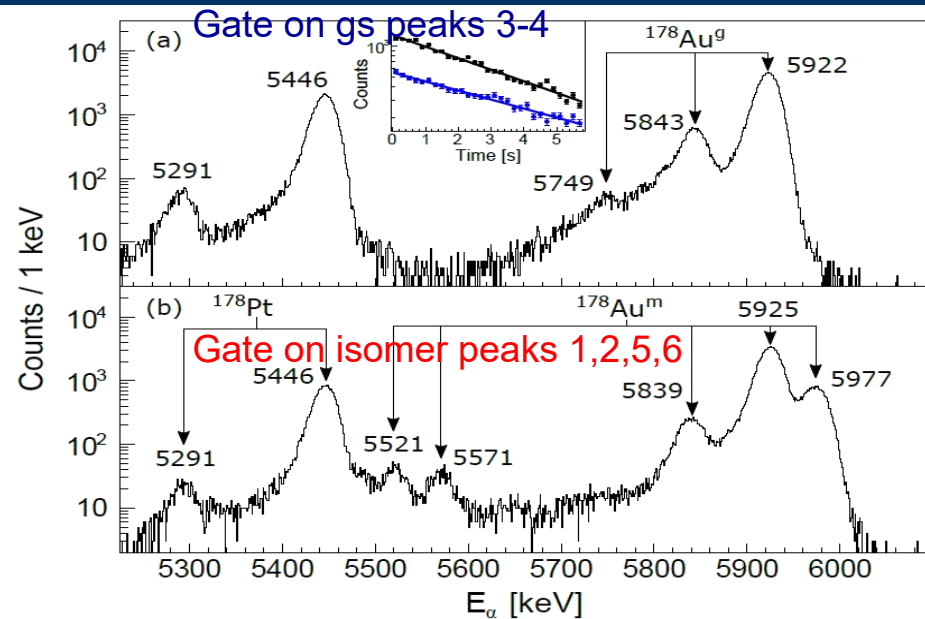
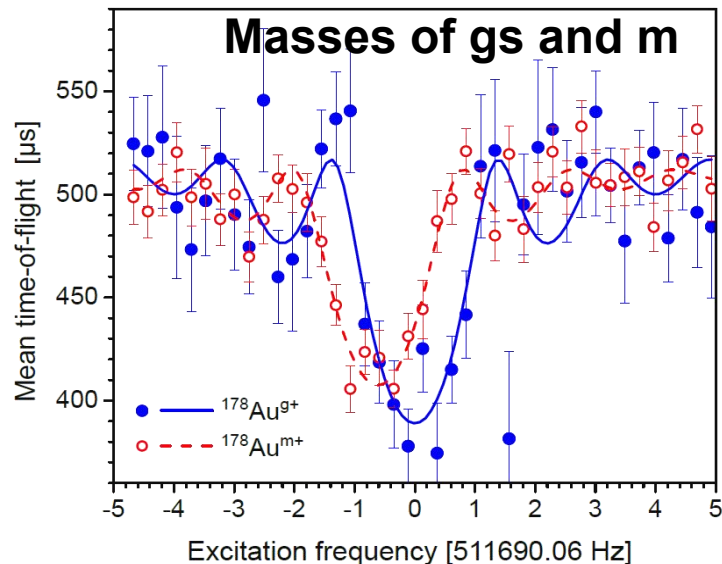
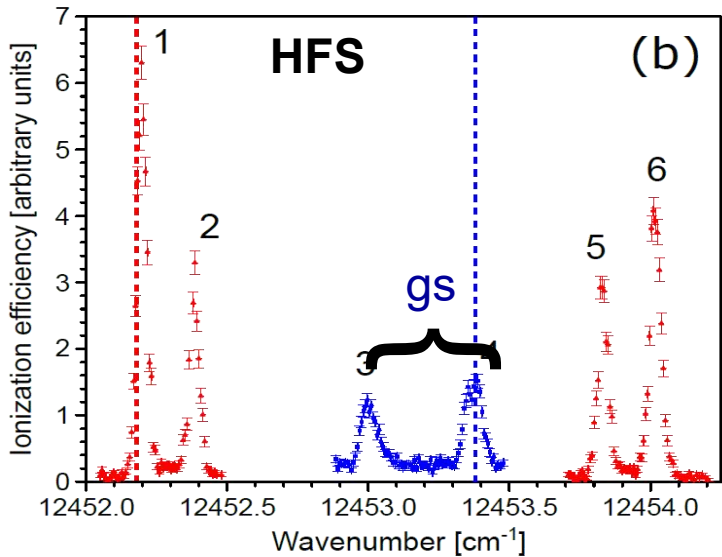
^{188}Bi : Isomer separation



Comparison of α -decay spectra for different laser modes: broad bandwidth, narrow bandwidth for high-spin isomer, narrow bandwidth for low-spin isomer.

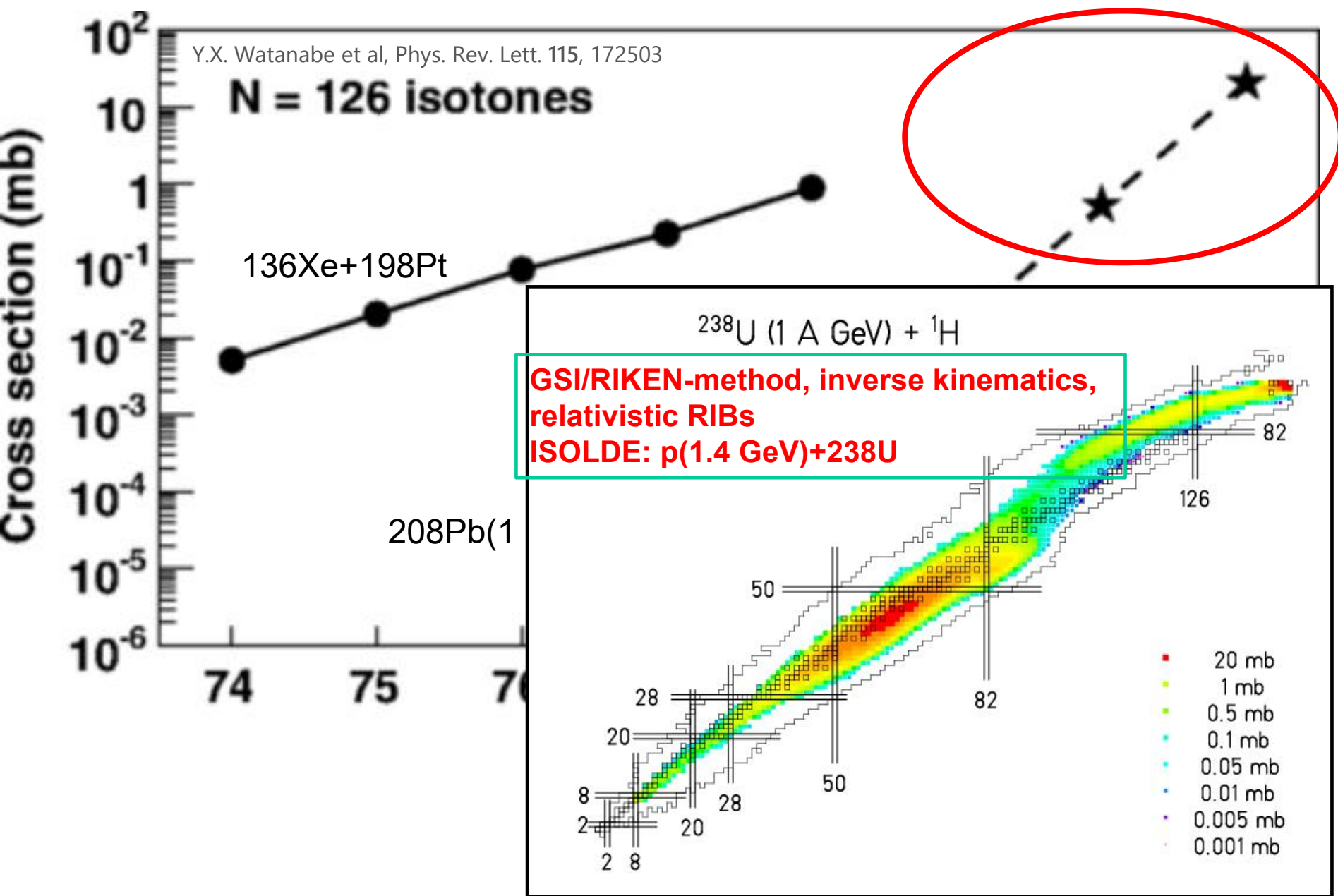
Example on Isomer Selectivity in $^{178}\text{gs},\text{m}\text{Au}$

J.G. Cubiss (York) et al., in preparation

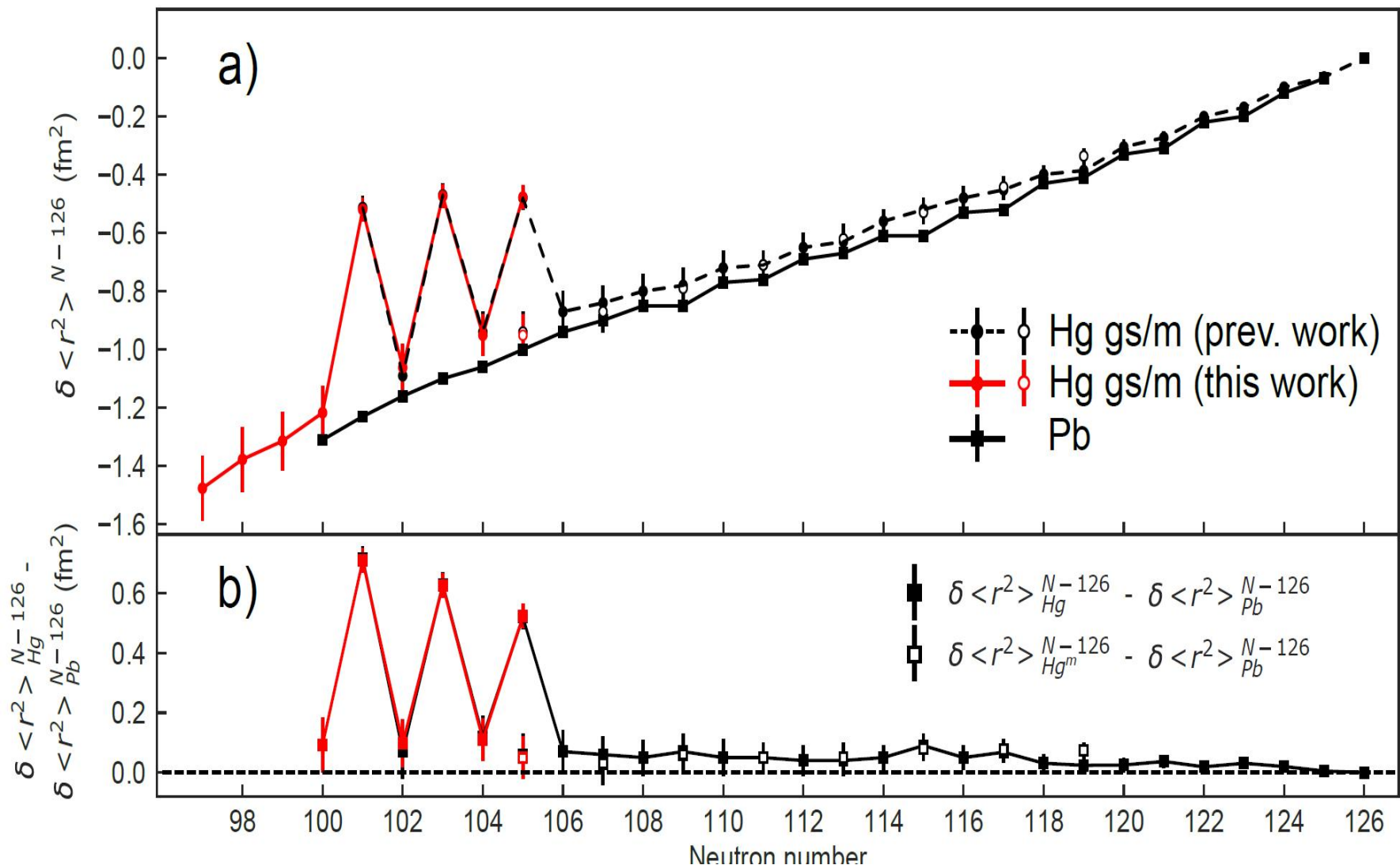


Opens up a totally new area of reactions studies with isomerically-clean beams! (e.g. spin-dependence of reactions, in this case with low spin ground state or with high-spin isomeric beam)

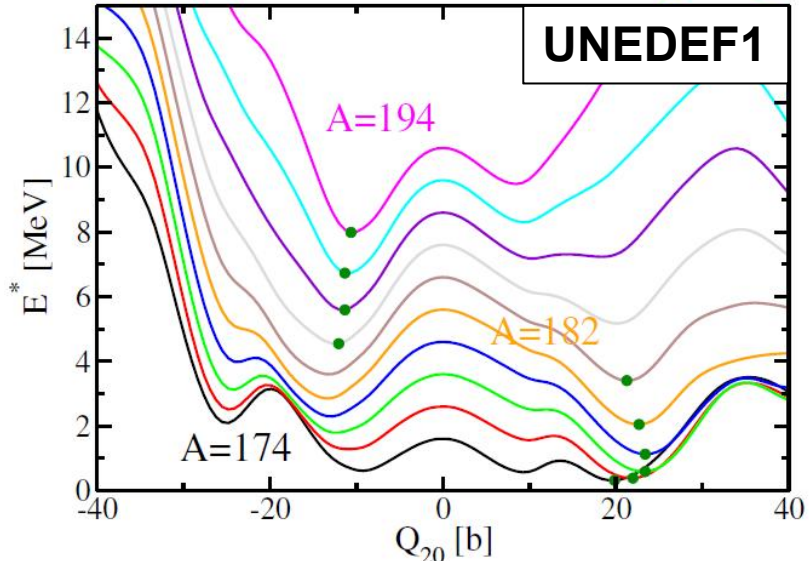
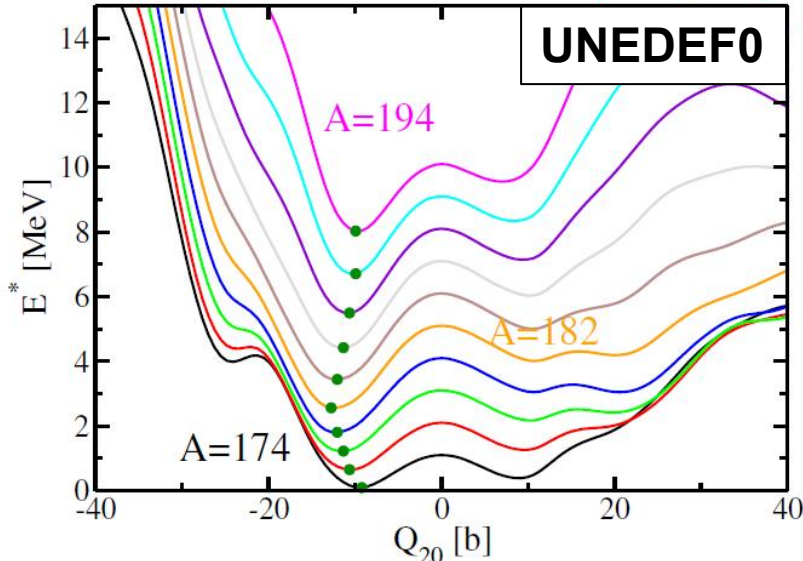
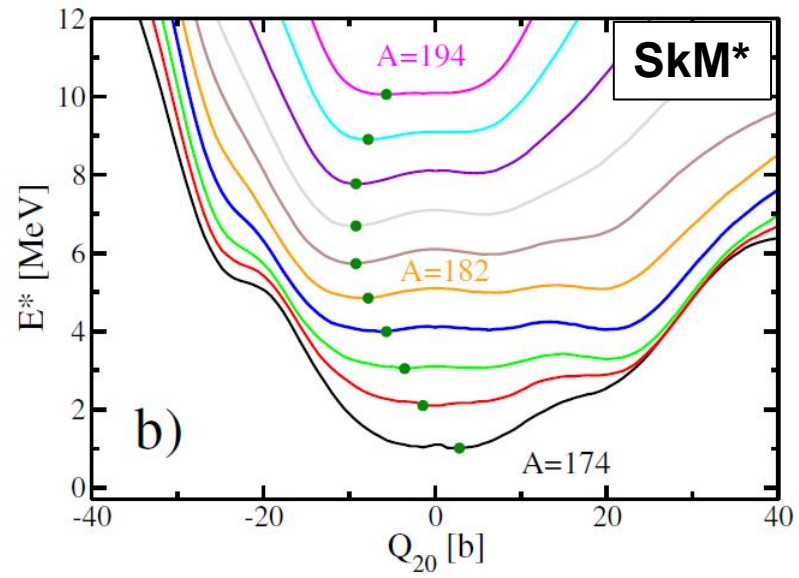
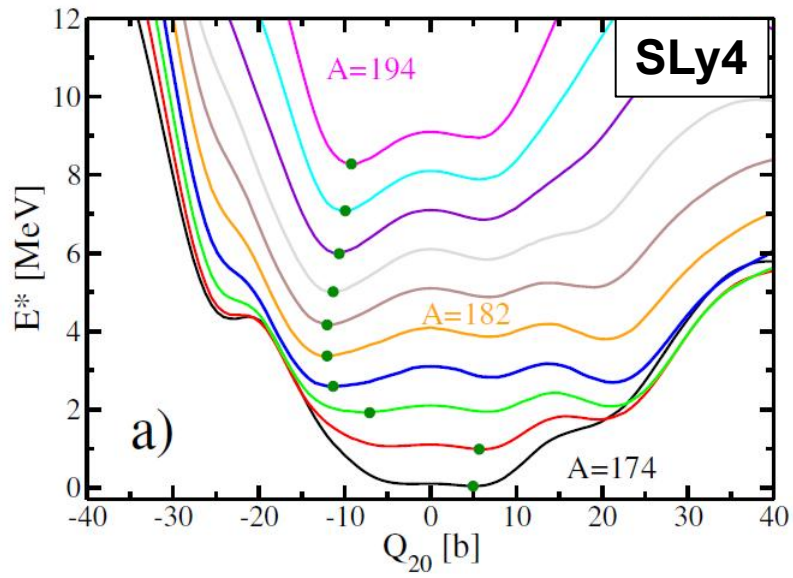
How to get to N=126 nuclei (and beyond)?



Comparison Hg vs Pb chains

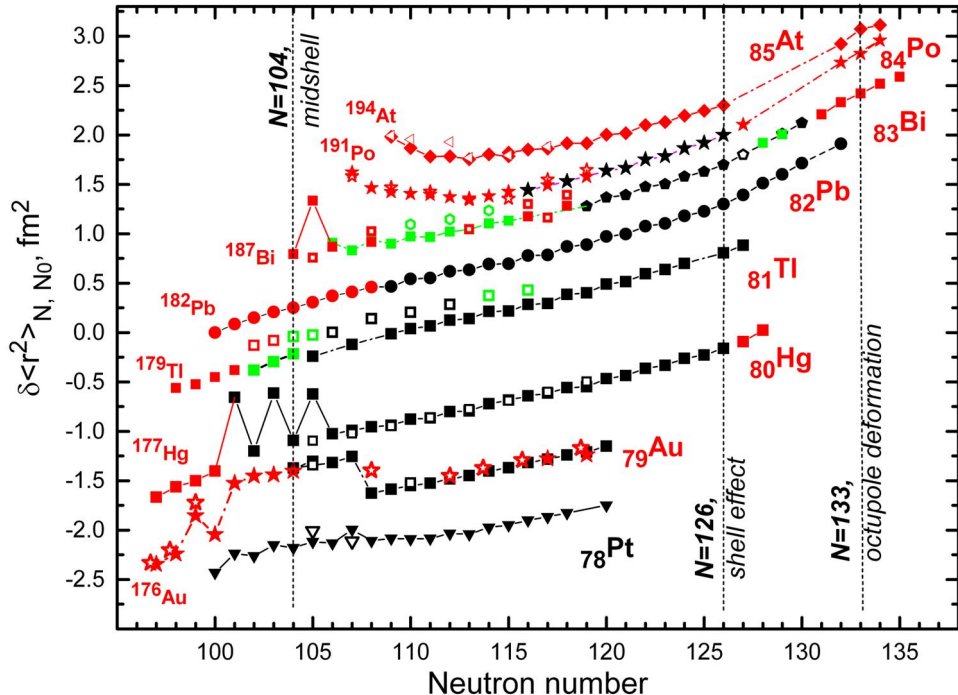


DFT Potential Energy Surfaces (even-even Hg's)



Summary

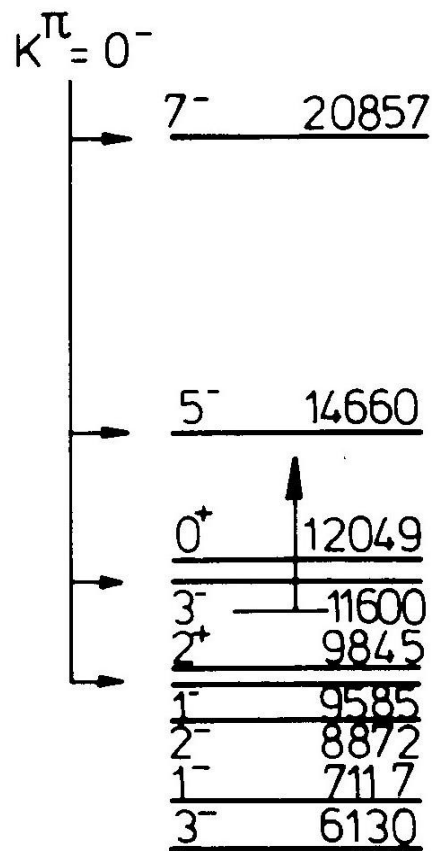
- **In-source laser spec. powerful and versatile tool**
 - Extensive campaign performed throughout Pb region
 - Unique sensitivity vital for most exotic cases
 - Wealth of spectroscopic info. to challenge models
- **“Global” models do much better than expected**
 - Candidate states present for all ground states
 - Magnetic moments powerful identifying tool
 - Shape mixing at microscopic level needs introducing
- **Kink phenomenon still needs exploring**
 - Different mechanisms proposed for producing trend, RMF and Fayans calculations look very promising
 - Moments of odd-N cases could be key
 - High-spin Bi isomers experiment to provide further tests
 - Search for global Fayans parameterisation ongoing
- **Still much to learn and explore**
 - LIST opens up new opportunities in n-rich region
 - Still plenty to explore, to learn and fun to be had.



Red data = our data from ISOLDE
Green points = Gatchina
Black points = literature

Shape Coexistence in Nuclei *(a brief introduction)*

Spherical Doubly-Magic ^{16}O ($Z=N=8$)



Ground State 0p-0h Spherical configuration

Protons π

$1d_{5/2}$

8

$1p_{1/2}$

$1p_{3/2}$

$1s_{1/2}$

Neutrons ν

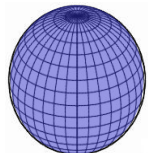
$1d_{5/2}$

8

$1p_{1/2}$

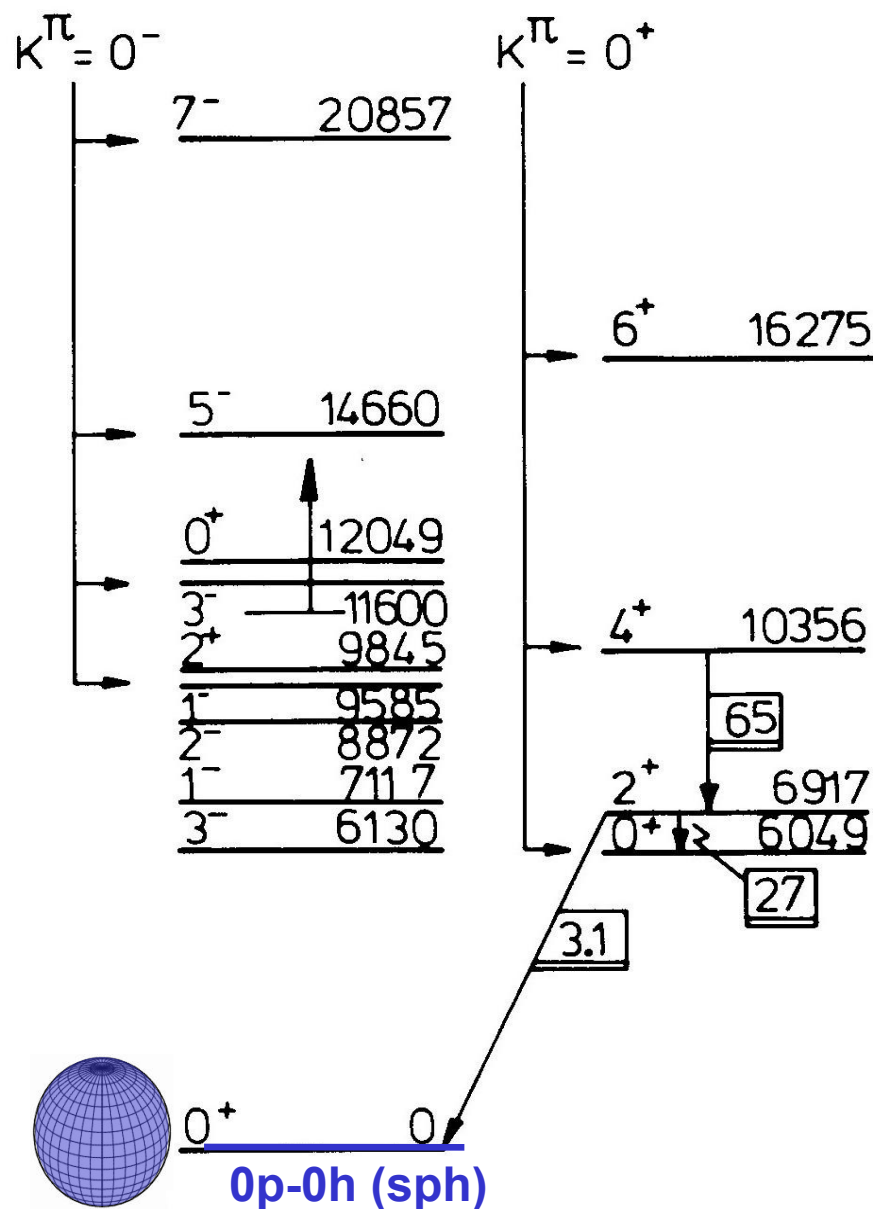
$1p_{3/2}$

$1s_{1/2}$



0^+
 0^-
0p-0h (sph)

Rotational Band in Doubly-Magic ^{16}O ?



Ground State 0p-0h Spherical configuration

Protons π

$1d_{5/2}$

8

$1p_{1/2}$

$1p_{3/2}$

$1s_{1/2}$

Neutrons ν

$1d_{5/2}$

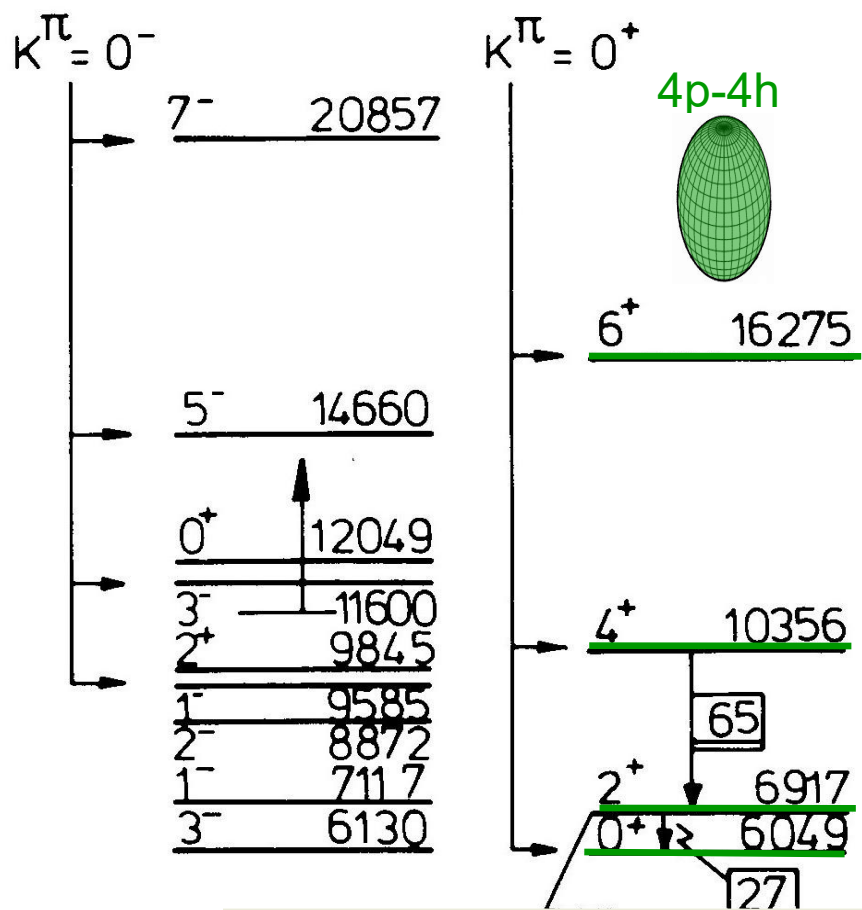
8

$1p_{1/2}$

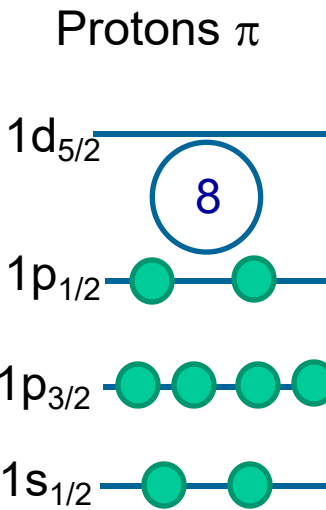
$1p_{3/2}$

$1s_{1/2}$

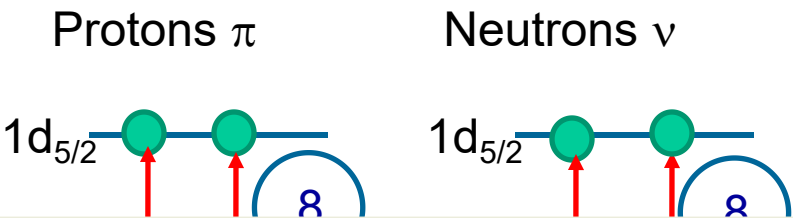
Shape Coexistence in Doubly-Magic ^{16}O ($Z=N=8$) (intruder states)



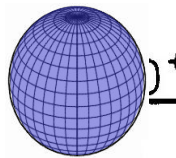
0⁺ Ground State 0p-0h Spherical configuration



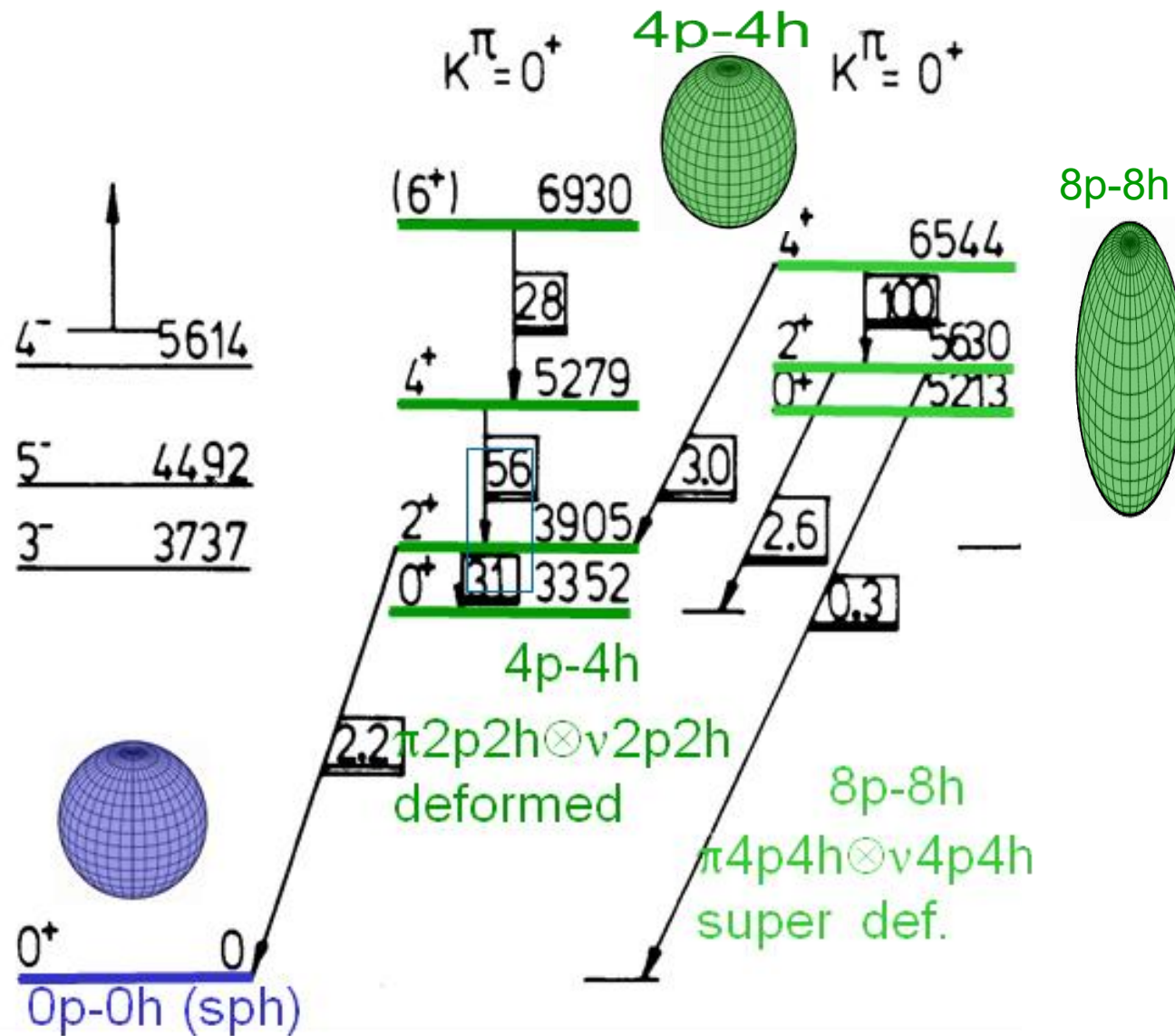
0⁺ Excited State 4p-4h Deformed configuration



Shape Coexistence: coexistence of two or more configurations in the same atomic nucleus (so, the same N and Z)

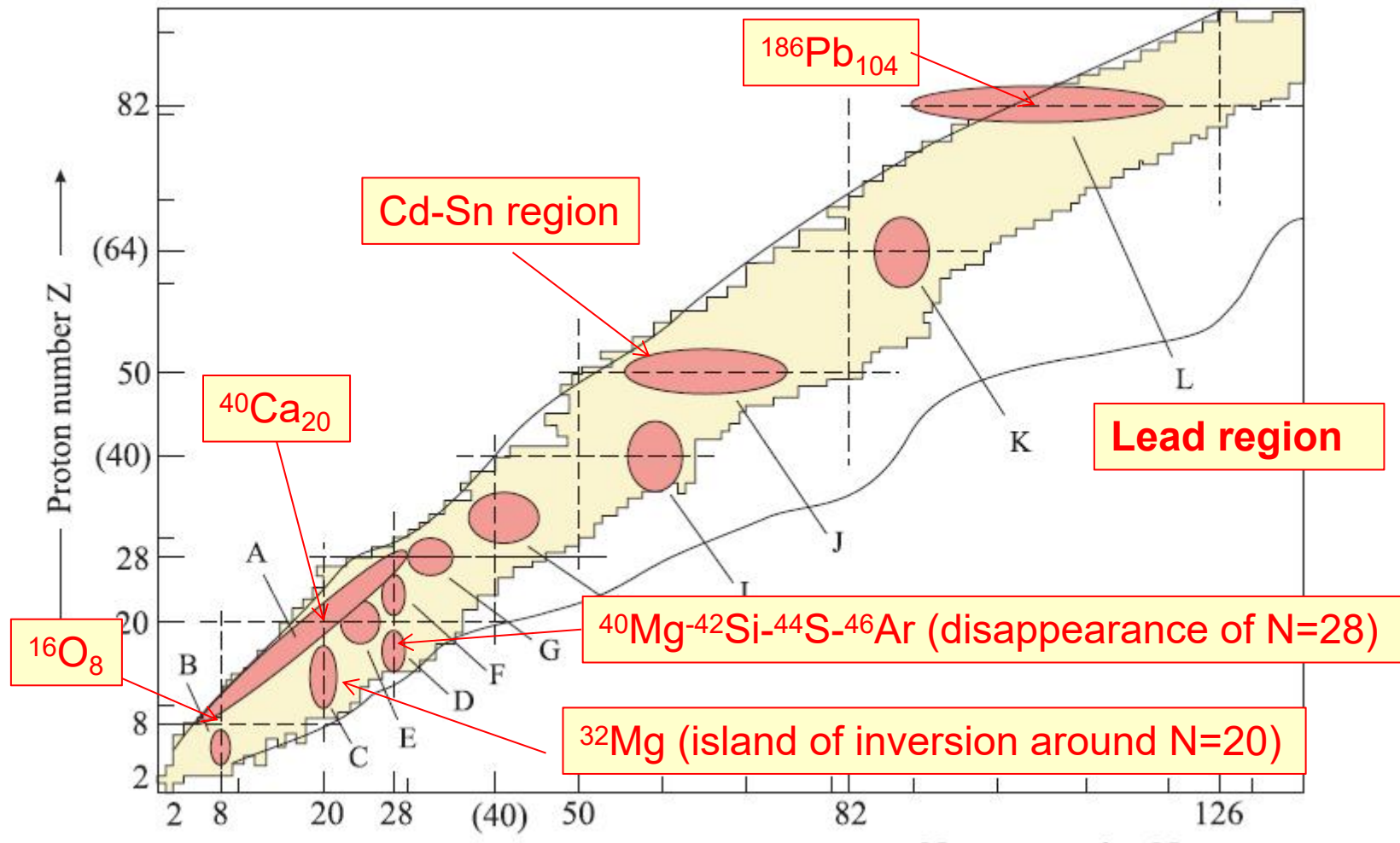


3 coexisting shapes in Doubly-Magic ^{40}Ca ($Z=N=20$)

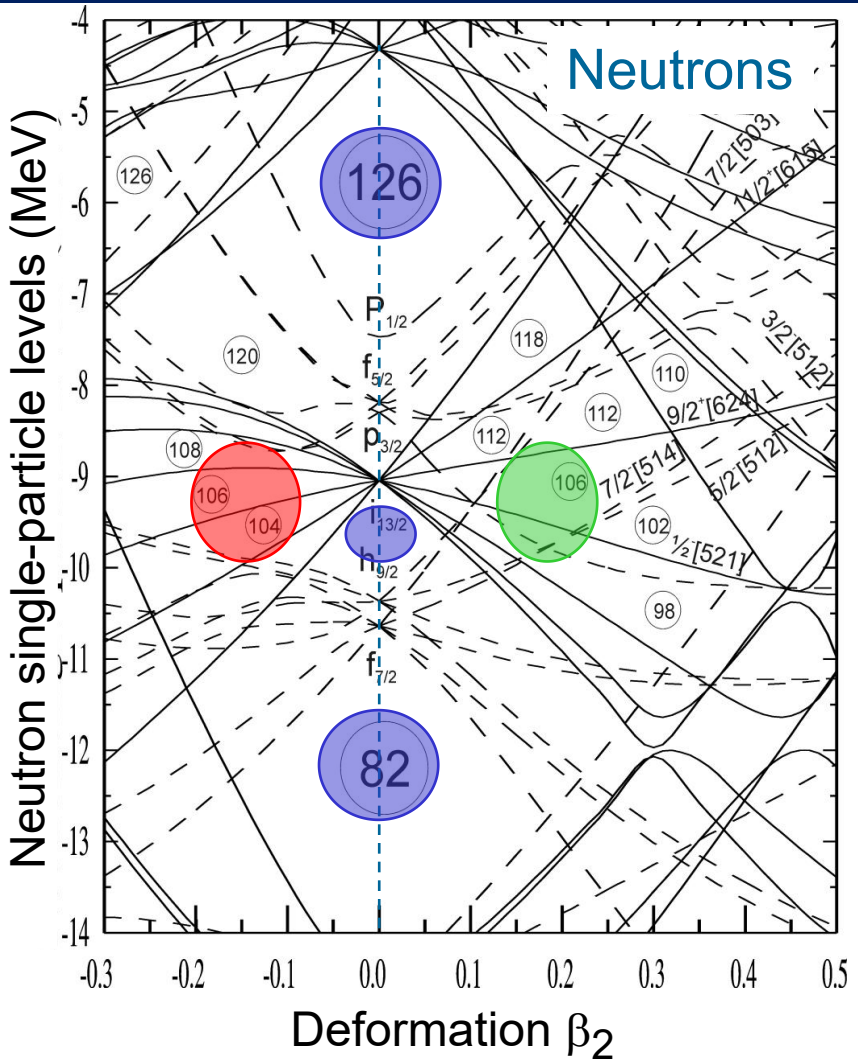
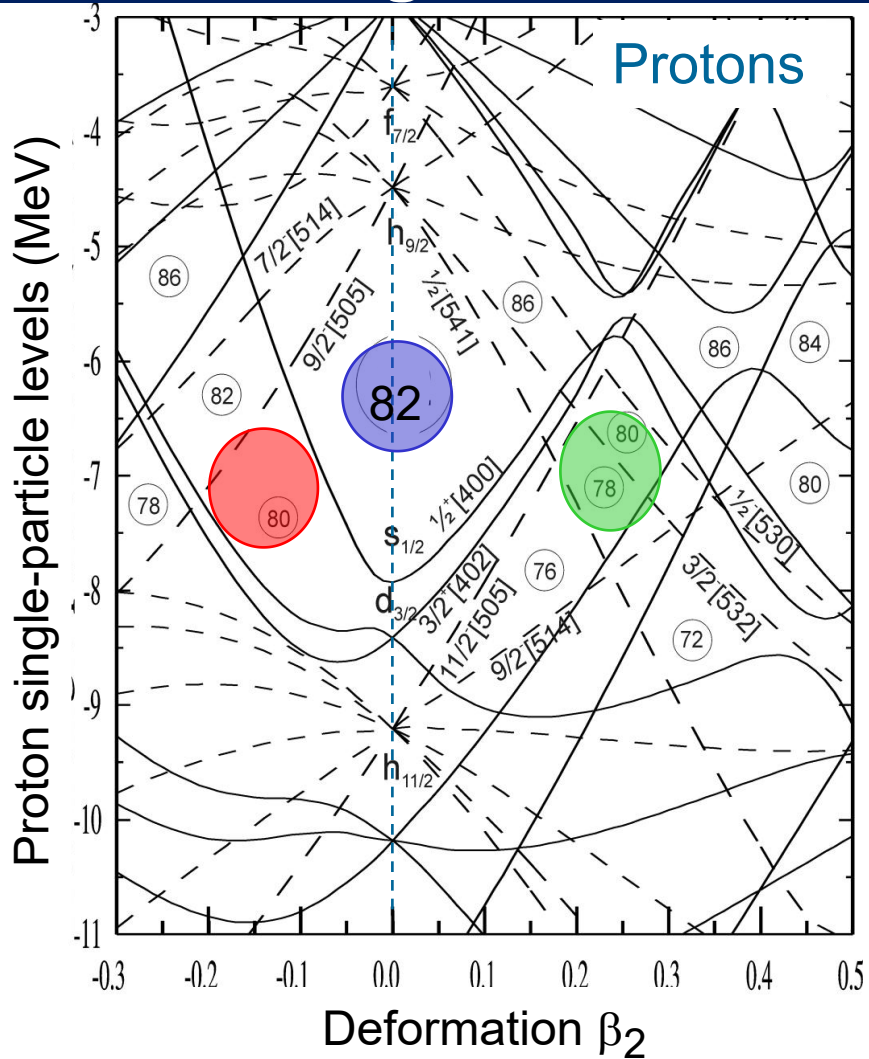


Shape coexistence around closed proton and/or neutron shells (and subshells)

- spherical and deformed structures co-exist in the nucleus at low energy
- its study can contribute in finding a unified description for atomic nuclei
- supplies information about the mixing between these configurations



Nilsson Diagrams around Z~82 & 82< N<126 (WS)



Around Z=82 and neutron mid-shell N=102-108, protons and neutrons coherently produce low-lying coexisting oblate and prolate shapes



Spherical

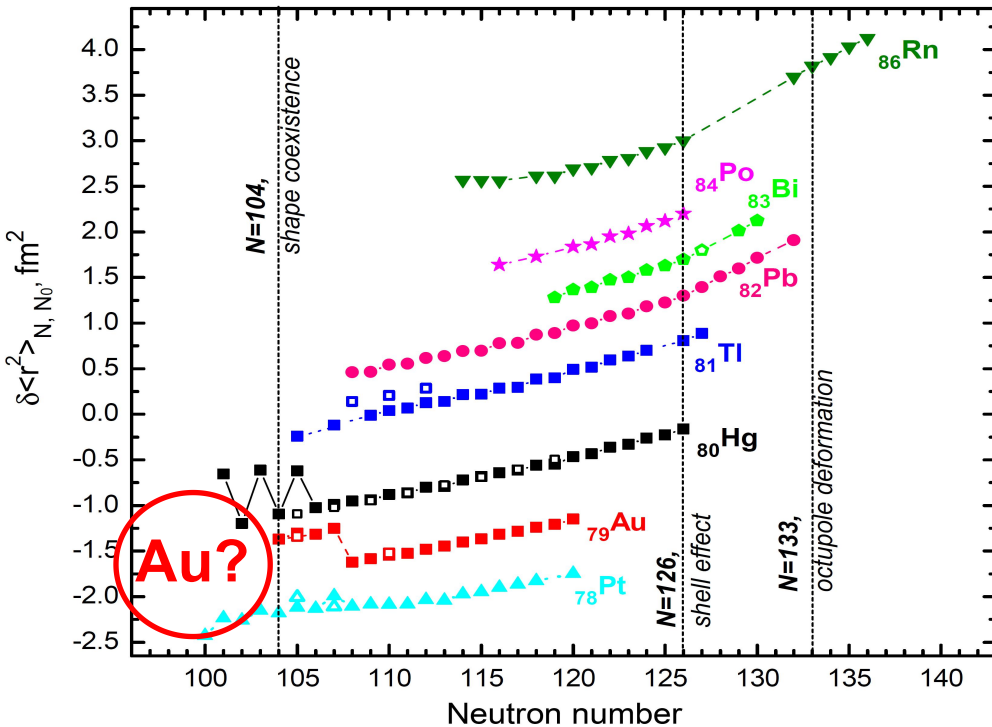


Oblate



Prolate

IS534@ISOLDE: Charge radii of Au isotopes



- Are the light gold isotopes deformed, $A(\text{Au}) < 183$?
- What are the spins of ground and isomeric states?

Previous radii data (ISOLDE)

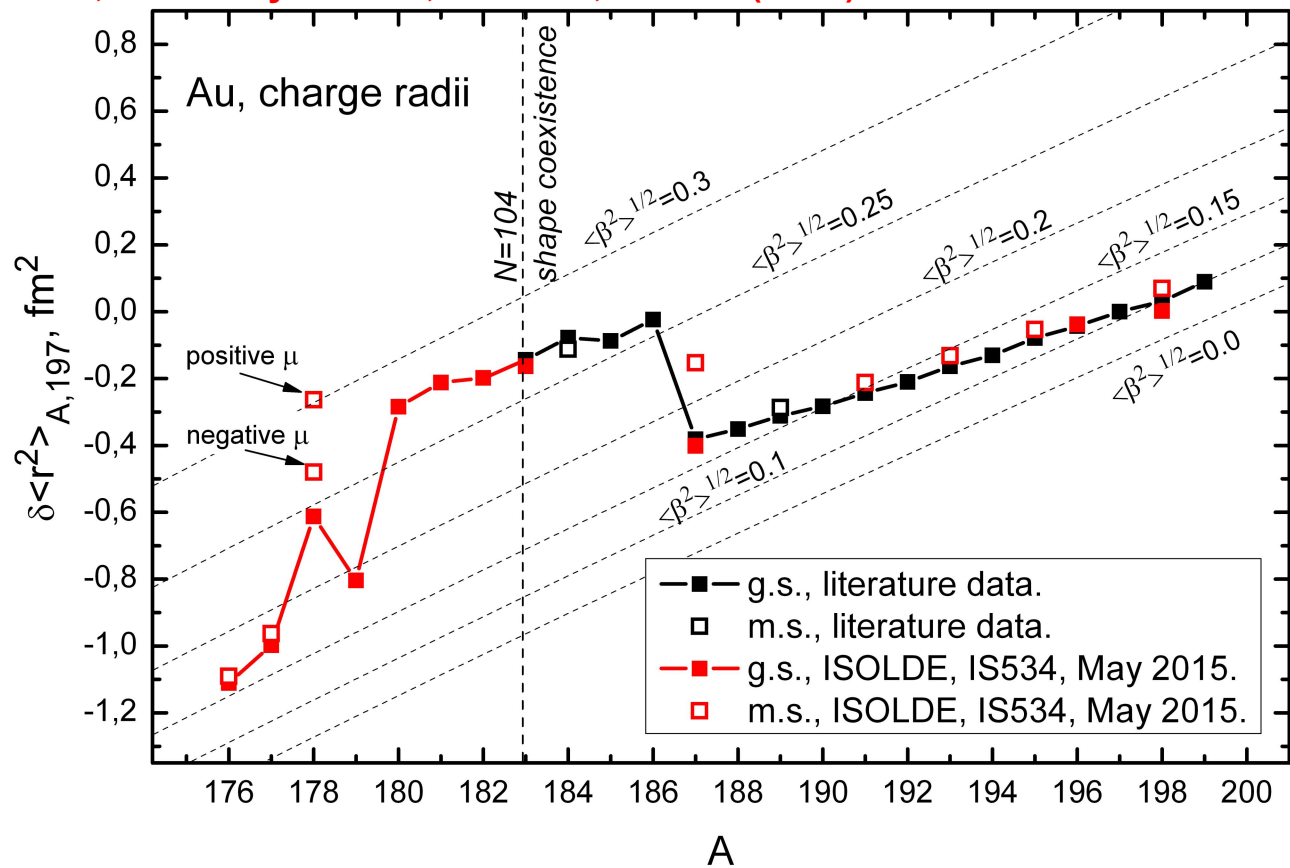
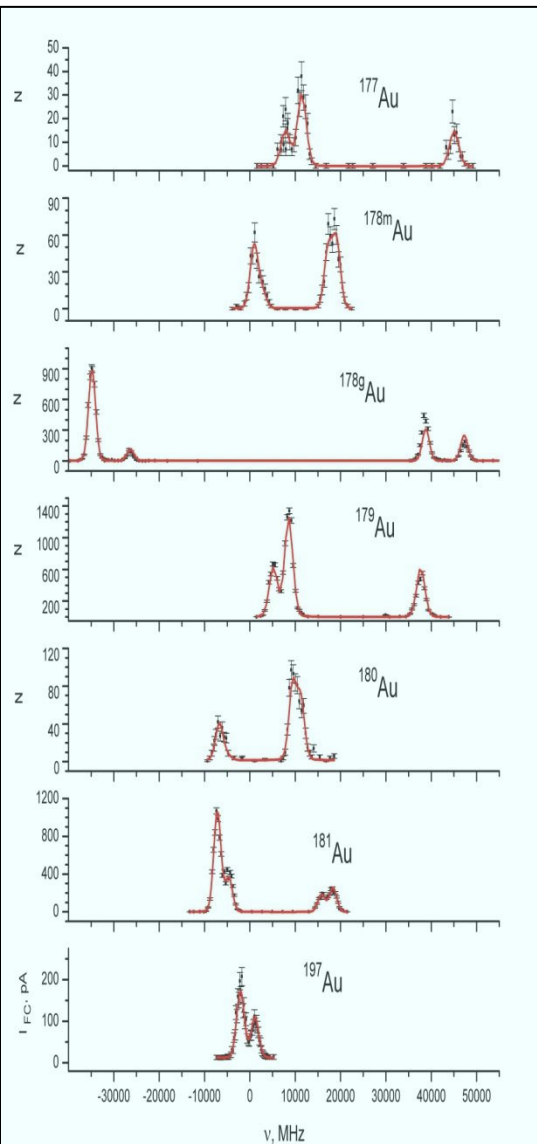
$^{185-190}\text{Au}$: K. Wallmeroth et al, NPA493,224 (1989)

$^{183,184}\text{Au}$: U. Kronert et al, Z.Phys. A331, 521 (1988)

$^{184\text{mg}}\text{Au}$: F. Le Blanc et al. PRL79, 2213 (1997)

HFS spectra and Charge Radii for Au

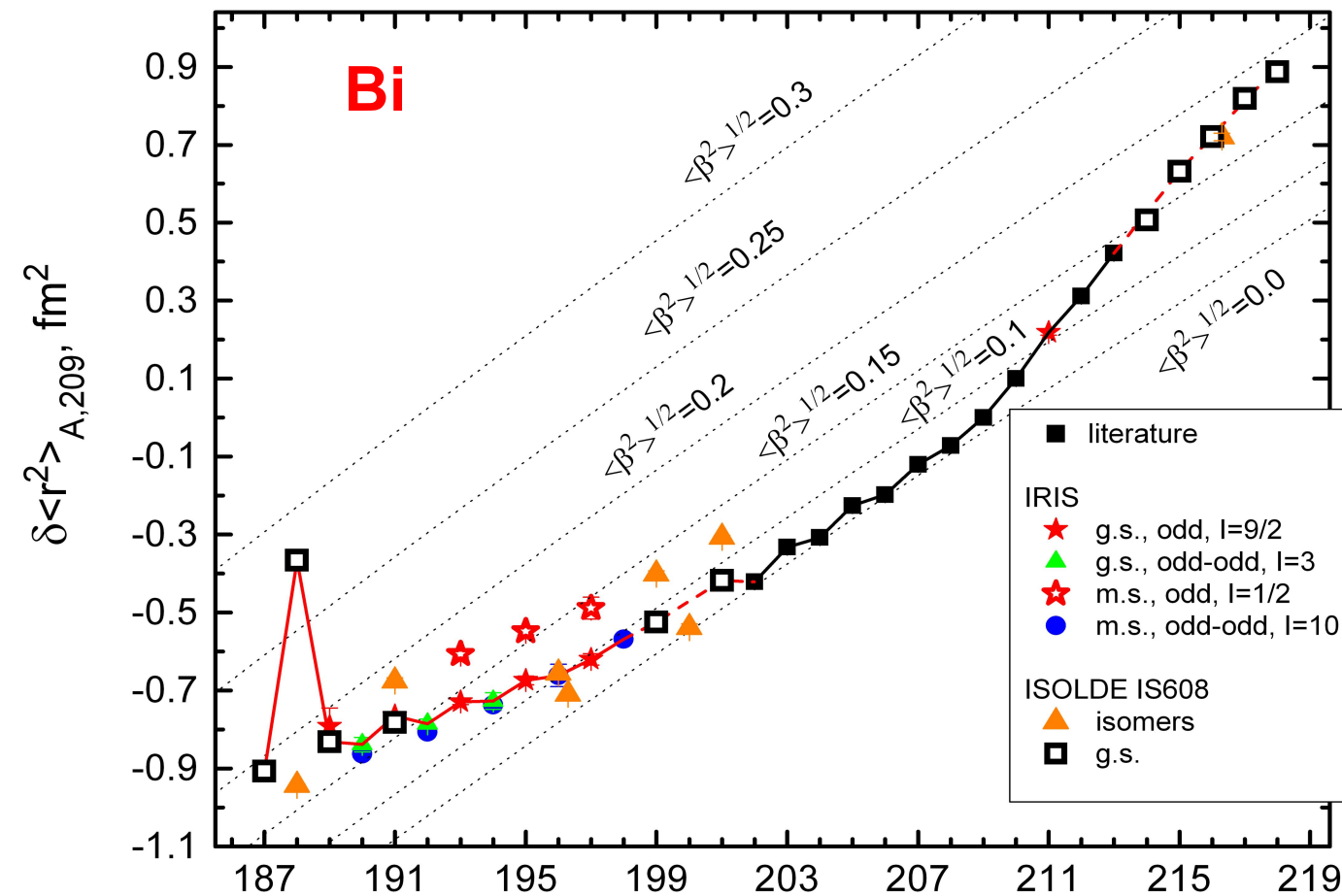
J. G. Cubiss, A. Andreyev et al., PRL 131, 202501 (2023)



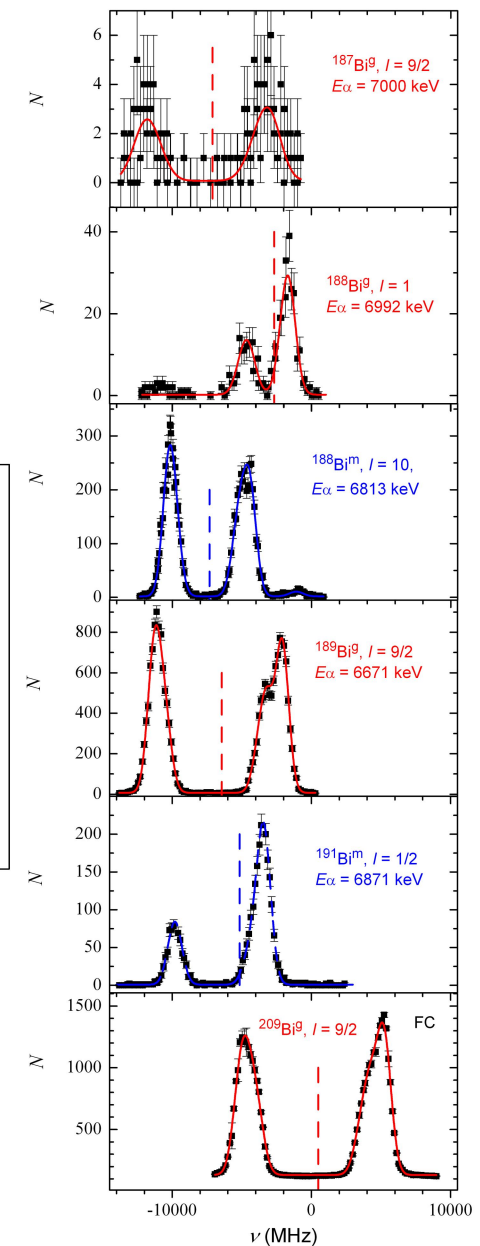
- 180-182Au- stay strongly deformed
- 176mg,177mg,179Au – trend towards sphericity
- 178mgAu: both isomers are deformed

Shape Staggering in $^{187-189}\text{Bi}$

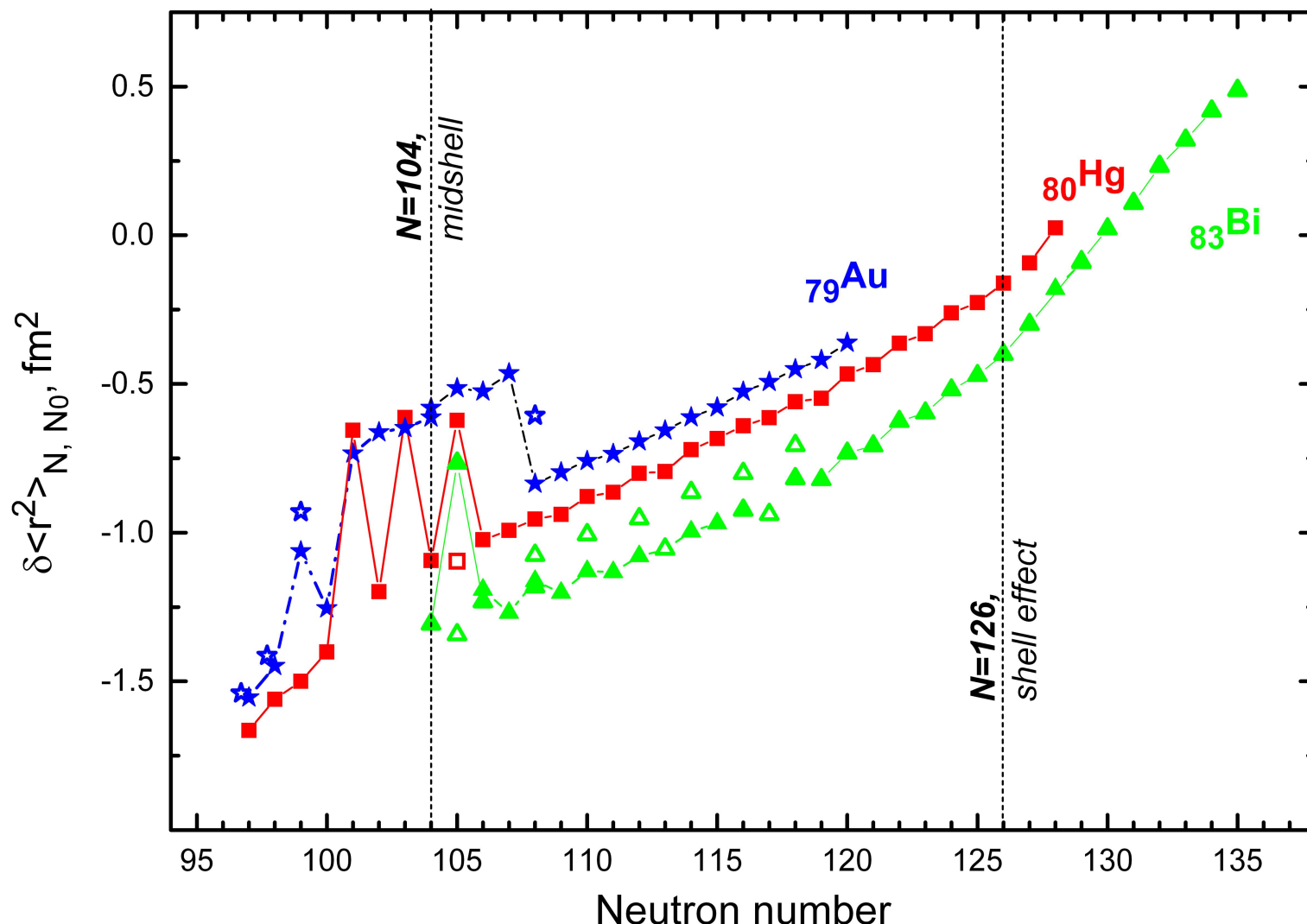
A.E. Barzakh, A. Andreyev et al., PRL 127, 192501 (2021)



- PhD project of Chris Raison (York)
- $^{187,189-209}\text{Bi}$ – follow the spherical Pb trend
- $^{188\text{m,g}}\text{Bi}$ ($N=105$) – Large stagger!
- Kink at $N=126$ observed



Charge radii for Hg, Au and Bi



The sudden jump in ¹⁸⁸Bi happens at the same neutron number N=105 as in odd-A Hg's

(An example) Modern 'state-of-the art' beyond mean-field calculations (SLy6+GCM)

J.M. Yao, M. Bender, P.-H. Heenen, PRC87, 034322(2013)

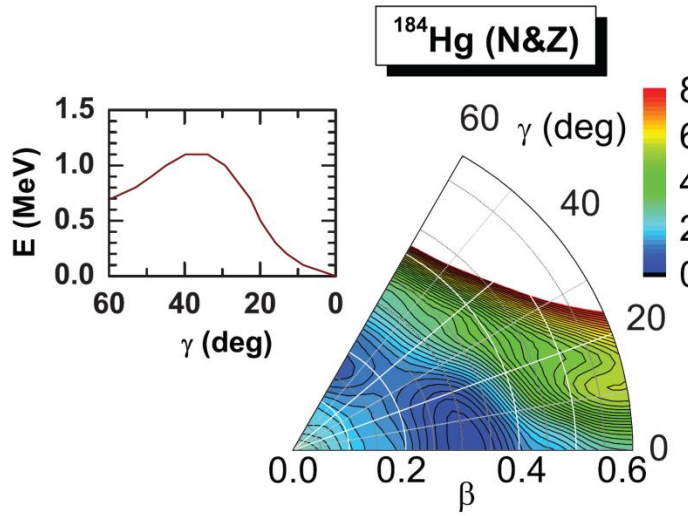
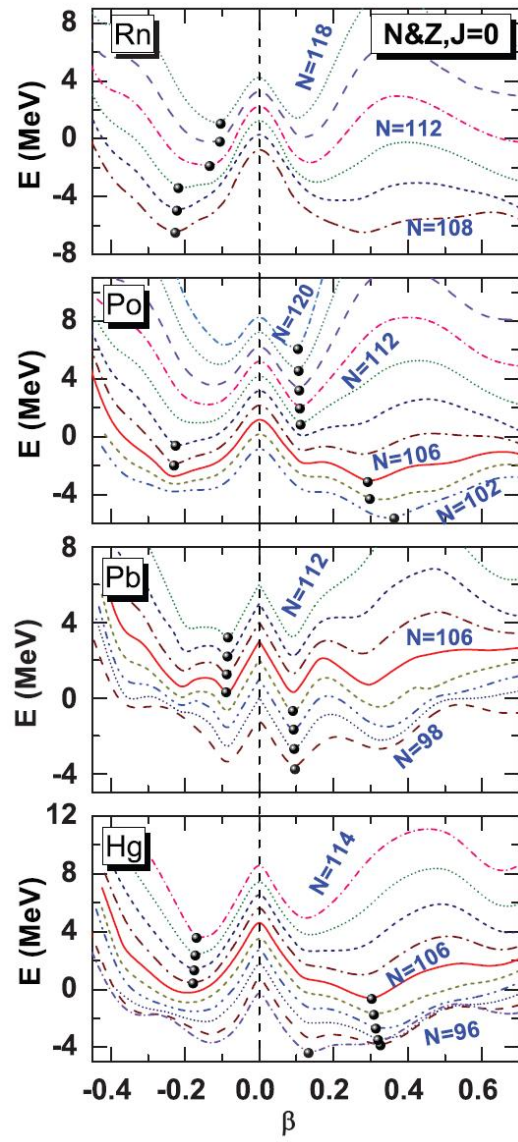
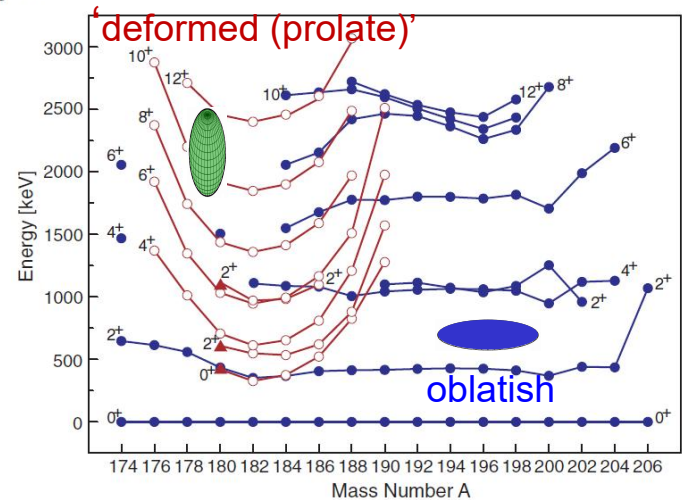


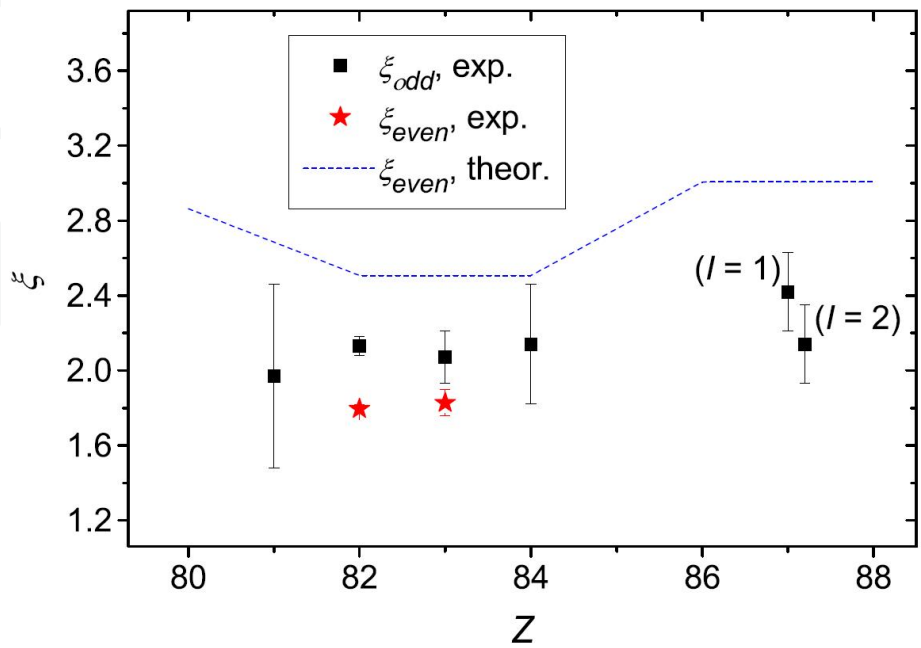
FIG. 4. (Color online) Quadrupole deformation energy surface for ^{184}Hg , normalized to the absolute minimum and projected on particle numbers. Each contour line is separated by 0.2 MeV. The inset shows the energy as a function of γ deformation along the path joining the two axial minima.

R. Julin, K. Helariutta, M. Muikku, J. Phys. G 27 (2001)

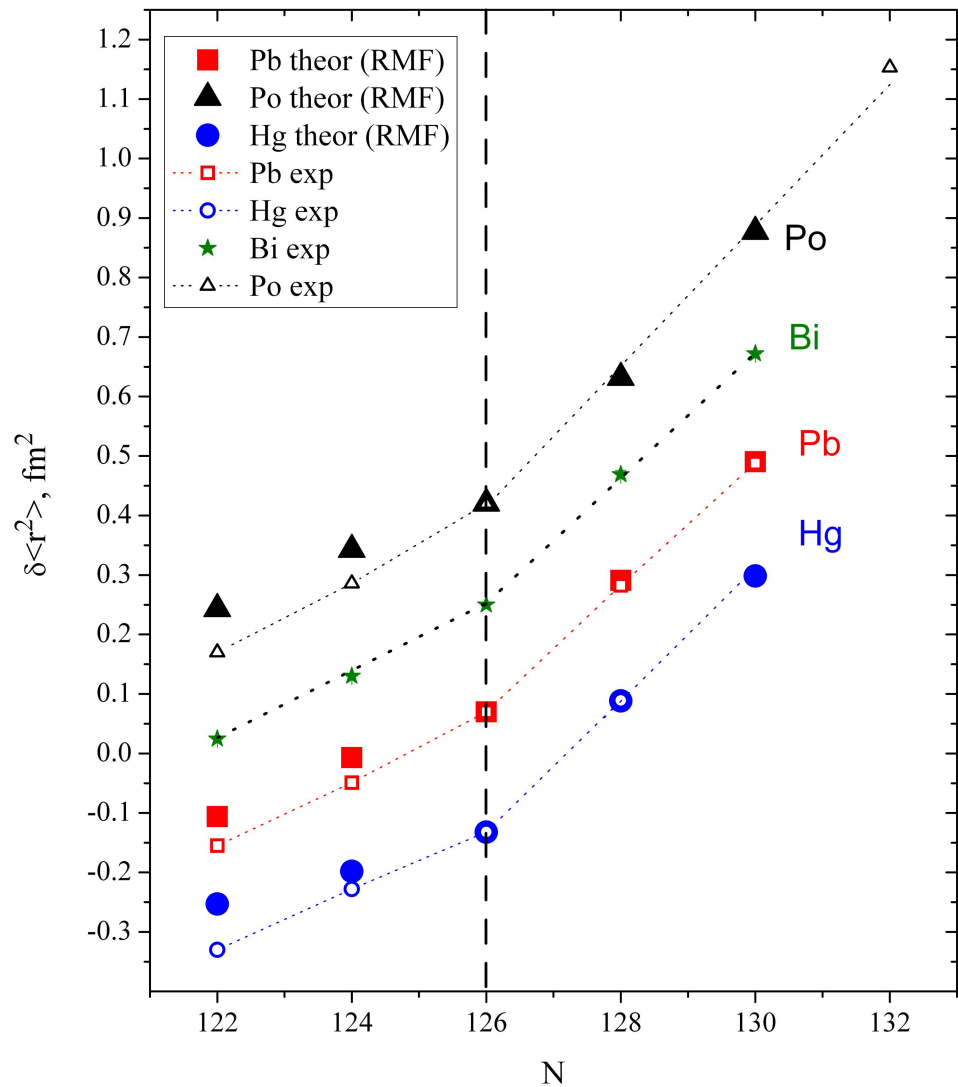


(In)Famous Kink at N=126

- Slope in $\delta\langle r^2 \rangle$ seen to increase when passing N=126
- Seen in elements both above and below Z=82
- Effect is seen in both odd- and even-n nuclei



A.E. Barzakh *et al.*, PRC 97, 014322 (2018)



(In)Famous Kink at N=126?

PRL 110, 032503 (2013)

PHYSICAL REVIEW LETTERS

week ending
18 JANUARY 2013

Charge Radius Isotope Shift Across the $N = 126$ Shell Gap

P. M. Goddard, P. D. Stevenson, and A. Rios

Department of Physics, University of Surrey, Guildford GU2 7XH, United Kingdom

(Received 9 October 2012; revised manuscript received 26 November 2012; published 15 January 2013)

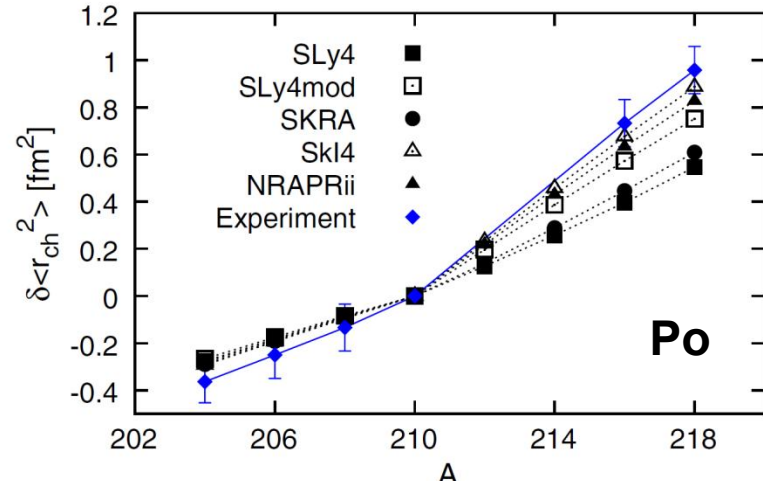
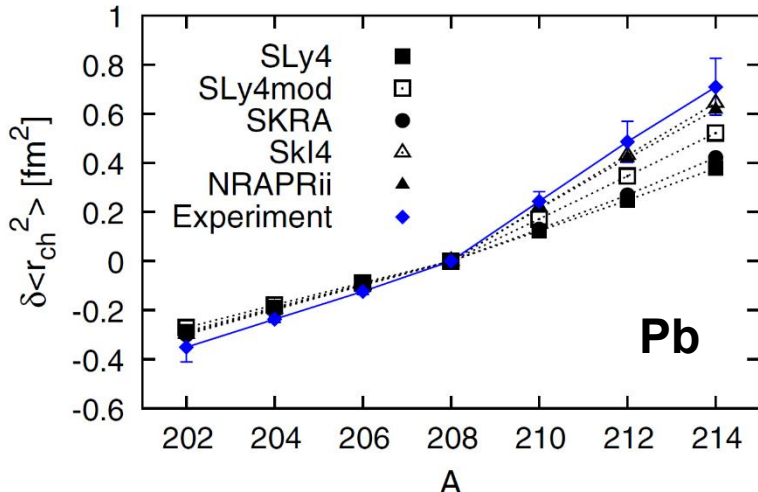


FIG. 1 (color online). Isotope shifts are given by the difference in the mean square charge radius between a series of even isotopes, denoted by their mass number A , and that of ^{208}Pb . Across the $N = 126$ shell closure, a strong increase in the slope of the experimental data (diamonds) is observed. Theoretical predictions, obtained with different Skyrme parametrizations, are also presented. Only a handful of Skyrme sets are able to reproduce the increase of slope above $N = 126$.

Occupation of the neutron $1\text{h}_{11/2}$ orbital provides a better overlap with majority of $n=1$ proton orbitals (via symmetry energy), thus driving them to a larger radius?

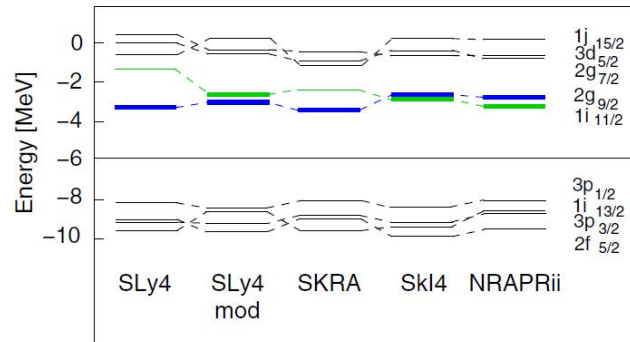


FIG. 3 (color online). Neutron single-particle energies around the Fermi surface in ^{210}Pb for five sets of Skyrme forces. States with a significant BCS occupation, $>3\%$, above $N = 126$ are emboldened. Whenever the $1i_{11/2}$ state is substantially populated, the kink in isotope shift can be reproduced.